

Blind Estuaries during Drought: The Influence of a Sandbar on Mangrove Trees

S. de Vries
MSc. Thesis Water Resources Management



Delft University of Technology



Blind estuaries during drought: The influences of a sandbar on mangrove trees

Estuarios ciegos durante la sequía: Las influencias de un
banco de arena en los árboles de mangle

Thesis report

by

Sandra de Vries

February 25, 2016

For the degree of Master of Science
in Civil Engineering at Delft University of Technology.
To be defended publicly on March 4, 2016 at 1:00 PM.

Committee:

Prof. dr. ir. Hubert H.G. Savenije
Ir. Willem Luxemburg
Dr. Bregje van Wesenbeeck
Dr. Ir. Klaas Metselaar
Dr. Heyddy Calderon

Delft University of Technology
Delft University of Technology
Delft University of Technology, Deltares
Wageningen University
Centro para la Investigacion en Recursos Acu-
aticos de Nicaragua (CIRA/UNAN-Managua)



Preface

The report now lying in front of you is the final product of my thesis, a mandatory part to graduate for the master 'Water Resources Management' at Delft University of Technology. The research has been performed in close coöperation with the Center for Research on Aquatic Resources of Nicaragua (CIRA), who have been doing research in the study area and its surroundings for many years now. It was thus on their request that fundamental research would be continued in the small mangrove forest located there. Although compulsory, it never felt as such, since I performed the research with much pleasure and enthusiasm.

The research has focused mainly on combining ecological and hydrological factors, and in that way creating a multi-method to answer the main question without much data being available. In that way I could use the skills I had picked-up during my studies in Delft, and also learn a lot about mangrove ecosystems. The study was fortunately not only performed behind a computer, since it was back-boned by the information collected in the area of research itself.

The possibility to live in a friendly community next to the research area, is something to be grateful for. I would thus like to start thanking the inhabitants of El Ostional, who have welcomed me with such warmth and who were so patient with my Spanish. In fact, they gave me the opportunity to improve my Spanish by involving me in their daily habits. Thanks Blanca and Yorlenis, for the great cooking, Glenda and the kids for the cozy and happy stay, Fatima for the everyday chats, and Salvador and Carolina for their constant support for my research. Thanks to their kayak, I could go into the estuary without sinking waist-deep into the mud every time. I still remember the parties at their hostel together with the previous mentioned villagers, whom I all consider as friends now. My special thanks goes also to the absent crocodiles that seemed to have taken a short holiday during my stay there. My job in the estuary would have been much more difficult with them popping up from the water surface every moment.

The constant help from Heyddy Calderon, who gave input and assistance for my everyday needs in Nicaragua, was essential for the success of the data collection. She was assisted by Camilo Fuentes and many others at CIRA to whom I owe much. They all helped me through setbacks due to the weather or equipment errors, and included me into their daily life at the research institute. Heyddy, thank you for the relaxed evenings and hospitality.

The research environment in Nicaragua was certainly not the only good working place. Before as well as after my fieldwork period I was surrounded with my beloved fellow friends and students in our so called 'den'; room 4.84. They inspired me with our sometimes heated and energetic thesis related discussions, where questions that popped up were immediately taken up by half of the group present. Thanks for all the philosophical and animating conversations, the jokes, papers-of-the-day, dragon fire, self-made coffee and tea, procrastinating, enervating news topics, Christmas trees, study music, everyday lunches, after hour drinks, and so much more! I am of course talking about Daniël, Bas, Emiel, Raoul, Lotte, Louise, Janneke, Bianca, Anke, Tessa, Eva, Nadja, Bernadien, and Marja.

Thanks goes to Esther, Marloes and Anke for reading the complete draft version of the report, and to many of my friends and family, with whom I could always spruce on my topic. Thanks to the enthusiasm of my family and friends, and their immense trust in me, which allowed me to never falter in following my intuition.

Credits for sure go to the professionals in ecology and biology I called upon, who informed me on topics that did not lie in my field of study. They supplied me of indispensable information and expertise. Thanks Dr. Riley, Dr. Olson and Dr. Jimenez.

Courtesy goes to the evaluation committee, that justly corrected me when necessary, to Lydia, who was always interested in my coming and goings, and to the rest of the Water Management section, who provided a great working atmosphere. Thank you Anna, for all the effort you have put in lending me the sap flow device, giving me instructions on how to use it, and not being annoyed when the equipment did not survive the test. This device would furthermore never have worked without the huge help of Ronald, who supported me on the electronics in order to fix the device.

And of course, last but certainly not least, my foremost gratitude goes to Hubert Savenije. Thanks to him I ended up in this field of research; he inspired me with his passionated lectures and visions on hydrology. Thanks to his input just when I needed it, while he mostly let me go my own way, I could freely do this research, which I enjoyed very much.

Sandra

Delft, February 25, 2016

Summary

Small blind estuaries are a common phenomenon on the coast of Nicaragua, but unfortunately not much is known on their hydrological characteristics. A blind estuary can be identified by a sandbar that temporarily closes the estuary from sea. These blind estuaries often have very diverse flora and fauna on which they play an important ecological role. Mangrove forests growing in this ecosystem often play a central position, and are valued for a wide range of functions, productivities, uses and values. Unfortunately these forests are also under threat of destruction, which is often caused by human influences. In this research human impact, as well as the impact of drought caused by an El Niño event, have been included to understand the influence of a blind estuary on the condition of the mangrove forest.

The study was performed in a blind estuary at the Pacific coast of Nicaragua, located near the village El Ostional. During a fieldwork period of approximately three months, the study area was observed and among others, measurements on water levels and salinity were conducted. The resulting information was used (1) to classify the separate morphologic, biologic, and social structures in the area, (2) to identify the interactions between mangrove well being and hydrological characteristics, and finally (3) to do more in-depth analyses on the salt intrusion occurring in the area using a steady state salt intrusion model and the Ghyben-Herzberg method.

The estuary contains two main landforms; the sandbar separating estuary and sea, and the back-barrier floodplain behind it. The sandbar is formed by wave action, and can be ruptured due to a highly seasonal river discharge. The floodplain inundates when accumulation of water behind the sandbar increases. A variety of common mangroves like the Red mangrove - *Rhizophora racemosa* and *Rhizophora mangle* -, White mangrove - *Laguncularia racemosa*, and the Buttonwood - *Conocarpus erecta* can be found in the floodplain. The floodplain next to this, is home to the Tea Mangrove - *Pelluciera rhizophorae*, a very rare and low salt tolerance mangrove tree. Together, these mangrove trees form an interior mangrove forest during the periods in which the sandbar is closed. The inhabitants of El Ostional mainly use the floodplain to shortcut their route to the shore, and from time to time they use the mangrove trees for firewood. Their main interest in the estuary is for the fishing possibilities it provides. The inhabitants on occasions like to 'help' the sandbar to open, for them to have easy fishing possibilities.

Inundation in the floodplain is shown to be extremely beneficial for the mangrove population. During drought, inundation does not take place and several problems arise. Germination of the mangrove propagules does not occur when inundation is absent. It further decreases dominance over other tree species. When drought persists, water tables in the floodplain aquifer decrease even further and this stresses the mangrove trees, inducing a growth stop. The crab population in the floodplain turned out to play an important ecological role, where their burrows increase permeability. This enhances infiltration into the soil, which increases soil moisture and decreases soil salinity. The blind estuary is, although stressed by drought, able to maintain relatively low salinity levels. This is caused by a steady fresh groundwater inflow. An overall outflow of estuary water occurs through the sandbar, where head differences between sea tide and estuary water level are the main forces that induce a transmission through the sandbar. The resulting relatively fresh water in the estuary permits the growth of the Tea mangrove.

A mainly pressure induced muted tide is shown to occur in the estuary. Together with the fresh water inflow and wind influence, a circulation is established that results in a well-mixed salt

intrusion, which is caused by over-wash events. Would the sandbar be ruptured manually during drought, then the result is an increase in salinity. That could turn out to be devastating for the Tea mangrove, but would also supply the estuary and mangrove trees with more water and it would provide the connection between sea and estuary necessary for fish reproduction. Salt intrudes the floodplain during inundation, when sea water evaporates and salt is left behind, which accumulates in the soil. The more infrequent the inundation, the higher the salinity in the soil. Salt intrusion in the subsurface of the Ostional area however, is due to pressure differences between fresh water in the aquifer and sea tide. This induces a mixing zone of which the interface is still near the shore; most of the wells in Ostional maintain potable water salinities.

In order to protect the mangrove forest, it is thus important to protect the complete ecosystem, in this case especially the crab population. It further is important to ensure the maintenance of a groundwater inflow, by protecting the upstream forests that enhance infiltration to the groundwater system. Whether the manual rupture of the sandbar during drought is considered problematic depends on the the value given to the Tea mangrove, the other mangrove population, or the nursery function the estuary provides. Further research and monitoring for the Ostional area is necessary to confirm the results of this research, and to keep track of salt intrusion in the estuary and subsurface.

Resumen

Pequeños estuarios ciegos son un fenómeno común en la costa de Nicaragua, pero por desgracia no se sabe mucho sobre sus características hidrológicas. Un estuario ciego puede ser identificado por un banco de arena que cierra temporalmente el estuario del mar. Estos estuarios ciegos a menudo tienen muy diversa flora y fauna los que juegan un importante papel ecológico. Los bosques de manglares que crecen en este ecosistema a menudo desempeñan una posición central, y son valorados por una amplia gama de funciones, productividades, usos y valores. Lamentablemente, estos bosques están también bajo amenaza de destrucción, que a menudo es causada por la influencia humana. En este impacto humano de investigación, así como el impacto de la sequía causada por un fenómeno de El Niño ningún caso, se tienen en cuenta a fin de comprender la influencia de un estuario de ciegos en el bienestar de los bosques de mangle.

El estudio se realizó en un estuario ciego en la costa del Pacífico de Nicaragua; ubicada cerca del pueblo El Ostional. Durante un período de trabajo de campo de aproximadamente tres meses, se observó el área de estudio y se realizaron mediciones de los niveles de agua predominantemente y la salinidad. La información resultante se utilizó (1) para clasificar las características morfológicas separada, biológico, y las estructuras sociales de la zona, (2) identificar las interacciones entre el bienestar del manglar y las características hidrológicas, y finalmente (3) hacer más análisis en profundidad sobre la intrusión salina se producen en la zona.

El estuario contiene dos formas de relieve principales; la barra de arena que separa el estuario del mar, y la llanura de inundación detrás de la barrera. La barra de arena está formada por la acción del oleaje, y se puede romper debido a una descarga del río, la cual es altamente estacional. La llanura de inundación se inunda cuando la acumulación de agua detrás de la barra de arena aumenta. Una variedad de manglares comunes como el mangle Rojo - *Rhizophora racemosa* y *Rhizophora mangle* -, mangle Blanco - *Laguncularia racemosa*-, y el Buttonwood - *Conocarpus erecta*- se pueden encontrar en el llanura de inundación. La llanura de inundación al lado de esta es el hogar del mangle Té - *Pelliciera rhizophorae*-, un árbol de mangle tolerancia a la sal con poca frecuencia y baja. En conjunto, estos árboles de mangle forman un bosque de manglar interior durante los períodos en que se cierra el banco de arena. Los habitantes de El Ostional utilizan, sobre todo la zona de inundación como atajo hacia la costa, y los árboles de mangle como leña. Su principal interés en el estuario es para las posibilidades de pesca que ofrece. Los habitantes en ocasiones ayudan al estero a abrir la barra de arena para tener posibilidades fáciles de pesca.

La inundación en la planicie de inundación se revela como extremadamente beneficioso para la población de manglares. Durante la sequía, la inundación no tiene lugar y surgen varios problemas. La germinación de los propágulos de mangle no se produce cuando la inundación está ausente. Se disminuye aún más el dominio sobre otras especies de árboles. Cuando la sequía persiste, niveles de agua en el acuífero de inundación disminuyen aún más y esto causa mayor estrés en los árboles, deteniendo su crecimiento. La población de cangrejos en la zona de inundación juega un importante papel ecológico, donde sus madrigueras aumentan la permeabilidad. Esto mejora la infiltración en el suelo, lo que aumenta la humedad del suelo y disminuye la salinidad del suelo. El estuario ciego, aunque estresado por la sequía, es capaz de mantener niveles relativamente bajos de salinidad. Esto es causado por un flujo de agua subterránea estable. Una salida total de agua del estuario se produce a través del banco de arena, donde las diferencias principales entre la marea del mar y el nivel del agua del estuario son las principales fuerzas que inducen una transmisión a través de la barra de arena. El agua resultante, relativamente fresca, permite el crecimiento del mangle de Té.

Una marea inducida por presión se observa en el estuario. Junto con la entrada de agua dulce y, probablemente, del viento, se establece una circulación que revela una intrusión salina bien mezclada, que es causada por un exceso de lavado eventos. Si el banco de arena se rompe de forma manual durante la sequía, entonces el resultado es un aumento de la salinidad que sería devastador para el mangle Té, pero suministrará el estuario y manglares con más agua y proporcionar la conexión entre el mar y el estuario necesario para la reproducción de peces. La sal se entromete la llanura de inundación durante la inundación, cuando el agua de mar se evapora y deja la sal, que se acumula en el suelo. Mientras más infrecuente la inundación, mayor es la salinidad del suelo. Esto sólo ocurre en la llanura de inundación. Intrusión salina en el subsuelo de la zona de Ostional es debido a las diferencias de presión entre el agua dulce en el acuífero de la marea y el mar. Esto induce una zona de mezcla de la cual la interfaz es todavía cerca de la orilla; la mayor parte de los pozos en Ostional mantienen salinidades de agua potable.

Con el fin de proteger el bosque de manglar, es importante proteger el ecosistema completo, en este caso en especial la población de cangrejos. Además, es importante para garantizar el mantenimiento de un flujo de entrada de las aguas subterráneas, mediante la protección de los bosques aguas arriba que mejoran la infiltración en el sistema de aguas subterráneas. Si la rotura manual de la barra de arena durante la sequía se considera problemática depende del valor dado al manglar del Té, la otra población de manglares, o la función de vivero ofrece la ría. Nuevas investigaciones y monitoreo para el área de Ostional es necesario confirmar las hipótesis formuladas, y con el fin de realizar un seguimiento de la intrusión salina en el estuario y del subsuelo.

Contents

1	Introduction	13
1.1	Research matter	13
1.2	Protection of mangrove trees	14
1.3	Research objective	14
1.4	Case study	15
1.5	Outline of the report	16
2	Methodology	17
2.1	Data collection	17
2.2	Data analysis	18
I	System analysis	21
1	Introduction	23
2	Results and conceptualization	25
2.1	Geomorphologic structure	25
2.2	Biologic structure	28
2.3	Social structure	33
3	Conclusions	37
II	Symbiosis between hydrology and ecology	39
1	Introduction	41
2	Results and conceptualization	43
2.1	Water shortage	43
2.2	Improvement of soil conditions by crabs	47
2.3	A relative fresh water estuary	50

3	Conclusions	55
III	Saline conditions of the Ostional area	57
1	Introduction	59
2	Results and conceptualization	61
2.1	Salt intrusion in a blind estuary	61
2.2	Salt intrusion in the subsurface	69
2.3	Salt intrusion with an opened sandbar	74
3	Conclusions	77
IV	Concluding remarks and recommendations	79
1	Synthesis	81
1.1	Retrospect on the objective	81
1.2	New hypotheses	82
2	Discussion	83
2.1	Measurements	83
2.2	Steady state salt intrusion model	84
2.3	Blind estuaries in general	84
3	Recommendations	85
3.1	Protection of the ecosystem	85
3.2	Maintenance of groundwater flow	85
3.3	Manual rupture of the sandbar	86
3.4	Recommended research topics	86
	Appendices	103
A	Establishing the database	103
A.1	Survey	103
A.2	Further retrieved data	108
B	Used theories	109
B.1	Recalculation methods	109
B.2	Ghyben-Herzberg approximation	110
B.3	Steady state model	111

C Complete results	117
C.1 Applicable data	117
C.2 Fresh-salt water interface	135
C.3 The 1-D analytical salt intrusion model	135
C.4 Further retrieved data	140

Chapter 1

Introduction

The title of this report will be explained in order to introduce the objective of the research. Furthermore the research is motivated and a keynote is given on the procedure used to reach the objective.

1.1 Research matter

1.1.1 Blind estuaries

An estuary is a coastal body of water which is either permanently or periodically open to the sea and within which there is a measurable variation of salinity due to the mixture of sea water with fresh water derived from land drainage. This definition for estuaries by Day [1] is one of many, but especially appropriate here since it was the first to include estuaries that are (temporarily) closed off from the sea by an ephemeral bar, and which are called 'blind' estuaries [2]. This bar arises when littoral transport, one of the main driving forces affecting the character of an estuary, is strong in relation to the erosive power of the tide and of the river discharge. When the estuary is only temporarily closed off, this can for example be due to a seasonal river discharge, found often at tropical coasts. The circulation processes and type of biological occurrences differ whether the connection is open or closed [3]. Under closed circumstances opinions differ whether a 'blind estuary' even resembles a true estuary, since the other main driving forces affecting the character of an estuary - tide, waves, river discharge, and density difference [2] - are hard to detect or not occurring at all. These main driving forces and their resulting characteristics, have not yet been researched in detail in a blind estuary.

Blind estuaries have been described not only by Day [1], but also by Anthony [4], Cooper [5] and Roy [6] for African, Asian [7] and Australian estuaries. Estuaries in this category are relatively small, both in length and catchment and are characteristic for areas of low rainfall or highly seasonal rainfall. Blind estuaries often have very diverse flora and fauna and play an important ecological role [7]. Sandbars in front of estuaries are also common on the Pacific Coast of Central America according to Jimenez et al. [8,9]. Not yet defined as blind estuaries, some at least bear the same characteristics [10–12], giving incentive to believe that blind estuaries occur at the Pacific Coast of Central America.

1.1.2 Mangrove forests

Mangrove forests play a central position in the estuarine and near shore marine environment [13]. These forests are tropical inter-tidal habitats which form wetlands in coastal areas [10,14]. A broad definition for mangroves can be; an assemblage of plants all adapted to a wet, saline habitat. The mangrove tree environment is typically with anaerobic sediments, fluctuating water levels, and high

salt content [15]. Mangrove trees are defined as halophilic, but high salt content is not a necessary condition. The trees just thrive in their habitat because of evolved adaptations to the saline conditions, and since fewer species are able to live in such an environment, mangrove trees have the upper hand. Mangrove forests are appreciated for a wide range of functions, productivities, uses and values for adjacent ecosystems and human societies. Several examples are (1) the nursery habitats they provide for many fish and invertebrate species, (2) protection for inland sites from storm surges and flooding, (3) enhancing sedimentation and thus development of new land, (4) reduction of variations in salinity, (5) building materials, (6) firewood, (7) medical applications, and (8) tourism [13,14].

1.1.3 El Niño 2015

The National Oceanic and Atmospheric Administration announced around March 2015 that an El Niño event emerged [16]. El Niño is the name for an appearance of anomalously warm water in the eastern tropical Pacific Ocean. This event usually persists for about 6 to 18 months and occurs irregularly around every two to seven years. El Niño is accompanied by high air pressure in the western Pacific and low air pressure in the eastern Pacific that causes global changes of both temperature and rainfall [16]. Recent studies report a robust tendency to more frequent and extreme El Niños [17,18]. The intensity of an El Niño matters for impacts on freshwater fisheries, river and coastal water quality, and wetlands.

One of the countries at the Pacific Coast affected by El Niño is Nicaragua, where the main effect is a sharp reduction in available atmospheric humidity leading to significant rainfall deficits and an irregular, sporadic rainy season from May to October [19]. Together with an already dry year during 2014 with a record reduction in rainfall, drought is the result [19,20]. In Nicaragua it means, among others, dry riverbeds of seasonal rivers during the rainy season. This results in estuaries bordering the Pacific Coast that are continuously closed off by a sandbar. These estuaries in general are bordered by mangrove forests, thus also secluded for longer periods from sea influences.

1.2 Protection of mangrove trees

Human destruction of mangrove habitat by shoreline or fishery development is a great threat [7,15,21]. Preservation and conservation of mangroves is thus a worldwide point of attention, and in Nicaragua has been a high priority for the Centre for Aquatic Resources Research (CIRA) and Paso Pacifico [10,22]. Management of the estuaries containing these mangrove trees could effectively improve the situation. However, official water resources management plans have not been published in Nicaragua yet [10]. Realizing management plans for ecosystems without an understanding of hydrology, sociology or ecology is hard to say the least. Many catchments in the world are ungauged or poorly gauged and the capability to optimally integrate social, economic and ecological perspectives without the continuous information of observed data limits water management in these catchments [23]. Hydrological research on blind estuaries at the Pacific Coast has not been performed yet and the hydrological influence of these estuaries on the function and survival of mangrove forests has not been researched at all [10]. Without more knowledge about these systems, management and thus protection of the mangrove forests might not be effective, especially during such extreme circumstances caused by El Niño.

1.3 Research objective

To overcome this lack of data and understanding, the research objective is **to understand the influence of a sandbar in front of a blind estuary, on the well being of a mangrove forest during a drought**, in order to recommend management plans that can combine a healthy ecosystem with an upcoming community life.

Three different research questions have been formulated to reach this main objective:

1. Can the different geomorphologic-, biologic-, and social structures contained by the blind estuary be classified according to known classification systems? This information will provide a clear understanding of these structures and their inter-linkages, and give the possibility to apply or compare the case study to other areas with similar structures.
2. In what way does the hydrology influence the ecology and visa versa?
3. Can the salt intrusion of the blind estuary and its surrounding groundwater system be described and predicted during a drought?

By answering these questions, results of the case study can be used in a global context. These questions also induce a focus on the appearance of salt water conditions in the estuary which change due to the sandbar, and try to find other influences of the sandbar on mangrove trees.

1.4 Case study

1.4.1 Study area

The study was performed in a catchment previously studied by Dr. Heyddy Calderon [10], in which a typical example of a 'blind' estuary bordered by a mangrove forest was described, and which lies on the Pacific Coast of Nicaragua. This mangrove ecosystem can be found along the floodplain of the seasonal river Ostional. It is a small forest of approximately 0.2 km^2 , yet it provides valuable economic and ecological services in terms of habitat provision for numerous species, and flood protection and tourist attraction for the village El Ostional [10,11].

The mangrove forest forms a wetland along the Southwestern coast in the Ostional catchment that has an approximate area of 46 km^2 . The area is located in the tropical wet forest life zone [24]. The Ostional mangrove forest is particularly important to conserve, for it is home to one of the rarest trees in the country, if not the entire Pacific Coast [25]. The Ostional estuary is the most Northern estuary containing this mangrove species; the Tea Mangrove, *Pelliciera rhizophorae*, or La Piñuela in Spanish. The location of the Ostional catchment in Nicaragua, and the village El Ostional together with the estuary, the sandbar, and its mangrove forest are shown in figure 1.1.

The climate in the area of El Ostional is tropical wet and dry according to the Köppen climate classification [10, 26]. The wettest months during the rainy season of May till November are September and October. The accumulated rainfall in September and October is on average around 480 mm/season , while annually it is 1475 mm/a with a mean pan evaporation of 1976 mm/a [10]. The nearest station however, is located in Rivas, about 40 km North West from El Ostional. This station measured a mean temperature of $27.1 \text{ }^\circ\text{C}$ over the last 40 years. River discharge can vary between $0.1 \text{ m}^3/\text{s}$ in March and $13 \text{ m}^3/\text{s}$ in October [27], while in dry months the riverbed can be completely dry in the lower catchment area.

1.4.2 Fieldwork conditions

During a fieldwork period of approximately two and a half months, the study area was observed and measurements were done. The study was performed during the wettest months of the rainy season, starting from August 15 till October 30 of the year 2015. Due to the El Niño event, the usual amount of rainfall remained unseen, establishing a noteworthy dry period with only 177 mm of precipitation measured during the complete study period of 2.5 months. The riverbed became completely empty, and the sandbar continued to exist. The estuary behind the sandbar remained filled with water, although the water levels were low compared to the usual standards [10]. The floodplain and its mangrove forest did not become inundated, except for occasional over wash events due to high spring tide.

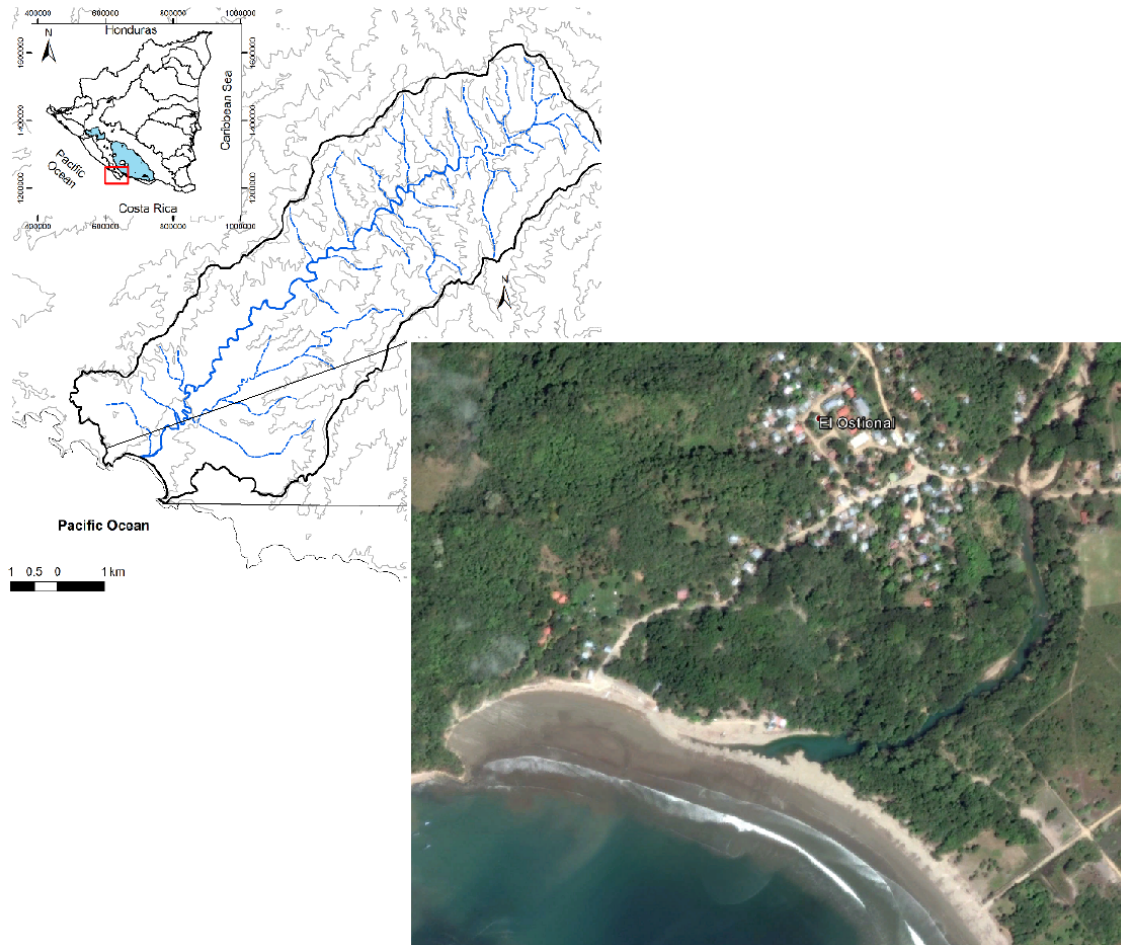


Figure 1.1: The location of the village and estuary, in the Ostional catchment, Nicaragua. Figure was edited from an official map of catchment areas [10], combined with a Google Earth image of the area in 2011 [28].

1.5 Outline of the report

This thesis is organized according to the three different research questions. Before going into those questions, first a description will be given on the research methodology, showing how and with what equipment the questions were answered. Thereafter, each question is touched upon in a different part of the report. Part I: System Analysis goes deeper into question 1. Question 2 will be answered in Part II. Part III will explain the results related to question 3. Each part introduces the subject and hereafter enters the results. Immediately an expert conceptualization of the results will be made. Following the results and conception are the conclusions for the different research questions. These conclusions are then used in Part IV, where first they will be synthesized to find if the objective of the research was achieved. This is then discussed in Chapter 2, where after recommendations on management plans will be formulated in the third chapter; Recommendations.

Chapter 2

Methodology

This chapter will set forth the methods and materials used to retrieve and analyze data. Research on this type of estuaries in Nicaragua and their relation with mangrove trees was not encountered. Neither has there been much research in El Ostional until now. This research thus mainly starts from scratch.

2.1 Data collection

During the fieldwork period of 2.5 months, observations were made, interviews were taken, and measurements were done.

2.1.1 Observations

Observing the Ostional area was especially important in order to identify and classify the different structures; geomorphology, biology and social. The main observations were thus aiming to:

- Understand and know the different stages the sand bar went through. Pictures were regularly taken from the same location and angle, in order to capture the different stages that might occur.
- Get an overview of the sediment distribution throughout the estuary and more upstream in the Ostional river.
- Determine the types of mangrove trees and other vegetation in the floodplain and surroundings.
- Determine the present fauna in the floodplain and its interaction with flora and morphology.
- Know the main uses of the floodplain by and its services for, the community.
- Understand the benefits of the estuary for the community.
- Understand human influence on the estuary and its floodplain.

2.1.2 Interviews

In the Ostional community

Interviews with the community members of El Ostional were conducted for background information and further understanding of the observations made during the fieldwork. There has been no formal

social data collection or analysis. The main informant was Mr. Salvador Manual Sanchez Santana, who owns a hostel at the beach of El Ostional and plays a key role in the village. He also grew up in El Ostional and together with Dr. Eric Olson, from Brandeis University, takes personal interest in conserving and protecting the mangrove forest. Additional interviews were conducted, mainly with community members working in the fishing-business of El Ostional.

With experts

In order to solve some of the major questions about ecological factors of mangrove trees and other herbivores, contact was sought with several experts in those fields. This resulted in a number of extensive email conversations, providing much insight information into mangrove preferences and leaf damage. For specific mangrove related questions, Dr. Jorge Jimenez was consulted, whereas Dr. Eric Olson and Dr. Edward Riley provided help concerning herbivore activity in the mangrove forest.

2.1.3 Survey

The following measurements were done in the the area of El Ostional:

1. Meteorology: precipitation, evaporation, pressure, temperature;
2. Surface water levels and aquifer water tables;
3. Salinity and temperature of the water;
4. Salinity of soil samples;
5. Seepage;
6. Inverse-auger hole tests;
7. Way points and tracks of the area;
8. Cross sections of the estuary;
9. Sap flow in a mangrove tree.

All measurement locations are depicted in figure 2.1. More information and details on the installations and materials that have been used, can be found in Appendix A.

2.2 Data analysis

The collected data was subsequently used to do a qualitative and quantitative analysis on the blind estuary and its mangrove trees. Each different research question, tackled in a different part of the report, used a combination of the data types collected in the field. In Part I only the observations and interviews are used to answer the question. The second question is answered in Part II with the use of observations, expert knowledge on ecology, and measurements on water and salinity levels. The third Part answers the question by using solely the conducted measurements.

2.2.1 Qualification

The information obtained with observations and interviews was subjected to observational analysis, where literature is combined with knowledge gained on the area. This was then used to either classify structures with known classification system, or to originate new hypotheses. Classification systems are structured organizers used to determine groups based on similar characteristics [29].

When structures are thus classified, one can compare it to other structures throughout the world, and more generic conclusions can be formulated. These new hypotheses are proposed to explain phenomena that cannot satisfactorily be explained with the available scientific theories.

2.2.2 Quantification

The survey measurements were first recalculated to retrieve applicable data:

- Precipitation and evaporation measurements were conducted with self made instruments and thus were measured in mL and then transferred to mm per day.
- Surface water levels and aquifer water tables were measured relative to the (floodplain) soil surface (b.s.s.). Due to the lack on elevation data, the soil surface was assumed to have equal elevation height anywhere in the floodplain. Although this is not the case, it gives the possibility to compare the separately measured values.
- Salinity was measured in Electrical Conductivity (EC) and thus for several applications needed to be converted into total dissolved solids (TDS).
- Seepage measurements were converted into infiltration and ex-filtration rates.
- Inverse-auger hole tests were converted with the inverse-auger hole method of Kessler and Oosterbaan [30] to retrieve permeability values of the soil.
- Sap flow measurements were converted into sap flow velocities.

An explanation of the methods used for these calculations can be found in Appendix B. The resulting applicable data is documented in Appendix C. Sap flow measurements unfortunately did not result in accessible data. The sap flow measurement data is included in Appendix C, for perhaps it may be pertinent for other researchers.

In part III further analysis of certain measurements have been performed in order to describe salt intrusion patterns. The 1-D analytical salt intrusion model for alluvial estuaries, developed by Savenije [31], is tested on the blind estuary in El Ostional. Further, the Ghyben-Herzberg relation [32] is used to estimate the depth of the fresh-salt water interface in the coast subsurface. These methods of analysis are further exploited in Appendix B. Complete results of this analysis can be found in Appendix C.

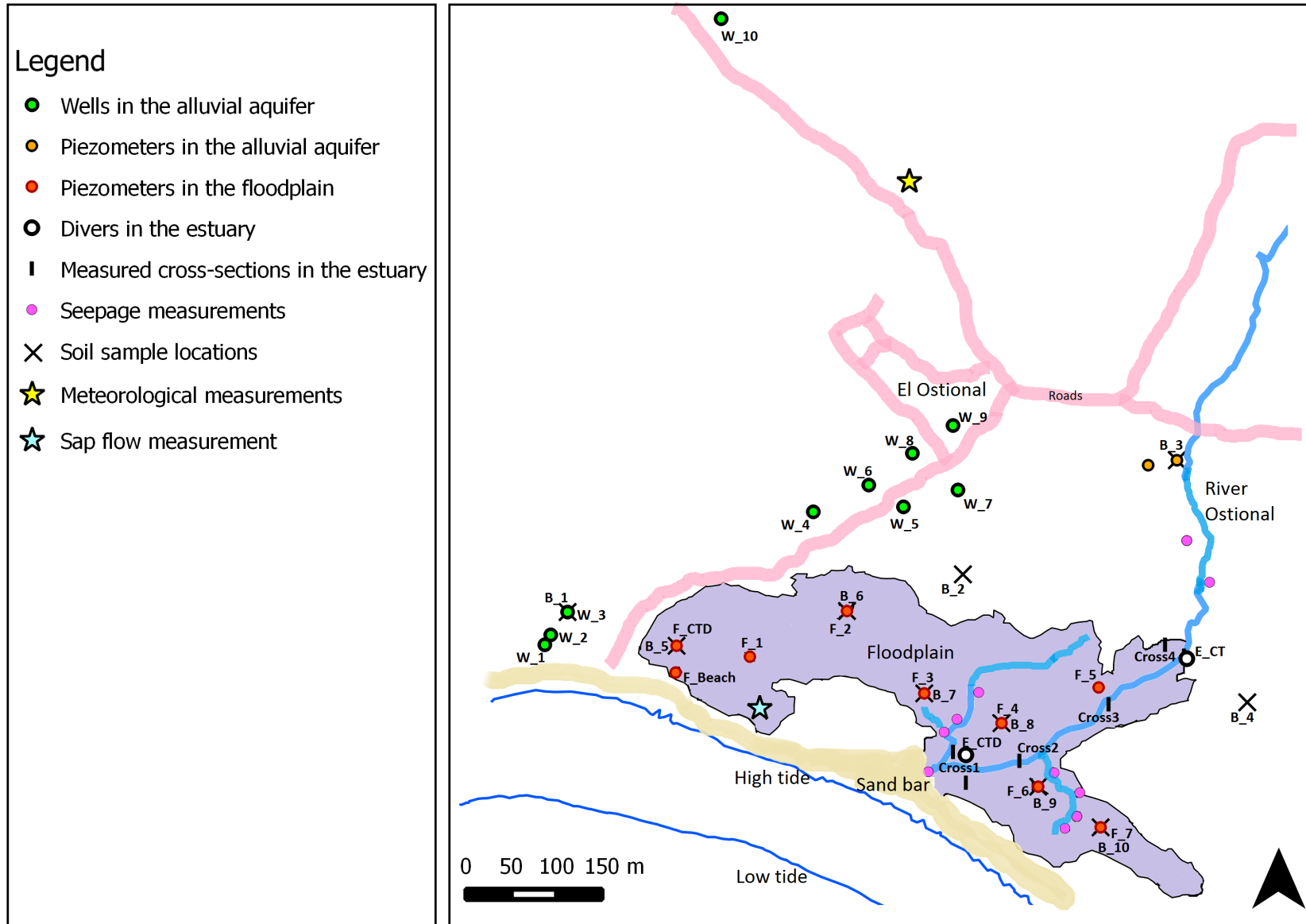


Figure 2.1: Locations of the different measurements in the study area.

Part I

System analysis

Chapter 1

Introduction

The objective in this part of the report, is to find an answer to the following question: *Can the different geomorphologic-, biologic-, and social structures contained by the blind estuary be classified according to known classification systems?* This information will provide a clear understanding of these structures and their inter-linkages, and give the possibility to apply or compare the case study to other areas with similar structures.

During the study period of Dr. Heyddy Calderon [10], the sandbar prevented direct surface connection between the mangrove forest and the sea; thus allowing surface water storage as backwater in the estuary and creating a temporal reservoir controlling in- and outflows. Accumulation of water of the river Ostional takes place into the floodplains, where the mangroves grow, and the estuary, both adjacent to the town El Ostional. According to the National System of Disaster Prevention the town is prone to flooding during high precipitation season, September till October [33]. Sudden release of water occurs when accumulated water causes rupture of the sandbar due to a larger precipitation event. If such a larger event does not occur, flooding of the area prompts the local community to remove the sandbar manually [10]. The three structures seem to influence each other, and by classifying the separate structures, these inter-linkages can be formulated.

A schematic overview of the Ostional estuary can be seen in figure 1.1. The numbered parts will be described in the following chapter, where the results from observations and interviews will be set forth per structure.

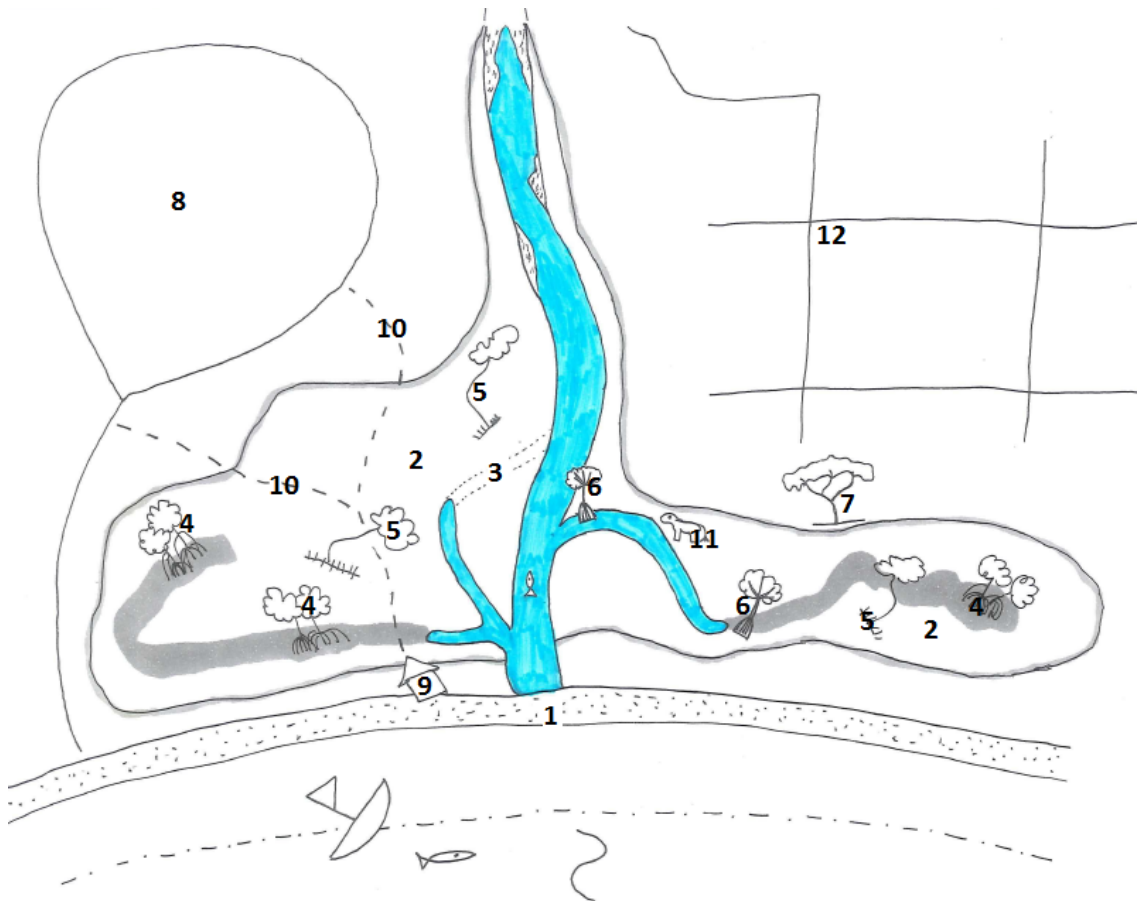


Figure 1.1: Schematic overview of the Ostional estuary, showing the key items: (1) the sandbar, (2) the floodplain, (3) a former estuary branch, (4 - 7) examples of locations for Red, White, Tea, and Buttonwood mangrove trees, (8) El Ostional, (9) the fishing cooperation, (10) trails, (11) watering areas for livestock, and (12) cleared land.

Chapter 2

Results and conceptualization

2.1 Geomorphologic structure

Geomorphology is generally defined as the study of landforms and their formation. In this section the landforms of the Ostional area will be described and thereafter classified.

Estuaries containing a barrier which closes off the estuary partly or completely, and temporarily or permanently, are a result of the Glacio-eustatic sea level rise of about 6000-8000 years ago, which flooded the old riverbeds [8, 34]. The river valley was flooded and quickly formed a sandy barrier separating the estuary coastal body of water. The estuaries thereafter went through different stages of Holocene evolution, as a result of sediment input by the contributing river and landward reworking of sand by wave and tidal processes [8, 35]. After years of progressive infill of the muddy estuarine embayment, the river becomes channelised through wetlands, leaving the estuary in the state it is now; a blind estuary.

In a regional study of Krasny and Hecht [36], the area of Ostional is stated to contain the sedimentary Brito formation. The composition of this formation is mainly volcanic breccias, tuffs, shales and limestones. In the lower catchment a wide alluvial valley is found, forming an alluvial aquifer on top of the shale layer. On top of the alluvium near the river banks, a 3 meter thick discontinuous clay layer was observed by Calderon [10].

2.1.1 The sandbar

The forming and rupture of the sandbar is caused by two different forces. The amount of rain and therefore the amount of discharge produced by the river is the first force, the second being the wave and tidal impact. The bars are formed by an amount of sand, gravel, and pebbles, thrown back by sea into the mouth of the estuary. The moment the river discharge is high, and the pressure behind the sandbar increases due to an accumulation of water, the sandbar ruptures [10]. When the rainy season ends, the discharge slowly decreases and the forcing caused by wave action takes the overhand, causing the bar to close again. This creates four different stages during an average year in the estuary, repeating itself the following year:

1. Rain; discharge; closed sandbar; inundation of fresh water in the floodplain.
2. Rain; high discharge; open sandbar; inundation of fresh and salt water.
3. No rain; low discharge; open sandbar; inundation of mostly salt water.
4. No rain; no discharge; closed sandbar; no inundation, water evaporates.

The above cycle was described by the inhabitants of the Ostional community as an average year. During drought however, the first two stages do not occur, and stage 4 continues. An exception is to be made throughout stage 4, when either inundation occurs due to (a) over-wash during high spring tide, or (b) a high precipitation event. This induces inundation of either salt water, or fresh water.

There is a clear longitudinal sequence from the estuary mouth where in particular fine sand can be found, to the top of the bar, where mostly pebbles lie. The sea beach is again formed by fine sand. This perfect sequence is proof for the formation of a wave-induced sandbar. The energy necessary to move pebbles is highest, and when losing this energy at the top of the bar, the pebbles are deposited. The washing sea water that over-flows the top, transports less heavy material, and loses this material according to weight, again due to a loss of energy on its way to the estuary mouth. The gravel and pebbles show clear similarities with the gravel, pebbles and stones found in the river bed upstream of the estuary. See figure 2.1 to compare. This is confirmed by Jimenez [8], who claims that the bars are formed due to the accumulation of terrigenous material found in the area. This material is either deposited there by direct discharge of the river, or has been transported by currents arising along the coast from other river depositions.

2.1.2 Floodplain

Behind the sandbar, the estuary stretches out in upstream direction, with several small branches and one main channel. Around the estuary, a low elevation plain can be found, also visible in figure 1.1, number 2. In the above mentioned stages 1, 2, and 3, this plain is partly or completely flooded, depending on the amount of inundation. From now on, this plain will therefore be referred to as the floodplain. The floodplain consists mainly of red clay mixed with some silt. There is however a layer at a depth of around 70 to 80 cm that is mainly formed by brown clay with a picric smell, very humid, and containing much iron. This layer is highly impermeable and seems to confine an aquifer below consisting of gray material; fine sandy clay combined with organic material containing abundant gas, methane and sulfide. During the research period the soil became moist at a depth of approximately 45 cm, and there was indeed water found in the floodplain aquifer.

Sediment transport

The occurrence of this clay layer was already mentioned by Calderon [10], and in all probability has its origin in the sediments from the upstream catchment, transported by the river, and captured by the sandbar. Through erosion in the upstream catchment, the water transports sediments. Slowly, these sediments are dropped in the alluvial valley when energy is lost during a slope decrease. The water remains flowing down into the direction of sea, containing only fine suspended sediments, mostly clay. During the accumulation of water in front of the sandbar, and before it ruptures, there is enough retention time in the floodplain and estuary for the suspended sediments to settle.

As the upstream part of the river can be highly erosive during flood flows, the abundance of the coarse-grained bed deposits like the former mentioned pebbles and stones are its result. Figure 2.1 shows examples of evidence for this erosion, also found previously by Rains [12]. In the same figure, evidence of a high rate of sedimentation that can occur in the floodplain in only 25 years, is shown. According to Mr. Salvador Sanchez, he and his friends could still dive into the river from this tree, which hung over the former estuary branch, see also figure 1.1, item number 3, for the location of this former branch.



Figure 2.1: The sediments found, in the front and top of the sandbar (top figure), in the upstream river catchment (lower three left figures), and the tree trapped in sediment which 25 years ago hung above an estuary branch (lower right figure).

2.1.3 Estuary classification

During the research period, the semi-diurnal tide could range from 1.5 to 3 meters. The 3 meter tidal difference was devised by an extreme high spring tide, only occurring in October and March in this area, and the average tidal range is thus taken to be 2 *m* and less. This is a limited tidal amplitude, creating a micro-tidal estuary [8,37]. Micro-tidal estuarine processes are dominated by both the upland discharge and the wave and storm action from the sea [37].

Especially without the upland discharge, this estuary falls into the category of a typical wave-dominated estuary [38]. Waves are the main force forming the sandbar, where the bar again prevents most of the wave energy from entering the estuary [8,38]. Within most wave-dominated estuaries, a clearly-defined, coarse-fine-course distribution of lithofacies is produced. In the Optional estuary, this distribution is also clearly visible, as was already described and can be seen in figure 2.2. In the figure, the energy distribution in the estuary is also shown, what induces the morphological shape.

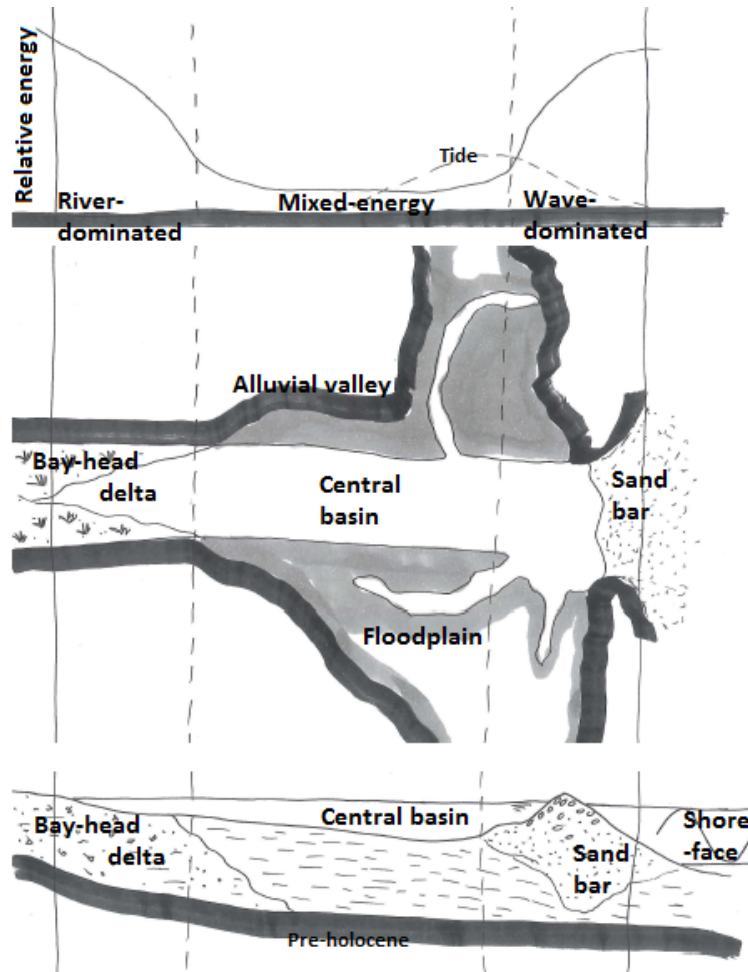


Figure 2.2: Distribution of energy (top sketch), morphological components in a plan view (middle sketch), and distribution of sedimentary facies in a longitudinal section (bottom sketch), within the Ostional estuary. Based on observations and an idealized wave-dominated estuary of Dalrymple [38].

2.2 Biologic structure

Biology can be defined as the study of living things - biota, organisms - and their vital processes in order to survive. The most important present flora and fauna in the Ostional estuary, and its vital processes, will be described, and a forest classification will be made.

2.2.1 Present flora and fauna

The occurrence of the sandbar causes the formation of a shallow floodplain towards inland. It is in this environment where extensive mangrove areas are located in Ostional, as in all of Central America [8].

Mangrove trees

The Ostional floodplain contains the following four types of mangrove trees [8], which can also be seen in figure 2.3:

- The Red mangrove; *Rhizophora racemosa* and *Rhizophora mangle*
- The White mangrove; *Laguncularia racemosa*
- The Tea Mangrove, better known as La Piñuela; *Pelliciera rhizophorae*
- And, the Buttonwood; *Conocarpus erecta*



Figure 2.3: The different mangrove trees and their seeds, in the Ostional floodplain: The Tea mangrove (left top figure), the Red Mangrove (middle top figure), the Buttonwood (right top figure), and the White mangrove (bottom figure).

The Red mangrove is easily distinguished from other species by its tangled prop roots, originating from trunk and branches, extending one meter or more above the soil surface. The roots increase stability of, and supply oxygen for the tree [8,39]. Under optimal conditions, this mangrove tree can grow to heights of over 25 m, which indeed were occasionally observed in the Ostional floodplain. Reproductive adaptations enable seedlings to germinate while still attached to the parent tree. Seeds sprout into 15 cm pencil-shaped propagules. Seed germination while still attached to the tree gives this mangrove a higher chance of survival. When the seedling falls into the water, it may either take root alongside its parent or be carried by the tides and currents to other suitable habitat.

The White mangrove is less easy distinguished, and sometimes does not have visible aerial roots. However, like in the Ostional floodplain, when this mangrove tree is found in oxygen-depleted

sediments or flooded for extended periods of time, it often develops peg roots [8, 39]. This small tree grows rapidly in rich soils to heights of 15 *m*. White mangroves produce small propagules, usually less than 0.5 *cm*.

The Tea Mangrove is one of the rarest mangrove trees existing, and endangered [8, 40]. The rib-like buttress roots have several functions. The most essential reasons are to provide stability and oxygen, with the help of pores called lenticels that cover the buttresses. The ribbed fruit of the Tea mangrove, about 10 *cm* in diameter, contains the already very well developed sprout, which can be a couple of centimeters long.

Literature differs in its opinion if the Buttonwood tree is to be mangrove or mangrove-fringe flora. In this research however, it is assumed to be one of the mangrove trees. This plant does not reproduce via propagules, but instead produces seed cases [8, 39]. Furthermore, the tree does not have any special aerial roots.

Mangrove-fringing vegetation

Next to these mangrove trees, the floodplain and surroundings are mainly occupied by Manchineel, Jicaro, and Neem trees. In the floodplain almost no undergrowth is found. The Manchineel tree, *Hippomane mancinella*, is native to tropical southern North America and northern South America. In present-day Spanish, the tree is called "Manzanilla de la muerte", "little apple of death". This refers to the fact that Manchineel is one of the most poisonous trees in the world and its fruit and leaves resemble an apple tree [41]. The tree grows in coastal areas, on sandy soils of high salt concentration, and with occasional inundation. The Jicaro, *Crescentia alata*, is a kind of tree that grows in the dry tropical forest areas in the Pacific region [42]. Its uses are varied, especially for its rounded fruit. Although the tree has a high drought tolerance, it can withstand periodic flooding during the rainy season. It is known to have a medium salt tolerance. The Neem tree, *Azadirachta indica*, is native to India and the Indian subcontinent. It typically grows in tropical and semi-tropical regions [43]. The tree has been brought to Central America mainly for its use as a key ingredient for a natural repellent. Neem is also a fast-growing tree, and is now mainly seen as a weed. The tree grows in many different types of soil, but it thrives best on well drained deep and sandy soils. Also the Neem tree is tolerant against slightly salt groundwater.

Animal population

Fauna in the Ostional estuary is diverse and beautiful; some examples can be seen in figure 2.4. In particular birds living in the estuary, like the Roseate spoonbill, *Ajaia ajaja* [8], are valued highly for their beauty. The estuary water is filled with fish and the trees are inhabited by the Howler monkey.



Figure 2.4: Fauna in the Ostional estuary. The Roseate spoonbill (left figure), the Howler monkey (middle figure), and the crab inhabitants, one of them the Mouthless crab (top right figure).

Going into the Ostional floodplains, especially crabs are in abundance and always visible. There are two crab species, of which one is the Mouthless crab, *Cardisoma crassum* [44], which is known to live in tropical forests along the Pacific Ocean. Unlike others, this crab is not able to stay submerged in

water for long periods of time [45]. As a terrestrial crab it lives in J-shaped burrows which are one or two meters deep. It burrows in drier soils within mangrove forests and in transition areas of humid or dry forest, with the only requirement that it needs a brackish source nearby. The Mouthless crab helps conserve the mangrove ecosystem, by for example accelerating the decomposition of organic matter during feeding and hence working as a catalyst, or by regenerating the wetland plant community [46–50]. Crabs furthermore are known to pronounce sediment properties and biochemical processes by enhancing porosity and water flow through the sediment [46–50], hence increasing infiltration and drainage.

2.2.2 Spatial distribution of the mangrove species

Mangrove forests often show marked zonation patterns that are correlated with a number of factors; salinity gradients, site elevation, soil type and chemistry, and nutrient availability [10, 35, 51–53]. Thus, by combining the knowledge on the preferences of specific mangrove species with the zonation patterns observed, information can be gained on the relative factors - resources, regulators and hydro period - controlling mangrove growth in the estuary, now and in the future [13].

Figure 1.1 shows the location of the four different mangrove species in the floodplain, items number 4 till 7. The Red mangrove species tend to grow in groups of trees, never standing alone. These trees are found mainly in the areas of the floodplain with the lowest elevation, marked in gray. The White mangroves on the other hand, grow scattered and separate of each other. They fill the complete floodplain, not showing a clear preference for any location other than their absence outside the floodplain border. The Buttonwood tree conversely only prefers to grow on the floodplain borders, fringing the mangroves, or growing on small elevated mounds in the floodplain. For the Tea mangrove, the pattern is a little less clear, since also in this estuary there is a relative small amount of them. This mangrove has a predilection for places boarding the estuary waters, but can also be found in the lower elevations of the floodplain. Still, they are mostly found on the left side of the estuary (the left side when looking in downstream direction of the river).

Site elevations mainly influence the duration and height of inundation. Inundation can be with fresh, brackish or salt water. Inundation can be due to the tide and/or discharge, creating certain turbulence in the water. Considering the relative low elevation of the floodplain, inundation must be the prime reason for the zonation pattern of the mangroves [52]. Inundation influences the oxygen availability for the roots of the mangrove tree, the stability of the tree, the distribution of the propagules, and the availability of fresh and salt water. Every mangrove species manages the oxygen supply, the size of the propagules and the tolerance for salt differently. The manner of adaptation that mangrove trees have to inundated circumstances is mostly why they predominate coastal areas, and why they outweigh other trees in the floodplain.

Mangrove roots

Respiration is an essential process in all plants. During the day, the necessary oxygen for this is produced by photosynthesis through the leaves. However, during the night the lack of light stops photosynthesis and roots absorb the oxygen through lenticels. That is, when roots stay in contact with the air. Normal roots can absorb the oxygen from air in the soil pore space. However, the roots of mangrove trees are often inundated, and thus in anoxic conditions. For this reason mangrove trees have developed three different root systems, which are shown in figure 2.5, in order to respire [8]. All three types of root systems are present in the Ostional estuary, providing oxygen during inundation for the Red mangrove (*Rhizophora*), White mangrove (*Avicennia*) and Tea mangrove (*Pelliciera*). Only the Buttonwood lacks this adaptation, explaining why it cannot survive in the floodplain and only grows at its borders or on the elevated mounds.

Root adaptations of mangrove trees also increase stability of mangrove trees in the soft sediments along shorelines, especially since their root systems are very shallow - almost all of the root system is in the first 50 cm of the soil - [8, 54–56], and they need a higher stability due to turbulent waters. Figure 2.5 shows this function for all three species. It might even be hypothesized that

the thin prop roots of a young *Rhizophora* have a higher stability when they can intertwine with their families' roots, what could explain why the Red mangroves prefer to group together.

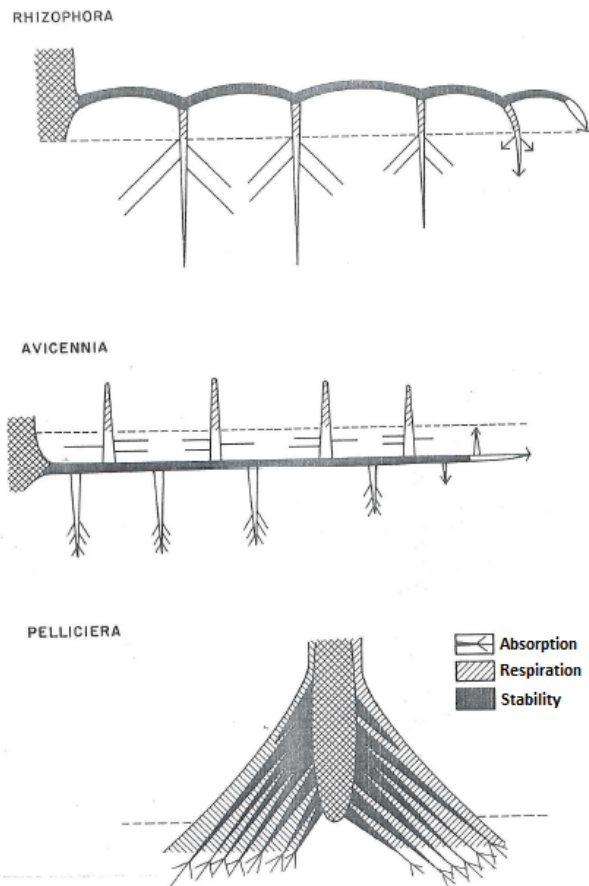


Figure 2.5: Main components in the root systems of the mangroves. All roots of the species *Rhizophora*, *Avicennia*, and *Pelliciera* consists of the components absorption, ventilation and stability. The figure has been adapted from Jimenez [8].

Propagules

The size of each trees' propagules influences the possibilities for transportation and germination. When the inundation height is low and/or the inundation duration is short, transportation is more difficult for bigger propagules than for smaller ones [53]. Since the propagules of the White mangrove are especially small and light, they are more easy distributed over the floodplain and can already germinate with very low inundation heights. On the other hand, the Tea mangroves propagule is heavy and big, decreasing transportation possibilities dramatically. And while the Red Mangrove's propagules are not heavy and can be transported relatively easy, they are long and need higher inundation in order to stand straight and germinate. This explains the high distribution of the White mangroves all over the floodplain, the Red mangroves' liking for lower elevations and the occurrence of the Tea mangrove near the estuary waters [8, 9, 13, 53].

Salinity tolerance

The ranges of pore salinity tolerance for each species [8] are listed here. These amounts can be compared to an average sea salinity of around 35 (kg/m^3) or an electrical conductivity (EC) of approximately 50 mS/cm .

- Red mangrove: 0 - 65 kg/m^3 , or 0 - 93 mS/cm
- White mangrove: 0 - 90 kg/m^3 , or 0 - 129 mS/cm
- Tea mangrove: 0 - 37 kg/m^3 , or 0 - 53 mS/cm
- And, Buttonwood: 0 - 90 kg/m^3 , or 0 - 129 mS/cm

Striking is the low salinity tolerance of the Tea mangrove. The existence of the Tea Mangrove in the Ostional estuary indicates in this way that salinities, at least in the estuary waters, are lower than 37 kg/m^3 . In order for such saline conditions to occur, there must be fresh water seepage into this estuary during the dry season, creating a low salinity mangrove site [54].

2.2.3 Forest classification

Several classification methods are found in mangrove literature, of which the comprehensive eco-geomorphological classification scheme of Woodroffe [35, 52] is used here. First, the geomorphological estuary classification is used as a starting point since in many cases, mangroves respond opportunistically to the geomorphological habitats that are available, adjusting to morphodynamic changes in the landforms. In the previous section, the estuary was classified as a wave-dominated, blind estuary. Due to the sandbar in this estuary, the mangroves, which occur in the back-barrier settings, are protected from direct wave action.

The Woodroffe classification divides the mangrove habitats in terms of relative dominance of river, tidal or interior processes [35]. Combining that knowledge, the closed sandbar creates an interior mangrove forest; a sink for organic matter, nutrients and sediment. During the rainy season though, when the sandbar is ruptured and riverine discharge is high, the forest becomes river-dominated; where sediments are deposited from the river, and organic production, enhanced by the freshwater, can be exported with the flow. Once in a while, in extreme circumstances, high spring tide creates over-wash events, creating an over-wash mangrove forest, dominated by the tides. This happens only twice a year and is thus not the dominating setting. That the Ostional mangrove forest can be both an interior and a river-dominated mangrove forest, was already confirmed by Rains [12].

2.3 Social structure

Human social organization in El Ostional, and especially its impact on the mangrove forest, floodplain, estuary and sand bar, has been analyzed and classified accordingly.

2.3.1 The Ostional community

The community of El Ostional exists for already three generations, and is on the map since at least 1970 [57]. Notable are the common surnames, showing a big family community, where most people know each other as niece, nephew, aunt, uncle, or cousin. Living in the area is only possible due to the groundwater availability, since river discharge is seasonal and other fresh water sources are too far away. Ostional therefore contains many old shallow excavated wells, which are mainly unused because lately a communal drilled well provides the necessary water with the use of a pump. For their sewage water the inhabitants of Ostional combine the use of septic tanks for toilet and shower wastewater, with a direct outflow into the environment for gray water [10, 12]. Most cooking is done with gas tanks, using firewood only when their gas provisions are temporarily depleted. This firewood is made from a variety of trees, including mangrove trees. Mainly dead tree branches are cut down, resulting in several tree branch stumps found in the mangrove forest, see figure 2.6. Garbage is collected with waste trucks, and then brought to a dump where it is processed. Old habits are difficult to forget; heaps of trash are still burned at the side of the road, or can be found back on the fringes of the mangrove forest.

2.3.2 Fishing Cooperative

The most interesting for the people of El Ostional concerning the estuary is that it is rich in fish. In the community, a fishing cooperative has been started some years ago between all separately working fisherman. The fishery is collected and sold and its haul distributed equally. With this, a bad day of fishing is compensated and insecurities in income are diminished. This fishing cooperative has made the fishing business in El Ostional expeditious.

The fishermen of El Ostional know that the rich estuarine fish production provides them with opportunities to catch fish for a living. This is confirmed by a number of studies, which show that estuarine and coastal systems are important fishery regions, and it is clear that estuaries are responsible for a proportionally large part of the fish yield [35]. During the fieldwork period, the fishermen tried to excavate a channel through the sandbar during a week with promising rainfall, in order to induce a manual rupture, see figure 2.6. They noticed a reduced fishing possibility that year due to the remaining drought. Unfortunately this did not work out, since water levels in the estuary were not high enough to make the connection viable and the rain did not last. In normal years, the sandbar would rupture and through the connection between estuary and sea, fishes move in and out. This should create an easy way for a high catch every year.

2.3.3 Inundated floodplain

According to the fishermen there were other reasons to manually dig a trench through the sandbar. When the estuary water levels increase, the floodplain inundates.

Trails

Inundation decreases the possibility to use the paths through the floodplain, which are depicted in figure 1.1 with item number 10. These paths are shortcuts, decreasing the distance from the village to the fishing cooperation by about half. They are, when dry, extensively used. Other trails are created by the communities livestock; mainly cows and horses. They are herded towards the estuary for its constant offer of water. At several places pastoral signs can be detected, like for example fenced areas which are now broken or incomplete and obviously not used anymore. Another example are the cow pies lying at specific water points, and which are decomposed by the small crab inhabitants of the floodplain, see figure 2.6.

While the trails are used by the community and livestock in a practical way, the occasional tourist visiting Ostional also uses the trails to walk around and enjoy themselves. During inundation, these tourists cannot use the trails either. In order to solve this, there are plans to construct elevated ramps through the floodplain that can be used as a walkway [58].

Cleared land

Fringing the floodplain on the left side of the estuary, some land has been cleared of its natural growth, and changes to drainage of the area have been made. This area is depicted in figure 1.1 with item number 12. These changes include elevated roads acting as levees that direct flow on a grid, and dug trenches throughout the lowland draining and reducing water levels [12]. The land has been cleared for agriculture, but seems to be forgotten and abandoned. According to several inhabitants, the area used to be prone to flooding, explaining the elevated roads and constructed ditches. In former times, this area might have looked more like the outskirts of the floodplain, inhabited by the land crabs, but experiencing a less frequent inundation.

Crab burrows

Inundation further increases nuisance from mosquitoes in the village, which then increases chances for mosquito borne diseases. Villagers tell that these mosquitoes propagate by laying eggs in the crab burrows when water levels in the burrows are high enough. This is confirmed by literature, where sand flies and mosquitoes are said to use land crab burrows as their breeding sites [59].



Figure 2.6: Noticeable human influences into the estuary of El Ostional. The top left figure shows the excavated trench, whereas the bottom left figure depicts a tree stump. The two right figures show the livestock and its manure, used by the crab as energy supply.

2.3.4 Human impact classification

A generic classification scheme defined by Day et al. [60] organizes the human impacts into four general categories; (1) enrichment, (2) physical alterations, (3) introduction of toxic materials, and (4) harvest or introduction of exotic species. At least three of these categories can be detected.

An amount of untreated waste water disposed by El Ostional flows into the mangrove forest and estuary, which is high in nutrients. This enrichment - 1 - is an addition of naturally occurring substances, and can lead to changes in the structure and metabolism of the ecosystem [60]. Unclear is what the effect of this change is, since when excessive it could have a negative impact, but when retained, the nutrients enrichment might increase mangrove productiveness [10–12]. Digging trenches in the sandbar and the floodplain fringing lowlands, are clear examples of physical alterations - 2. According to Rains [12], draining the lowlands leads to higher erosion and loss of nutrients in that area. For sure the trash dumped in the floodplain and mainly at the sides of the village, introduce toxic materials - 3 - into the area. Especially during inundation of the area, when plastics and metals are transported into the estuary and possibly the sea waters, this is problematic. Although livestock may be considered as a new species, this is hardly meant by Day et al. when they talk about harvest or introduction of exotic species. Until now, the exploitation of, or overfishing in the estuary, has not been done yet.

Considering these categories, it can be seen that Day et al. [60] define human impacts as stresses for the coastal system. Inasmuch as this might be true, human impacts seem to be able to have a positive impact on the ecological system as well. Examples are the manure of cows, which

benefit the crab community, or the possibly increased mangrove productiveness due to nutrients enrichment.

Chapter 3

Conclusions

The answer to the question *if the different geomorphologic-, biologic-, and social structures contained by the blind estuary be classified according to known classification systems*, is yes. A clear understanding of these structures and their inter-linkages was provided, making it possible to apply or compare the case study to other areas with similar structures.

The two main landforms contained by the Ostional estuary are the sandbar and the back-barrier floodplain behind it. The sandbar is mainly formed by the strength and sediment transport of seasonal river discharge, and wave and tidal impact. The seasonality of the river creates a dynamic estuary with four different stages. The study was performed during stage 4, when there was no rain, no discharge, a closed sand bar and no inundation. The sand and gravel forming the sandbar is transported by the river into the sea and thrown back by wave action. Behind the sandbar, the floodplain, a low elevation plain, consists mainly of silty clay. At an approximate depth of 75 cm, a confining layer of pure clay seals an aquifer of organic matter and clay. This floodplain exists in order to intercept the accumulation of water when the sandbar is closed and a river discharge exists. During that time, clay particles settle in the floodplain. With an average tidal range of 2 m or less, this micro-tidal estuary can be classified as a wave-dominated estuary, especially when river discharge fails.

In the floodplain a mangrove forest can be found, consisting of the Red mangrove - *Rhizophora racemosa* and *Rhizophora mangle* -, the White mangrove - *Laguncularia racemosa*, the Tea Mangrove - *Pelliciera rhizophorae*, and the Buttonwood - *Conocarpus erecta*. Surrounding these mangrove trees are Manchineel, Jicaro, and Neem trees. The mangrove forest and estuary are inhabited by several bird types, Howler monkeys and a huge amount of crabs, of which the Mouthless crab is especially abundant. The spatial distribution of the different mangrove trees can be attributed predominantly to inundation height and duration, for which the trees have adaptations in root systems for stability and oxygen acquirement, seed type, and salinity tolerance. The salinity tolerance of the Tea mangrove in particular shows that this estuary contains a low salinity mangrove site which can only be possible if there are seepage flows during the dry season. Using the Woodroffe classification for mangrove habitats, this mangrove forest is both an interior mangrove forest when the sandbar is closed, as well as a river-dominated forest during open sandbar conditions.

The Ostional village can exist mainly due to groundwater availability, which is used to provide for the necessary fresh water. The inhabitants of Ostional dispose waste water through septic tanks, or directly, into the environment. Cooking is done with gas and firewood, which can be mangrove wood. Garbage is collected, but also still disposed on the edges of the mangrove forest. Main interest of the estuary for the community is its fishing possibilities, which sometimes induces them to help nature by manually opening the sandbar. Another reason for the community to open the sandbar is their dislike for an inundated floodplain, because their shortcuts through the floodplain are barred, and the inundation increases mosquito nuisance. All in all, the impact of the Ostional community onto the estuary can be categorized into enrichment by wastewater release, physical alterations of the sandbar, and the introduction of toxic material by trash disposal.

The following inter-linkages were designated between the different structures:

- The interior mangrove forest exists thanks to the combined forces of sandbar and floodplain, which provide a protected environment where the mangroves have the upper hand on other trees.
- The existence of a Tea mangrove in this estuary seems to be mainly possible due to the combined forces of the sandbar which keeps out too high salinity levels and a possible fresh water seepage flow into the estuary.
- Crabs help conserve the mangrove ecosystem, and there were reasons to believe that the livestock manure benefits the crab community in turn.
- Manual rupture of the sandbar is beneficial in many ways for the community of El Ostional. Impacts of this during drought on the functioning of the mangrove trees are yet unknown.

Part II

Symbiosis between hydrology and ecology

Chapter 1

Introduction

An answer to the following question will be obtained in this report part: *In what way does the hydrology influence the ecology and visa versa?*

Hydrology is the science that describes the occurrence of water on our planet and the processes that drive the circulation of the water between different stocks and locations where the water resides. Ecology on the other hand is the study of the relationships between organisms and their environment, where the environment can be defined as factors that affect organisms. These factors can be abiotic, biotic, or anthropogenic. Hydrology is a physical element in an ecosystem, hence an abiotic factor. So actually ecology already holds the study of the relationships between organisms and hydrology. What needs to be known, is how this hydrological factor influences the organisms, in particular the mangrove trees in El Ostional. This also holds the other way round; would there be ecological factors driving the movement of the water between different locations, this could effect the mangrove population.

In the previous part, the System Analysis, factors that will be discussed in this part, were already introduced. It was concluded that the spatial distribution of the different mangrove trees could be attributed to inundation. Combining that knowledge with the occurring drought, the dependency for a high amount of water will be further explored. The Mouthless crab was mentioned to help conserve the mangrove ecosystem by accelerating the decomposition of organic matter. Now, we will look more closely into other ways the crab works to the benefit of the mangrove trees. And finally, it was hypothesized that a fresh water seepage flows into the estuary, even during drought, which would explain the existence of the Tea mangrove in this estuary. The inflow and outflow in the estuary will therefore be analyzed to proof the hypothesis.

Chapter 2

Results and conceptualization

2.1 Water shortage

Plants need oxygen in order to convert sugars into energy. During this process, called respiration, carbon dioxide and water are produced. The sugars plants use for this process, are made using photosynthesis, were they again release oxygen, and need carbon dioxide, sunlight and water. These two processes are basically its reverse, except that the sunlight is now converted into energy the plant can use. The needed oxygen and water are taken up by the roots of a plant, out of the pores in the soil, which are either filled with water, oxygen, or both. When the pores are completely filled with water during for example inundation, no oxygen is available. And vice versa, during drought pores are filled with oxygen, and no water is available. Plants thus need an equilibrium, not too much water, not too little. Mangrove trees however, have adapted in such a way that water levels can be higher than the soil surface, by expanding their roots into the air. Since mangrove trees are, on average, standing in soil which is fully saturated, these anoxic conditions and its associated toxics prevent mangrove trees to reach high depths [54]. Almost all of the root system is in the first 50 *cm* of the soil, and most of it is even in the top 20 *cm*.

During the fieldwork period, inundation of the area almost did not occur, except for three small periods of a couple of days due to over-wash or precipitation events. Over-wash events occurred around September 2nd, September 29, and October 28, and the precipitation event had its peak at October 16, which are displayed in figure 2.1. It goes further than the absence of inundation though, since the water table in the floodplain could drop to 100 *cm* below surface level for several weeks. Figure 2.1 shows the manually measured water table depths below the soil surface.

2.1.1 The need for inundation

Before and after the small periods of inundation, seedlings of different trees were observed, see figure 2.2. After inundation, these were germinated mangrove propagules. Already before the inundation however, these were Neem seedlings.

Propagules are out of time

At the end of August, many of the mangrove trees started to loose their fruit. This was in accordance with the observations made by Jimenez [61] in Costa Rica, and happened in the middle of a normal rainy season. The release of propagules occurs then when flooding levels in the floodplain are at their max; August till October. The timing of the propagule crop is very important for the establishment of the seedling; flooding or inundation after all, would assure proper propagule dispersal, and would ensure fast establishment of the seedling [61]. A fast establishment would ensure a deeper root system and thus a better chance to withstand the upcoming dry season.

Now however, there had been no rain at all in the past months, and the peak of the rainy season also failed to appear. Due to the small periods of inundation, some propagules finally managed to germinate. However, possibilities of establishing enough of their root systems was not high. Although the site was not observed any more after the end of October, the usual dry period started again, and thus the new seedlings will need to survive at least until next April. The drought now, will also influence future reproductive events. Jimenez found that flowering was found to be regulated by water stress, suggesting a necessity of high soil moisture levels in the forest prior to the development of flowers, which would be somewhere during the dry season [61]. Since this dry season started with unusual low soil moisture levels, it will probably result in extremely low and restricted flowering activities. Yet, possibilities are not depleted; mangrove propagules are viviparous and once independent of the mother tree can withstand dry conditions and can remain unrooted for long periods [18].

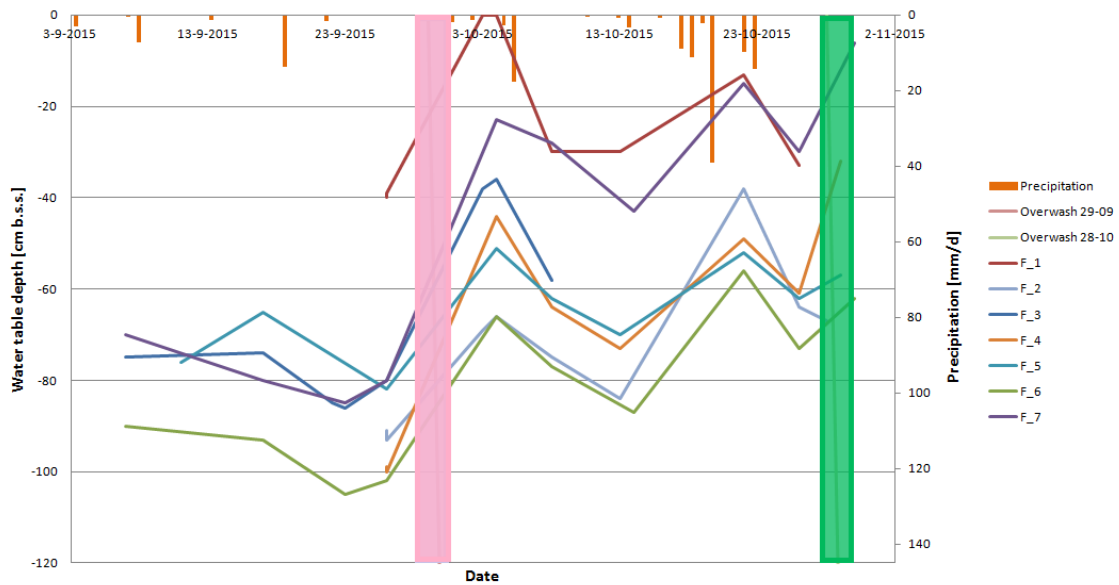


Figure 2.1: Water table depths below the soil surface (b.s.s.). These measurements were done manually at on average weekly intervals. The displayed trend is a linear interpolation between these moments of measurement. Precipitation in mm/day and the approximate moment of overwash events are also displayed in the graph.

Neem is taking over

Around the floodplain, Neem trees can be spotted everywhere, throughout the village and its surroundings. Neem, one of the mangrove-fringing trees, is non-native and fast-growing. Much faster than mangrove trees. Its mastery over native trees can be attributed to the fact that it thrives on well drained soils, so with small amounts of water. Usually its strength would be a weakness in mangrove areas were the soils are too wet for the Neem tree. Walking around in the floodplain and its surroundings, this preference to dry soils can be seen, since there are not yet young or full-grown Neem trees in the floodplain. The possibilities for Neem trees change when the soil stays dry while it would usually inundate. Neem seeds which are then dispersed in the floodplain, germinate, thriving on the dry soils like no mangrove propagule could ever do. During the next long period of inundation, the seedlings in all probability die. If drought holds on for a longer period however, the Neem seedlings will establish and grow fast. Their growth decreases possibilities for mangrove seedlings; Neem using precious nutrients and blocking sunlight. Still, Neem appears not to tolerate prolonged inundation [62]. And so if the area remains being flooded yearly, at least in the floodplain, Neem will not be able to spread.

Domination of Neem over the local flora is not only a threat for the mangrove trees however, it affects the complete ecosystem since Neem, an extremely toxic plant, does not participate in the

local food chain [63]. Insects cannot feed on the Neem tree, and since insects are part of the food chain, this means less food for birds, frogs, toads, and many other species playing an important role in the ecological balance. Also, once a Neem tree establishes, all undergrowth disappears, leaving the soil susceptible to erosion [62].



Figure 2.2: Seedlings growing in the floodplain; White mangrove (left figures), Red mangrove propagules (middle figure), and the Neem seedlings (right figure).

2.1.2 Beetles that enhance the effect of drought

It was assumed that water table levels have been low for at least a couple of months, and perhaps already before the usual water depletion in the dry season, since 2014 was a dry year as well [64]. This was based on the combined knowledge that water levels were measured to be at least 60 *cm* below surface level during a complete month, see figure 2.1, and that precipitation already failed the complete year of 2015. This engenders a lack of water for the low root systems of the mangroves, during a minimal period of three months and a maximum period of eight months. Mangroves can tolerate drought for about six to eight months [54], and while stressed just survive, making no fruits or new leaves [64]. Observing the mangrove trees, they seemed to be functioning just fine, even producing fruits, except for some of the White mangroves at the edges of the floodplain. These trees were left with little amount of leaves, and had partly dead branches. While only some of the White mangrove trees degenerated in such rate, all were in bad shape due to leaf damage. The same leaf damage, but in lesser amounts, was detected on the Buttonwood trees.

Leaf damage

This leaf damage, occurring as brown pits on the leaves, is shown in figure 2.3. The pitted damage on White mangrove and Buttonwood seems to be a chronic part of life for these species, and can be found in about every mangrove forest in Central America [64,65]. It is caused by a leaf beetle of the *Metachroma specie(s)* (*Coleoptera: Chrysomelidae: Eumolpinae*) [66], also shown in figure 2.3. The adults are associated with various vegetations in saline habitats, and are most active at night. Leaf damage density was not the same for every tree. Trees closer to the estuary waters showed less leaf damage, especially the leaves that hung above the water itself seemed to be without damage at all. The fact that almost no damage could be seen on the Red and Tea mangrove, is probably related to the physical and chemical defenses of this species. The leaves of at least the Red mangrove are known to be extremely resistant, and both Red and Tea mangrove have high concentrations of soluble tannins that render them especially unpalatable for herbivores such as this leaf beetle [54,65]. Leaf damage on trees means direct loss of photosynthetic area, and thus a lower productivity of the tree. In extreme cases, with high amount of leaf damage, this can lead to death of the tree [65].

Nectaries

The White mangrove and Buttonwood trees are of the same family, the *Combretaceae*, and both appeared to contain tiny bumps on the petioles of the leaves, which can be seen in figure 2.3. It was demonstrated that the bumps are in fact extra floral nectaries, secreting a clear, sweet-tasting nectar [67]. The reason for secreting this sugar is still unclear, though insects are said to feed on the sugar. This could indicate a mutualistic relationship between the insect and plant, where the insect defends the plants against damage typically caused by browsing herbivores. Several organisms are known to have evolved such obligate mutualism [64, 67, 68].

The bumps were observed, but the sugary substances were not. The bumps even contained black dots, as if unused. These black nectaries were also observed by Jimenez [54], and although not analyzed further, thought to be turned black only in the old leaves, which is also mentioned by Tilney and van Wyk [68]. According to them, nectaries are probably only (optimally) functional on new growth. Just outside of the mangrove forest, on the rocks of the beach of El Ostional, a lonely White mangrove tree can be found, almost constantly in direct contact with sea water. This tree, in contrast with its fellow trees in the floodplain, was almost impregnated with a white substance, shown in figure 2.3. After tasting this, it turned out to be sweet, and probably was nectar secreted by the nectaries, which were not blackened at all. And, most importantly, the leaves were not damaged either.

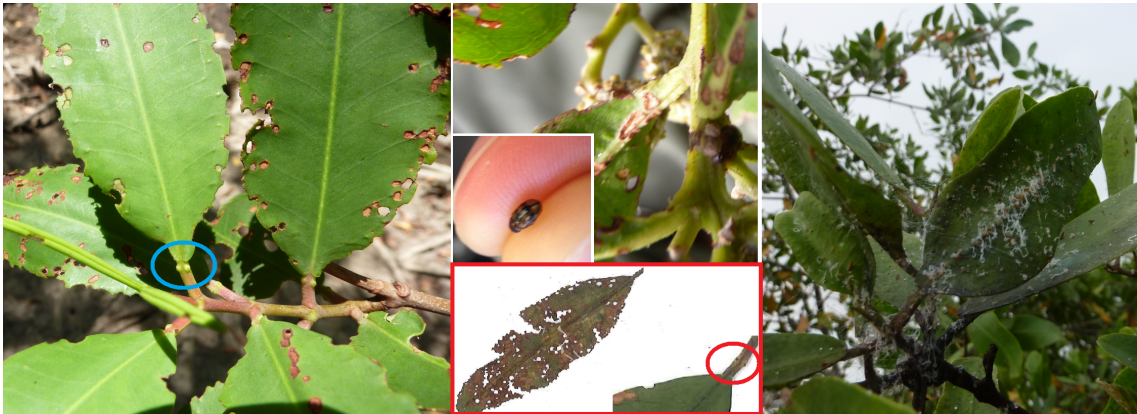


Figure 2.3: Effects of damage caused by beetles on leaves of the White mangrove and Buttonwood trees. The beetle is displayed, as are the nectaries. The blue circled nectaries are shown on a relatively undamaged leaf, while the red circled nectaries - blackened - can be seen next to a decaying, largely damaged leaf. The right figure displays the lonely tree away from the floodplain, covered with the sweet tasting substance.

Production of new leaves

The nectaries of the trees in the floodplain are dis-functional either because of old age, or because the tree requires a healthy condition to produce nectar. Presumably, a stressed tree weakens, and thus produces less nectar, which allows more herbivores, and weakens the tree further [64]. Whenever water is limiting, mangrove trees have to be more restrictive with water loss. Photosynthesis and transpiration rates are reduced, what means that plant carbon dioxide uptake for growth of leaves which occurs simultaneously will also be decreased [52]. The moment the tree experiences water stress, leaf production and other growth is put on the back burner [18]. New leaf production for most mangrove trees most certainly must have been low due to the drought, leaving only the old leaves. In combination with the leaf damage caused by the leaf beetle, total leaf area decreases substantially. A low amount of leaves reduces the possibility for photosynthesis, reducing the amount of sugar production even more. This downward cycle can eventually indeed lead to tree mortality, explaining the occasional dying White mangrove trees in the floodplain. These were the trees farthest from the estuary waters. This relationship between leaf damage and water stress, was also observed in Brazil [65], where leaf damage by herbivores was studied for two

years. Here, the greatest levels of leaf damage among White mangrove trees were observed during the dry months. This high percentage during the dry period, was appointed to leaf fall and the subsequent production of new leaves during the rainy season, which decreases the average amount of leaf damage subsequently.

2.2 Improvement of soil conditions by crabs

Mangrove trees have adapted to saline conditions, by using mechanisms as exclusion, secretion, tolerance, or a combination of these [67, 69]. These mechanisms basically mean that the tree can either filter the salt in the roots during assimilation, secrete the salt via secretion glands in the leaves using transport pathways, or wield an extensive damage repair system by for example transporting the salt into specific leaves which are then sacrificed. From the Red mangrove it is known that exclusion is mainly used to tolerate salt. The White mangrove is said to combine different mechanisms; it excludes salt, it can secrete salt via glands when salt conditions are extreme, and it transports salt into leaves that can be sacrificed, which is visible in the occasional yellow leaf hanging in the tree.

The difference in osmotic potential between the tree sap and the saline pore water, creates a negative osmotic pressure exerted on the roots of mangroves, which tries to draw precious fresh water out of the plants. In order to counteract this pressure, the trees use a process similar to reverse osmosis, to draw in water against the osmotic gradient. This pressure most likely is generated by transpiration at the leaf surfaces in combination with the filtration capabilities of root membranes [52, 67]. Mangrove trees are in this way able to exclude uptake of at least 90 % of the external salt [52]. When a tree uses salt secretion, it moves ions against large electrochemical potentials within the leaves. This energy-dependent process consequently demands higher levels of nutrition than when only salt exclusion is used. A trade-off against higher growth rates at lower salinity conditions [52]. It then secretes the salt through salt secretion glands, which can be observed as salt crystals on the leaves, and which are washed off during precipitation events.

Hence, the adaptive mechanisms of mangrove trees to saline conditions increase salinity levels in the surrounding soil. This needs to be balanced by flushing with water [52], in order to create a stable ecosystem for mangrove trees to grow. Flushing possibilities of the soil depend on the ease with which the soil transmits water [32]; the permeability of the soil. If materials have low permeability, most precipitation and inundation does not infiltrate the soil. Clay, compared to for example sand, has an extremely low permeability. Consequently, the clay found in the Ostional floodplain, led to the expectation that the below aquifer was confined by highly impermeable soil.

2.2.1 Confined or unconfined

To verify these expectations, infiltration tests were done in order to calculate the saturated hydraulic conductivity, a measure for the permeability of the soil. These tests resulted in an average hydraulic conductivity K_S of 0.79 m/day , extensive results can be found in Appendix C. Literature values for clay vary from 10^{-3} to 10^{-7} m/day [32], clearly much lower than the measured values. This implies that permeabilities in the floodplain are more or less in the order of sand instead of clay.

The difference in permeability can most likely be explained by the occurrence of preferential pathways. Preferential pathways can be old root channels, horizontal cracks, or - as is the case in El Ostional - burrows of crabs. At the sites where infiltration tests were performed, crab burrow entrances were counted in a 2 by 2 m area around the test hole. The calculated correlation between burrow amount and hydraulic conductivity was $R^2 = 0.64$. A correlation between total burrow surface area and hydraulic conductivity however, seemed non-existent; $R^2 = 0.06$. That the diameter size of a burrow is probably less important than the amount of burrows, was already found by Bouma during his research on preferential pathways [70].

The crab burrows in Ostional were abundant, and diameters could range from half a *cm* to five *cms*, depending on the type and age of the crab. Fresh burrowed clayey material, brought up to the surface, could be seen next to the burrows and often this had a gray color similar to the aquifer material. An example can be seen in figure 2.4, where also a high density of holes are displayed on the floodplain floor and between Red mangrove roots. The crabs thus penetrate the confining layer in order to reach the water in the aquifer. By burrowing to these depths, the crabs acquire the necessary brackish water source, but can mostly stay dry, as is their preference. Crabs are known to frequently exchange burrows, still burrows can remain actively occupied for more than one year, possibly exchanging hosts [47]. Abandoned burrows slowly fill with sediments again, still leaving a preferential pathway for long periods of time before completely being consolidated again. The Mouthless crab excavates burrows of almost one meter in length and depth [71], and often with more than one entrance [72]. This results in an underground network of macro pores, where suddenly the morphologically confined aquifer turns into an unconfined aquifer.



Figure 2.4: Crab burrows in the floodplain, including an example of fresh burrowed clayey material brought up to the surface in the left figure, and a burrow opening partly submerged after water level increase in the right figure.

2.2.2 Preferential flow through macro pores

The rate at which the groundwater table in the floodplain increased after precipitation or over-wash events was indeed high. In figure 2.5, continual measurements of the groundwater table in the floodplain are shown, together with the daily measured precipitation and the periods of high spring tide that caused over-wash events. These events created little periods of inundation. The immediate peaks resulting in the groundwater table are a result of the fast flow of inundation water into the aquifer water. Pressure is built up, and slowly the water percolates laterally into the aquifer. Remaining inundation slowly evaporates or subsequently infiltrates with the same speed as the spreading of water in the aquifer.

The manual groundwater measurements of figure 2.1 show the same increase, but lack the typical fast peak due to delay in measurement possibilities. The manual measurements however do show the effect of the interconnectivity between the separate burrows. Even though inundation due to over-wash events only reaches the areas adjacent to the beach, groundwater tables also increase in areas of the floodplain where no inundation takes place. Apparently, water flowing into the burrows does not flow downwards only, but follows also the burrow pathways in lateral directions. In this way increasing groundwater tables everywhere in the floodplain.

Threshold value

Alike to the burrow interconnectivity that shapes an underground network, a connection between the floodplain aquifer and estuary might be enhanced due to crab burrows. In figure 2.4 a burrow opening is shown that is partly submerged after water levels increased in the estuary. This water thereafter flows into the network of burrows and thus recharges the floodplain aquifer. A

demonstration of this connection was given when also groundwater tables in F_4 , see figure 2.5, immediately increased after an over-wash event. Location of can be found in figure 2.8 in Part III.

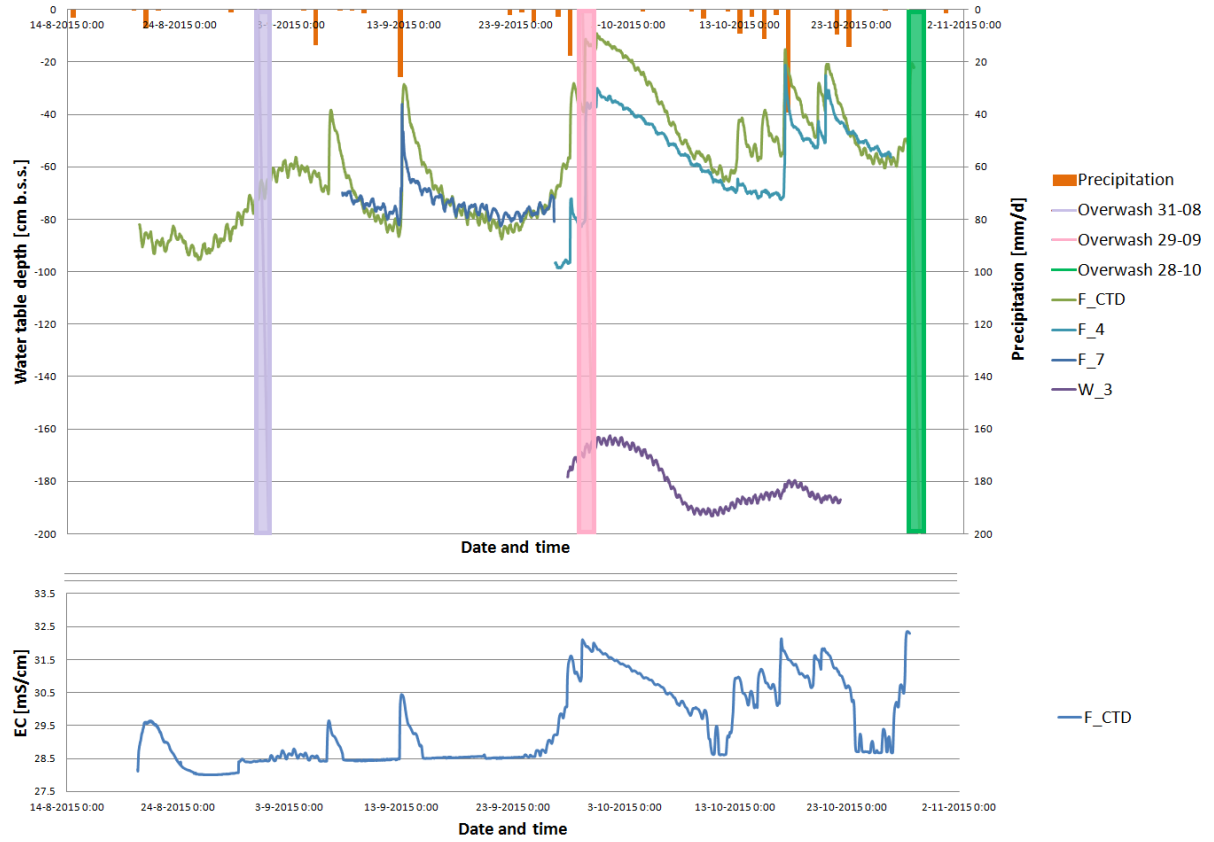


Figure 2.5: Continuous water table depths in the floodplain and well below soil surface (b.s.s.) in the upper graph. Continuous electrical conductivity (EC) levels measured in the floodplain in the bottom graph.

As can be seen in figure C.1 of the Methodology or figure 2.8 of Part III, this piezometer was located between the central basin and a branch of the estuary, and is thus unattainable for direct inundation through run-off due to over-wash. Over-wash events increase water levels in the estuary, where after groundwater tables in the floodplain can increase. It seems that the water level in the estuary needs to gain a certain height in order to reach the burrow openings. This would reveal a threshold value the water level needs to reach before connection with the floodplain aquifer exists.

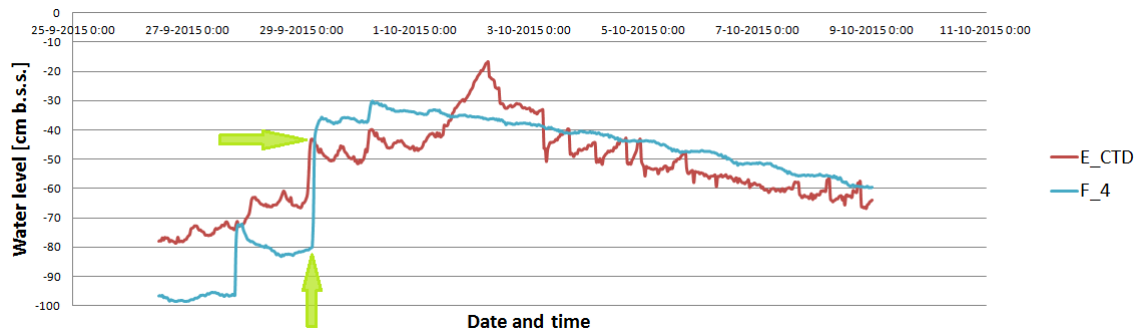


Figure 2.6: Continuous water table depths in the estuary basin E_{CTD} and floodplain at F_4 below soil surface (b.s.s.), for a small period around the over-wash event of 29-09.

To attain this threshold value, the moment of groundwater table increase was traced back in the

water level measurements of the estuary, delivering the height that needs to be reached. As can be seen in figure 2.6, this threshold is reached and an immediate water table increase in the piezometer is visible. When the water levels in the estuary rise up to approximately 43 *cm* below the floodplain soil surface due to the over-wash event around September 29, the burrow are flooded and water flows into the macro pore system. Of course, this is an approximate value since no absolute water levels are available and it is thus assumed that all soil surface levels have an equal elevation height.

Decrease of soil salinity

Figure 2.5 also displays the continuous salinity measurements in the floodplain; the location of F_{CTD} can be found in figure C.1 of the Methodology or figure 2.8 of Part III. The salinity on average shows a stable level of about 28.5 *mS/cm*. Like the groundwater table, salinity levels immediately increase after a precipitation or over-wash event. Caused by an over-wash event, this increase is not surprising since inundation water is then sea water, with an average salinity level of 50 *mS/cm*.

However, a salinity increase due to precipitation seems inexplicable. Overall, rainwater salinity levels do not even reach one thousandth of this value, and are thus expected to decrease salinity levels. Hence, to induce an increase in salinity levels, the fresh rainwater should be enriched with salt before it reaches the aquifer. During relative fresh water flow through the crab burrows, water dissolves the salt contained by the soil, flushing the soil. In that way, crab burrowing balances the mangroves suicidal habits to increase the saline conditions surrounding them, by decreasing soil salinity.

2.2.3 Crabs are the perfect eco-engineers

The positive effect of crab burrowing activities on mangrove trees has been noticed more often, and crabs have thus been named keystone species [73] or eco-engineers [48]. The crabs are known to promote nutrient recycling by feeding on the sediment surface and plant matter, and to pronounce sediment properties and biochemical processes by enhancing porosity and water flow through the sediment [46–50]. Crabs also are major seed predators, thus determining part of the plant community structure.

The role of crab burrows to provide an efficient mechanism for exchanging water between the anoxic substrate and overlying water in case of direct tidal influence, was researched by Ridd [74–76]. Tidal flushing of animal burrows in mangrove swamps turned out to be an effective and important mechanism for transport of salt and other soluble substances [76]. An even better confirmation of the hypothesis that crab burrows decrease soil salinity, is found during a research in a restored Florida coastal marsh [77]. Here crabs were experimentally removed in specific areas, and after a certain period interstitial water salinity was compared to control areas. Markedly less high salinities were measured in the areas with crab activity, than in the areas without crab burrow activity. Field studies in Japan [50] and Brazil [49] had similar results, finding significantly lower salinities in surface sediments with crabs than without crabs.

2.3 A relative fresh water estuary

In the complete Ostional estuary basin, measured salinity levels ranged from approximately 0.7 *mS/cm* at the beginning of the study period, to around a maximum of 17 *mS/cm* after an over-wash event. See Appendix C for an overview of the salinity measurements. Compared to the average brackish estuarine environment, these are very low values. Especially considering the amount of time that the estuary waters subsisted without river inflow. The existence of Tea mangrove trees in this particular estuary already indicated this estuary to be exceedingly fresh. Seepage measurements, conducted throughout the estuary waters, revealed where in- or ex-filtration occurred. Complete results of the seepage measurements can be found in Appendix C.

2.3.1 An underground river

A fresh water input was indeed found. At the upstream part of the estuary, the bay-head delta, only ex-filtration rates were found. These range from 0.3 to $13 \text{ cm}^3/\text{min}$. Although the ex-filtration rates differ greatly, they do indicate the existence of a flow from groundwater to estuary surface water [78]. A stratigraphic correlation of a cross-section in the bay-head delta has been created by Calderon [10], which can be found in figure C.20 in Appendix A. This cross-section shows that beneath a homogeneous clay layer, alluvial deposits with an average hydraulic conductivity of $K_S = 6.7 \text{ m/day}$ were found. Hydraulic head measurements during Calderon's [10] research also result in a general groundwater flow direction through this aquifer from northwest to southeast. With low water levels in the estuary, a positive hydraulic gradient originates from the alluvial aquifer to the estuary, resulting in a subterranean inflow of water into the estuary; an 'underground river' flowing into the estuary.



Figure 2.7: Bay-head delta, upstream in the estuary. The picture shows the cross-section where the ten piezometers are installed around. Pools of water can be seen that were mostly not connected to the downstream surface water.

At the cross-section where a stratigraphic correlation of the bay-head delta was created, ten piezometers were installed as well. These piezometers, depicted in figure C.21 in Appendix C, allowed manual water table and salinity measurements in the alluvial and shale aquifers below, which are listed in Appendix C, Section 1.3. The salinity measurements in the piezometers gave approximate values of 0.55 mS/cm , which match the measured salinities in pools of water in the bay-head delta depicted in figure 2.7. The conducted measurements in these piezometers were scarce, but a schematic view of the average heads in the aquifers is depicted in figure 2.8.

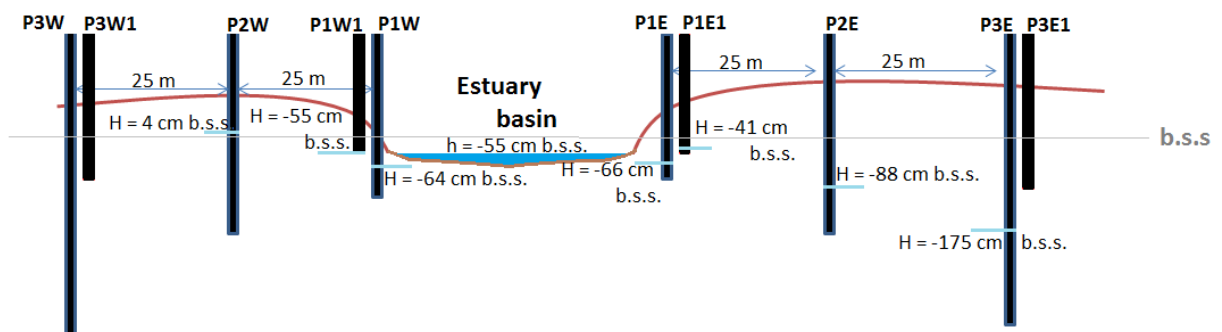


Figure 2.8: Schematic figure of the average measured head in the ten piezometers approximated with respect to b.s.s. level. These heads can be compared to the surface water level measured at October 5, 2015.

Although measurements were not leveled precisely due to missing elevation data, it can be seen that heads in $P1W$, $P1W1$, $P1E$, and $P1E1$ are approximately even to the water level in the bay-head delta. These piezometers are located in the clay layer surrounding the estuary, see figure C.21. Average heads in the shale layer on the west bank, $P2W$, show a much higher level compared to

surface water level, resulting in a positive hydraulic gradient. This is not the case on the east bank, *P2E*, where the head is lower than surface water level. It might indicate a loss of water again on the east side of the estuary to infiltration. The head differences between *P2W* and *P2E* does seem to confirm however, the reached conclusions from Calderon's research on a general groundwater flow direction from northwest to southeast.

2.3.2 A muted tide

At the mouth of the estuary, on the inner side of the sandbar, seepage measurement results were less consistent. Both in- and ex-filtration rates were found. Figure 2.9 contains continuous water levels measured in the estuary. No general increase is visible, except after over-wash events. What can be noticed however, is a diurnal change in water levels, which is similar to a diurnal tide. Tidal influence in this estuary is damped by the sandbar, and materializes as a muted tide.

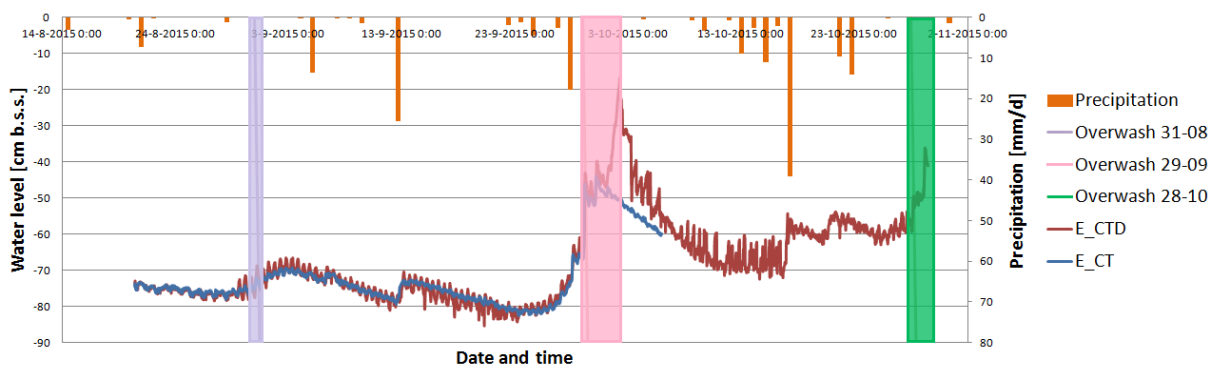


Figure 2.9: Surface water levels below soil surface (b.s.s.) in the estuary basin, measured continuously.

These tidal effects are caused by pressure changes in the subsurface, and in the estuary also by a tidal advance or ebb of water through the sand bar. Pressure changes in the subsurface are also visible in the continuous groundwater table measurements, already shown in figure 2.5. These tidal responses are confirmed by findings during the study period of Calderon [10], where groundwater levels in piezometers near the coast showed semi diurnal fluctuations due to the effect of sea tides. Tidal advance or ebb of water through the sandbar depends on sea water level, changing throughout a tidal day. At high tide, a little brackish water from the sandbar seeps into the estuary, while at low tide fresh estuary water seeps out of the estuary into the sandbar. This phenomenon corresponds to the seepage measurements, and is due to head differences between the estuary surface water and sea.

When sea tide from San Juan del Sur (located around 22 km to the north on the coast) is compared to the water level fluctuations in figure 2.10, a delay in high water level can be seen in the floodplain and in the estuary. The water table in the alluvial well aquifer seems to lack this delay however. The fluctuations in water level in W_3 follow the sea tide perfectly, although the amplitude is smaller. That the water level fluctuations in the alluvial aquifer are not similar to those in the floodplain aquifer and estuary, is possibly due to the subsurface soil type of the aquifers. Pressure changes in clayey soil will be less pronounced by cause of a smaller permeability. Where the alluvial layer has a hydraulic conductivity of $K = 6.7m/d$ [10], the floodplain clay layer revealed as previously explained a lower but still high permeability; $K = 0.79m/d$. A smaller hydraulic conductivity explains the delay seen in the floodplain aquifer. The estuary is surrounded by the floodplain and thus undergoes a similar delay due to subsurface pressure changes. It is however also connected with sea by the sandbar, which impacts the water level fluctuations as well. The tidal advance or ebb of water through the sandbar also occurs with a certain speed, depending on the permeability of the sandbar and the underlying subsurface. Thus, the inverse-auger hole method was used in the sandbar in order to determine the saturated permeability. Tests resulted in an average hydraulic

conductivity of $K_S = 23m/d$, see Appendix C, which is consistent to literature values of hydraulic conductivity in sand [32]. Figure 2.10 reveals this impact in the irregular fluctuations in E_{CTD} that differ from the fluctuations in F_{CTD} . The irregularities increase with a higher spring tide, when the sea tide more often reaches a higher head than the estuary surface water.

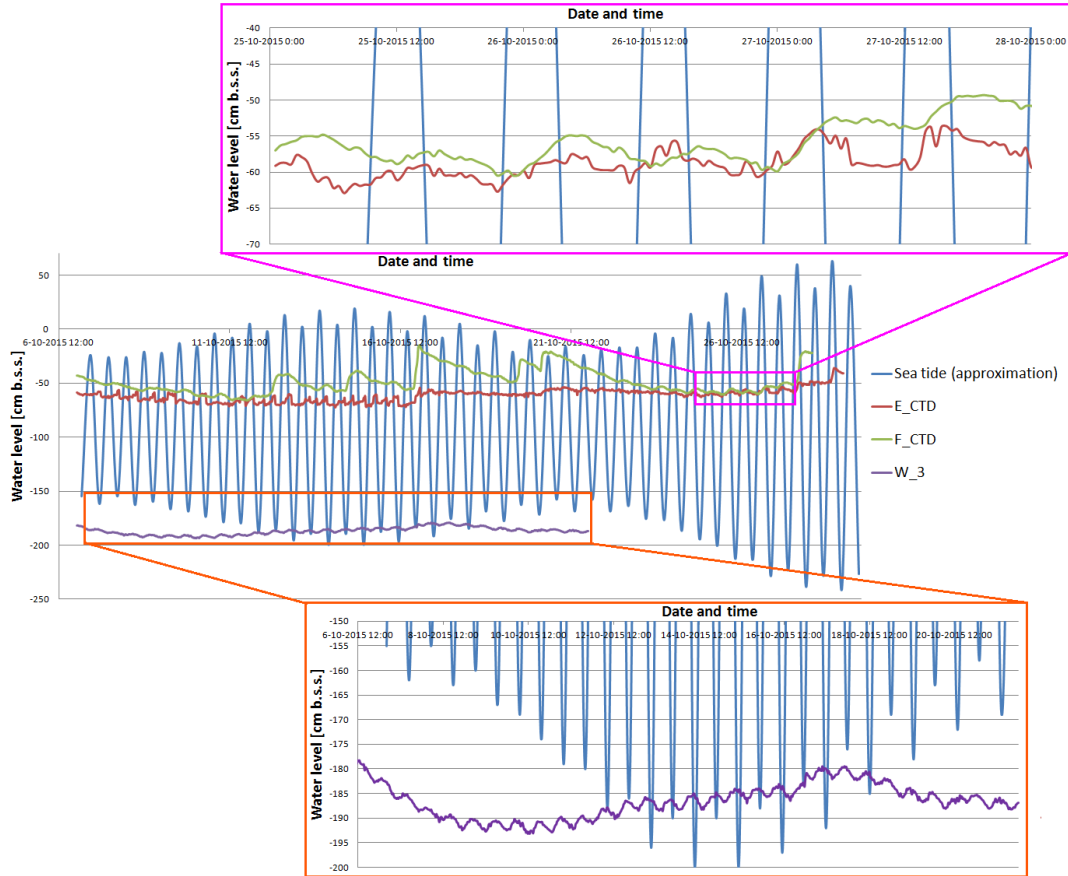


Figure 2.10: Water levels below soil surface (b.s.s.) in the estuary basin E_{CTD} , in the floodplain aquifer F_{CTD} , and in the alluvial aquifer W_3 , compared to sea tide from San Juan del Sur which has been leveled approximately to the datum b.s.s.

2.3.3 Immunity for interior sites

This blind estuary is apparently not static at all but dynamic. Driven by a fresh groundwater inflow and a damped and delayed tide, it starts resembling a general estuary. This estuary has even more in store, since it provides the perfect habitat for mangrove trees. By closing off the estuary mouth a natural protection is created against wave and storm impact, whenever an insufficient river flow is generated. Just a sand bar would not be able to attain the current Ostional estuary, where even during drought almost potable water is found.

The importance of freshwater flow to the sustenance and productivity of mangroves has been demonstrated in a variety of research settings [79–81]. Groundwater flow may permit mangroves to inhabit areas otherwise unsuitable for growth, and increase productivity in mangrove systems. In this estuary the Tea mangrove is a perfect example. The Ostional estuary further obtains mangrove trees with heights reaching over 30 m. This is not surprising, for trees of interior basins have been formerly found to be the tallest and of greatest girth when compared to river- and tide-dominated sites [81].

Thus, combined forces of a sand bar closing the estuary and a fresh water inflow might induce immunity from the negative impacts of for example drought. At least for a certain period of time.

Chapter 3

Conclusions

In conclusion; *in what way does the hydrology influence the ecology and visa versa?* Three different water residing locations were looked into more closely; (1) surface water which inundates the floodplain, (2) groundwater in the floodplain, and (3) surface water in the estuary. At all three locations, mangrove trees depend on the state in which the water appears. Contrarily, the way water affects the mangrove trees depends on fauna activities in the estuary.

Mangrove trees need water not only for their general growth cycle, but also to inundate the area. Inundation both ensures germination of propagules and thus reproduction, as well as the mastery of mangrove trees over other species, like Neem. And while Mangrove trees can withstand periods of drought for almost 8 months, the absence of water induces a growth stop. Drought in combination with leaf damage caused by herbivore insects may become disruptive, as seems to be the case for the White mangroves when drought persists.

Crabs turn out to play an important ecological role with their burrowing activities in the sediment. It was known that crabs in that way promote nutrient recycling, pronounce sediment properties and biochemical processes, help determine part of the plant community structure, and increase permeability of the soil. In this research it is shown that the increased permeability induces an increased soil moisture. The research further found an increase of salinity in the water, which is most probably flushed out of the soil through the crab burrows. That would result in a decreased soil salinity, a phenomenon which has been noticed more often in literature. Both effects influence mangrove growth and survival in a positive way.

The Ostional estuary surface waters are relatively fresh compared to other estuaries. This is caused by the combined efforts of a sand bar closing the estuary, and the continuous inflow of fresh groundwater. The groundwater inflow occurs at the bay-head delta and comes from an alluvial aquifer near the surface. Through the sand bar, also flow occurs, the direction depending on sea tide level. In combination with pressure changes in the subsurface, a muted tide is induced in the estuary instead of normal sea tide. The fresh water in the estuary has a positive influence on mangrove production and permits growth of the Tea mangrove.

Part III

Saline conditions of the Ostional area

Chapter 1

Introduction

The objective in this part is to find an answer to the following question: *Can the salt intrusion of the blind estuary and its surrounding groundwater system be described and predicted during a drought?*

According to Day [1], salinity varies under the ratio between evaporation and seepage through the sandbar on the one hand, and freshwater inflow plus precipitation on the other. In his description of a blind estuary, he assumes the estuary is under the influence of a river, and that seepage through the sandbar can be only outflow. During the study period in the Ostional estuary, a river current was non-existent and precipitation was minimal due to drought. Turns out, as can be read in Part II, that there still was an inflow of fresh groundwater, and that seepage through the sandbar occurred in two directions, depending on sea tide level. In figure 1.1, a sketch of these in and out flows is projected. The moment sea water flows over the sandbar and into the estuary waters during over-wash events, salt intrusion takes place. Salt intrusion is then driven by this muted tide and groundwater discharge into the estuary. A predictive theory developed by Savenije [31] was used to analyze the mixing mechanisms in this estuary in the period that it matters; the dry period.

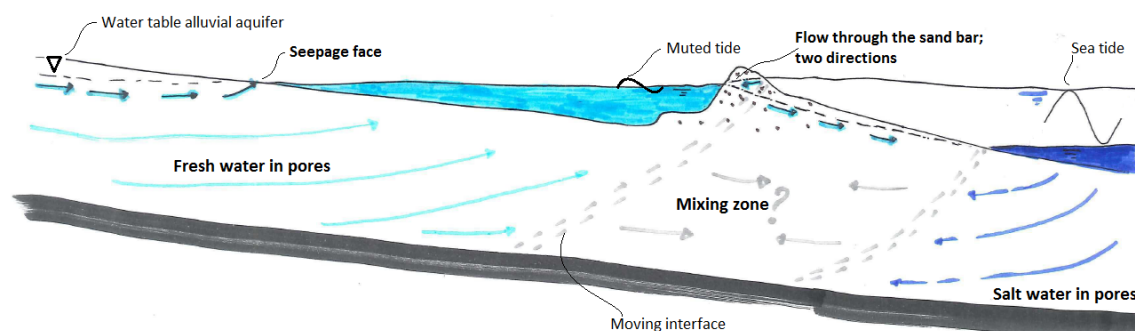


Figure 1.1: This sketch represents a longitudinal cross-section of the estuary waters and its subsurface flows. The assumed flows in the shallow aquifer are based on typical flow patterns in coastal aquifers [32]. The boundary between fresh and salt pore water is a diffuse mixing zone, a result of diffusion together with mixing caused by fluctuating tide and fresh water heads.

Figure 1.1 also shows the subsurface flows, suspected patterns of flow representing long-term averages usually occurring in coastal aquifers [32]. The location and direction of the fresh- and salt-water interface is unknown in El Ostional, and has even been hypothesized the other way round by Calderon [10], see figure C.19 in Appendix A. Fluctuation of fresh water heads can cause short-term variations in these flows, causing the interface of the mixing zone to shift [32]. During the study period, many residents of El Ostional confided in their fear for salt intrusion into their wells. The moment drought decreases fresh water heads, the mixing interface can shift landward,

increasing saline conditions further inland. The Ghyben-Herzberg relation is used as a method for estimating the depth to the fresh-salt water interface. This is then compared to salinity levels of the groundwater wells in the village.

Unfortunately, the Ghyben-Herzberg relation is unable to explain the high salinity levels measured in the floodplain. Saline conditions in the floodplain are an order of magnitude higher than those in the estuary and in most wells. According to Rains, groundwater flows beneath the Ostional mangroves floodplain and through the high-permeable beach deposits to discharge into the ocean [12]. That would be consistent with figure 1.1, but does not explain the high salinity levels that were measured. Relations between salinity measurements throughout the floodplain were thus mapped and plotted, in order to find a pattern and interpret its cause.

The above analyses assume that the sandbar is closed, since drought is the state of the art. During the study period already an attempt was made by the community to open the sandbar. This opening would most likely influence the water levels and salt intrusion in the estuary and floodplain. Some of the major consequences of the opened sandbar will be discussed in order to understand the effect that it will have on the mangrove population.

Chapter 2

Results and conceptualization

2.1 Salt intrusion in a blind estuary

During the study period, salinity was measured in the estuary with an Electrical Conductivity (EC) device, on a weekly basis. Results of these manual salinity measurements can be found in Appendix C. These measurements were conducted at several locations in the estuary, of which at least the four shown cross-sections. Salinity was measured over the complete depth, at half meter intervals. Salinity values measured at September 8 are shown in figure 2.1, and will be used to demonstrate the occurring salt intrusion in the Ostional estuary.

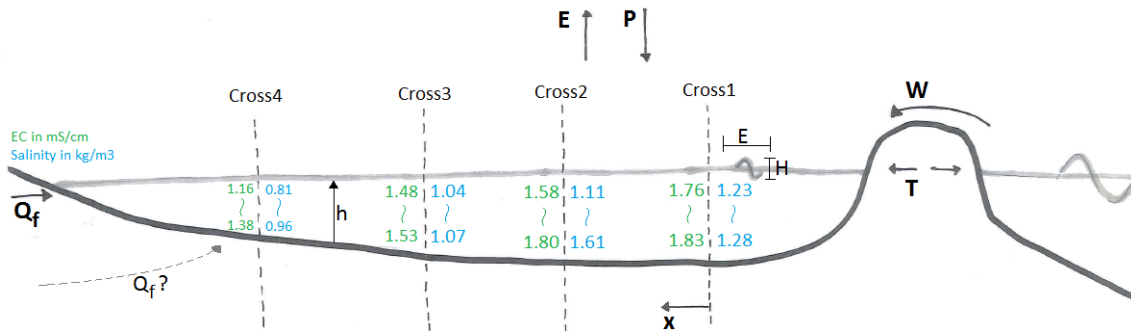


Figure 2.1: Schematic longitudinal cross-section of the estuary showing measured EC levels [mS/cm] in green, and recalculated salinity levels [kg/m³] in blue, at September 8 2015. These measurements were performed at four different cross-sections; cross1 till cross4. Represented in- and outflows are the groundwater seepage Q_f , the tidal period T , the evaporation E , the precipitation P , and the over-wash inflow W . The tide T then causes a certain tidal range H and a tidal excursion E .

2.1.1 Salt intrusion characteristics

The pattern that can be observed in figure 2.1, is the gradual change of higher saline conditions in cross-section 1, to the lower saline conditions in cross-section 4. It shows similar salinity distributions as a partially or well-mixed estuary [2]. A well-mixed estuary occurs when the fresh water discharge is small compared to the tidal flows, while for a partially mixed estuary the fresh water discharge and tidal flow evenly influence the mixing. The figure also shows the related vertical salinity gradient, which was smooth and thus only represented by the salinity at surface and bottom level. A smooth gradient is typical for a well-mixed estuary according to Savenije [2].

Estuary shape

The Ostional estuary has been classified in Part I based on the main driving forces affecting the character of an estuary and leading to different shapes of an estuary; the tide, the waves, the river discharge, and the lateral sediment transport [2]. These different shapes are also characteristic, forming parallel banks, or banks that converge in upstream direction. In the Ostional estuary it is almost impossible to discern converging banks.

In figure 2.2, it can be seen that the convergence, however slight, is present. The cross-sections and widths vary according to the exponential functions 2.1 and 2.2 along the estuary axis x , which is also visible in figure 2.2. The rate of longitudinal convergence is determined by the length scales a and b , called the cross-sectional and width convergence length [31]. The length scales are the distance from the mouth at which the tangent through the cross-sectional area or width at $x = 0$, A_0 and B_0 , intersect the axis.

$$A = A_0 \exp\left(-\frac{x}{a}\right) \quad (2.1)$$

$$B = B_0 \exp\left(-\frac{x}{b}\right) \quad (2.2)$$

The one-dimensional dispersion equation is developed by Savenije [31, 37] for alluvial estuaries with converging banks. It is based on the assumption that the geometries of an alluvial estuary correspond with the shape of an 'ideal estuary'. Such an ideal estuary is characterized by the ratio of the depth of flow h , to the convergence length a :

$$h = h_0 \exp\left(-\frac{x(a-b)}{ab}\right) \quad (2.3)$$

The mean estuary depth across the world does not significantly change over the longitudinal cross-section, and is therefore assumed to be constant for the Ostional estuary. For calculations see the Appendix C, Section 3.

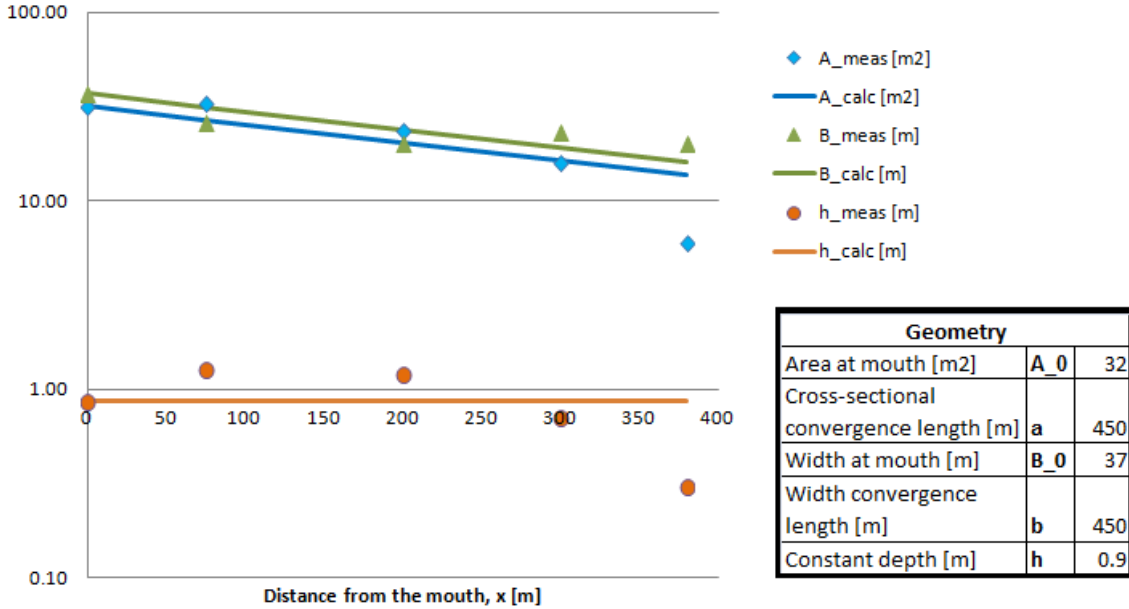


Figure 2.2: Shape of the Ostional estuary, depicting a semi-logarithmic plot with the cross-sectional area A in m^2 , the width B in m , and depth h in m . In the table the found convergence lengths a and b are listed, together with the cross-sectional area and width at $x = 0$; A_0 and B_0 . Since a and b are equal, the depth is constant along the estuary; $h = h_0$.

The shape of an estuary is a key driver of tidal hydraulics and mixing in estuaries, and as a result influences highly the shape of salt intrusion over the length of the estuary. According to

Savenije [2,31] there are four different shapes of well-mixed salt intrusion curves to be distinguished. One type, the recession shaped intrusion curve, occurs in narrow estuaries with a near-prismatic shape, comparable to the shape of the Ostional estuary, and high river discharges. The Ostional estuary was classified as river-dominated the moment that the sandbar is ruptured due to high river discharge. High river discharge is seasonal, but highly eroding, while a dry riverbed induces closed sand banks and little hydraulics. It is thus expected that the salt intrusion curve resembles the recession shape curve.

Sandbar influence

The tidal influence reaching the estuary through the sandbar is very small and not to be discerned by the eye. However small, measurements have shown us that there is indeed a tide. The tidal range H turns out to be only 4.1 *cm*. Also, wave type in the estuary is different now the sandbar turns it into a closed system similar to a tub. The moment the tide propagates through the bar, it 'rocks' the tub, where after the water continues to rock back and forth. While alluvial estuaries in general experience a mix of standing and progressive waves, the Ostional estuary is thus assumed to experience primarily a standing wave.

The tidal excursion is the distance that a water particle travels on the tide, in fact the horizontal tidal range. Savenije developed a Geometry-Tide relation [37], demonstrated in equation 2.4 and used here to calculate the tidal excursion, which is assumed to be constant for the complete estuary. Since a standing wave is assumed to occur in the Ostional estuary, the phase lag ε can be assumed equal to 0. The rate of longitudinal amplification of the tidal range δ , is assumed to be 0 since tidal range is already so small. And the ratio of storage width to stream width r_s is assumed to be approximately 1, with storage and stream width assumed to be almost alike. The Geometry-Tide relation can thus be simplified for the Ostional estuary into equation 2.4, where b is the width convergence length, which equals a .

$$E_0 = H \frac{r_s b \cos \varepsilon}{h(1 - \delta b)} \approx \frac{Ha}{h} = \frac{0.041 \cdot 450}{0.9} = 21m \quad (2.4)$$

It can be seen that the tidal excursion is extremely low, knowing that the typical length of a tidal excursion for a diurnal tide can be up to 10 *km*.

Driving forces for mixing

The Canter-Cremers number N and the Estuarine Richardson number N_R characterize the ratio of influence between tide and fresh water discharge [2]. The Canter-Cremers number can be calculated with equation 2.5, and is the ratio between the amount of fresh water (Q), and saline water (P_t), entering the estuary during a tidal period T . The saline volume entering is represented by the flood volume, or tidal prism P_t , and can be calculated with $P_t = E_0 * A_0 = 681m^3$ [37]. Seepage measurements resulted in ex-filtration rates of $Q_f = 0.001m^3/s$. The calculations for this value can be found in Appendix C, where is assumed that seepage only occurs through approximately one-eighth of the estuary bottom. This partition lies upstream in the estuary, where sludge is not present in thick layers retaining ex-filtration. The tidal period was estimated to be $T = 13h$, according to the water level changes visible in Appendix C, Section 3.1. This low value for the Canter-Cremers number indicates a well-mixed estuary, where fresh water inflow is small compared to the tidal flows.

$$N = \frac{Q_f T}{P_t} = \frac{0.001 \cdot 46800}{681} = 0.07 \quad (2.5)$$

The Estuarine Richardson number incorporates also the effect of the densimetric Froude number, defined as $F_d = (\rho/\Delta\rho)v^2/(gh)$. The (densimetric) Froude number is thus the ratio between the amplitude of the tidal velocity v and the celerity of a finite amplitude wave \sqrt{gh} . The amplitude

of the tidal velocity can be calculated with $v = (E\pi)/T$ and results in $v = 1.4 \cdot 10^{-3} m/s$. Such a small tidal velocity was to be expected with an extremely low tidal excursion. It also results into an extremely low densimetric Froude number $F_d = 9.83 \cdot 10^{-6}$. This amounts to an immensely slow flow. Hence, $N_R = N/F_d = 6988$, which when very large must mean that the estuary is strongly stratified and the flow is to be dominated by density currents. So the Canter-Cremers number and Richardson number disagree completely. The ultimate form of mixing due to fresh water inflow, gravitational circulation, is the saline wedge, corresponding with this high Richardson number, but which does not comply to the observed pattern in gradual salinity change over the depth.

What these numbers do not incorporate, and what could also not be measured during the study period, is mixing due to wind. The sandbar turns the estuary into a temporarily closed system similar to a tub, coastal lagoon, or lake, where wind-driven mixing can be dominant [82].

2.1.2 The steady state model

The analytical method of Savenije [31] uses one-dimensional dispersion and salt balance equations in combination with equations describing topography. It results in equation 2.6, describing salt intrusion when in the estuary an equilibrium condition is reached, a steady state.

$$\frac{S - S_f}{S_0 - S_f} = \frac{D}{D_0}^{\frac{1}{K}} \quad (2.6)$$

In equation 2.6, S is the salinity in kg/m^3 , S_f the fresh water salinity [kg/m^3], D stands for the dispersion, and S_0 and D_0 are boundary conditions at $x = 0$. The coefficient K was defined by Van den Burgh, and is a calibration parameter between 0 and 1 which functions as a shape factor on the salt intrusion curve. It is therefore a characteristic value for every estuary.

Longitudinal dispersion is driven by all mixing mechanisms occurring in the estuary at a certain moment. It can be described by:

$$\frac{D}{D_0} = 1 - \beta(\exp(x/a) - 1) \quad (2.7)$$

where β is the always positive dispersion reduction rate; $\beta = -(KaQ_f)/(D_0A_0)$. The dispersion D_0 is, in contrast to K , time-dependent. It is also used as a calibration parameter, but varies for every situation since it reflects tidal range and fresh water discharge which change over time. Measuring the fresh water discharge Q_f for the Ostional estuary was extremely difficult and only an average value could be obtained. By introducing the mixing coefficient $\alpha_0 = -D_0/Q_f$, D_0 can be used as a model parameter that can be obtained through calibration.

A fresh water salinity of $S_f = 0.5mS/cm = 0.4kg/m^3$ is used, based on salinity measurements in the alluvial aquifer, see Appendix C, Section 1.2. For the determination of the boundary condition S_0 , instead of sea salinity the measured salinity directly behind the sandbar in the estuary was taken. This value varies for every situation, and was $S_0 = 1.75mS/cm = 1.2kg/m^3$ at September 8.

Salinity measurements were performed all through a tidal period, while the model uses either tidal average, high water slack, or low water slack. While in most estuaries high water slack might be the most practical moment to measure, in the Ostional estuary the different tidal moments were not visible to the eye. However, with such a small tidal excursion and tidal velocity, this hardly seems a problem. Tidal average is thus assumed to be the moment of measurement.

Model results

The model has been applied to the El Ostional estuary for different measurements; on 31-08, 08-09, 16-09, 24-09, and 27-10. The results can be found in Appendix C, Section 1.2. The model result

for September 8 is shown here in figure 2.3, together with the used parameters. It can be seen that the model performs very well, where the correlation coefficient between model values at tidal average and measurements, is $R^2 = 0.97$. As can be seen in the Appendix, the high performance is also pretty consistent for the other measurements.

The shape of the salt intrusion curve actually is similar to a logarithmic convex shape, best compared with the Recession shape defined by Savenije [31]. A K -value of 0.1 turned out to fit all salt intrusion curves. A small value for K , means also that a high amount of tidal energy is converted into mixing [31]. This can also imply that in the Ostional estuary, tidal mixing has a relatively high importance while gravitational mixing is relatively low. A low dispersion at the mouth was found; at September 8 this was $D_0 = 0.035m^2/s$.

Interesting in the Ostional estuary is that the salt intrusion curve does not reach the $0kg/m^3$ line. In usual estuaries, one goes on measuring upstream until fresh water salinities are found. However, the Ostional estuary did not contain water any more further then about 400 m upstream of the sandbar. It could thus be that the actual salt intrusion would reach farther if possible. The salt intrusion length L can be calculated with the expression $L = a \ln(1/\beta + 1)$, and for the case of September 8 delivers an intrusion length of $L = 1461m$. This is almost four times the occurring estuary length.

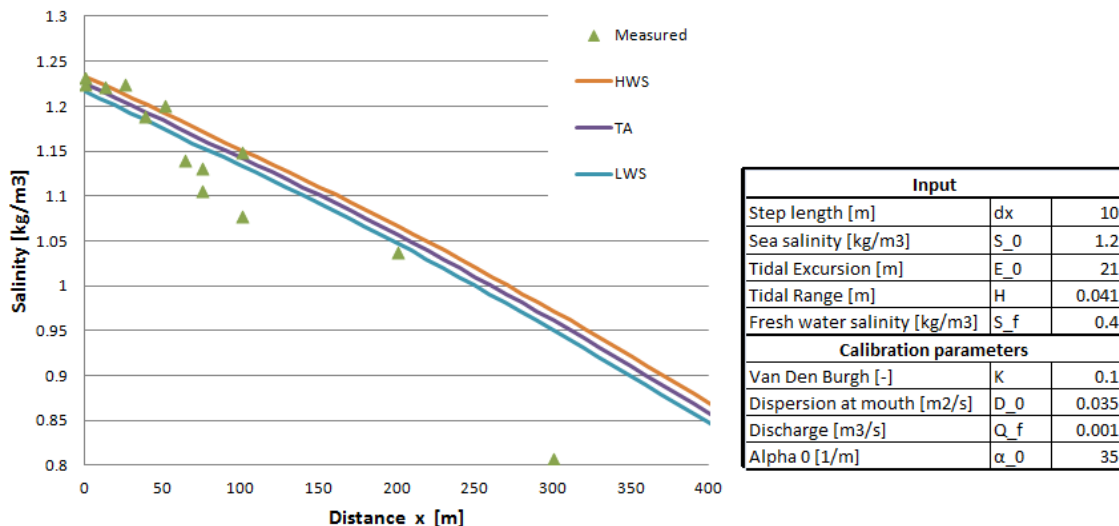


Figure 2.3: The El Ostional salinity curve at 08-09-2015. Measured values are shown, to be compared with the modeled values at tidal average (TA), high water slack (HWS), and low water slack (LWS).

Predictive model

To turn this steady state model into a predictive model to calculate the salinity in the Ostional estuary without new measurements, an empirical relation for α_0 , hence for D_0 , is required. Such an empirical relation was obtained by Savenije [31], to be used at high water slack. The equation, for which a relation was sought between non-dimensional parameters affecting dispersion, is based on a large number of observations in 13 different estuaries. These estuaries are nothing like a blind estuary, which explains the result of equation 2.8. The predicted D_0 is much higher than the found value with calibration.

$$\frac{D_0^{HWS}}{v_0 h} = 1400 \frac{E_0}{a} N_R^{0.5} = 6.91m^2/s \quad (2.8)$$

However, when the found value for the dispersion at the mouth of the estuary is assumed to be correct, the mixing coefficient α_0 should maintain its previous value to maintain the good fit of the

model to the measurements. Hence, the fresh water discharge fitting the predicted dispersion can be calculated by reversing the calculation for α_0 , what results in equation 2.9. Shown is immediately the calculation of Q_f at September 8. The value of the fresh water discharge is negative because the positive x-direction has been chosen in upstream direction.

$$Q_f = -\frac{D_0}{\alpha_0} = -\frac{6.91}{35} = -0.2m^3/s \quad (2.9)$$

This value is an order hundred higher then the measured fresh water inflow. The measured value is not completely trustworthy considering that it is based on a couple of seepage measurements that can contain measurement errors due to installation errors, equipment errors, etc. The measured value however is far more plausible than this predicted value, considering that the lowest reported discharge through the riverbanks itself, has been $0.12 m^3/s$ [10]. The Estuarine Richardson number that has been used for the calculation of D_0^{HWS} and hence Q_f , is extremely large. That explains the high values found in the prediction as well.

Unfortunately for the Ostional estuary, not only D_0 needs to be calculated but also the boundary coefficient S_0 suddenly becomes a problem. For normal estuaries sea salinity can be used to estimate S_0 , but this is not possible in a blind estuary. The coefficient S_0 is however a less important boundary condition, which depends here on over-wash or the opening of the sandbar. Perhaps the step to use the model for predictions of salt intrusion in blind estuaries is just to soon. With more measurements in different blind estuaries, the empirical relation for D_0 could possible be adjusted to blind estuaries and a good estimation for S_0 might be found.

2.1.3 Influence of other fluxes

Over-wash events

Use of the steady state model requires that the estuary indeed is in a state of equilibrium between convection by fresh water discharge and dispersion by tidal movement and gravitational circulation. The time required for the equilibrium to occur depends on the rate at which the boundary conditions vary, and the time required for the estuary system to adjust itself to a new situation. Whenever over-wash events occurred, a volume of salt water entered the estuary one-off. The new volume added at the mouth of the estuary, primarily induces a salt wedge, which slowly spreads through the entire estuary, increasing salinity levels. The estuary then first needs to find an equilibrium again. Over-wash events occurred around 31-08, 29-09 and 28-10, and especially the effects of over-wash around August 31 and September 29 were followed closely.

The over-wash event in the night of 31-08 was short and only a little amount of water entered the estuary. As can be seen in Section 1 and 3 of Appendix C, the measurements after this event could be modeled; the salinity distribution maintained a positive distribution. It does explain the somewhat less good fit for the measurements conducted at 31-08. Possibly the estuary was not yet in an equilibrium state. After the 29-09 over-wash event, salinity levels increased dramatically, resulting in several measurements that could not be used for modeling exercises. Due to the salt input, the estuary temporarily had a negative salinity distribution, showing increasing salinity in upstream direction, see also Appendix C. The amount of fresh water flow was insufficient to rapidly compensate the salt input, and not earlier then October 27, the estuary became positive again. Only to be disturbed by a new over-wash event. The measurements of October 27 have also been used in the modeling exercises. The model performed less well than it did for the other measurements. Whether or not the model could actually be used for this measurement is unsure. Possibly the equilibrium was not yet reached.

These two events show that the time required for the equilibrium to occur indeed depends on the rate at which the conditions vary. High spring tide that caused the over-wash event at 31-08 was lower than high spring tide that caused the over-wash event at 29-09. Hence, the amount of salt input was lower during the first event than during the second event. The estuary required far less

time to reach a steady state again. It also shows that the estuary system can adjust itself relatively fast to the new situation. That even with a significant increase in saline conditions, the estuary can return to positive circumstances during a drought, is a sign that indeed fresh water inflow has a serious influence on the salt distribution of the estuary.

Rainfall and evaporation

In most estuaries the relative importance of rainfall and evaporation in relation to discharge and dispersion is small. For this reason, it was not taken into account during the model exercises. The effect of rainfall and evaporation on the salt balance depends on the relative size of the two fluxes, but also on the size of discharge and dispersion. While precipitation was extremely low, evaporation in a tropical climate on open water is usually a substantial flux. It is thus important to realize whether the evaporation in the blind estuary influences the salt intrusion.

The relative importance of rainfall and evaporation on the change in salinity can be evaluated using non-dimensional coefficients determined by Savenije [31], described in Appendix B. Rainfall and evaporation data from Rivas has been used for these calculations, what can be found in Appendix A. Results can be found in Appendix C. Using this method, relative high values were found for the ratio of rainfall to fresh water inflow importance, and of rainfall to the dispersion. It seems that the overall importance of evaporation in dry conditions is high for the Ostional estuary. Whether the effect is important in quantitative terms for a blind estuary is still to be seen.

A closed blind estuary can more or less be represented as a simple bucket where fresh water flows in and brackish water flows out through the sandbar. Only during over-wash events, a volume of salt water enters the estuary. In between those events, the estuary does not experience any salt input except for the fresh water salinity S_f . This simplified and schematic view of the blind estuary can be seen in figure 2.4. Taking this into account, a new salt balance can be framed:

$$\frac{dVS}{dt} = V \frac{dS}{dt} + S \frac{dV}{dt} = Q_f S_f - Q_{out} S \quad (2.10)$$

Adding rainfall and evaporation, the water balance becomes:

$$\frac{dV}{dt} = Q_f - Q_{out} - (E - P)O_{estuary} \quad (2.11)$$

When the estuary is in a state of equilibrium, one can assume that the dispersion and advection are equal. When further is assumed that there is no overall change in volume of water contained by the estuary, $dV/dt = 0$, and thus the water balance can be rewritten to describe the outflow; $Q_{out} = Q_f - (E - P)O_{estuary}$. This results into an extremely simple salt balance:

$$\frac{dS}{dt} = \frac{Q_f}{hO_{estuary}}(S_f - S) - \frac{S(E - P)}{h} \quad (2.12)$$

For two different periods in between over-wash events, all fluxes of equation 2.12 are known. Until now, it was assumed that the fresh water inflow could be represented by the values derived from the seepage measurements. Two values for the fresh water flow were calculated, depending on what amount of the estuary bottom would let through seepage; $Q_{f(1/8)} = 0.001$ and $Q_{f(1/2)} = 0.004$. This assumption is not very thorough, and with the use of equation 2.12 it was estimated again. For these calculations, two scenarios have been used; scenario 1 being the period between over-wash events 31-08 and 29-09, scenario 2 representing the period between 29-09 and 28-10, see figure 2.4. The average daily evaporation and precipitation were measured manually in Ostional, and were compared to measurements conducted in Rivas by Ineter, see Appendix C, Section 4.1.

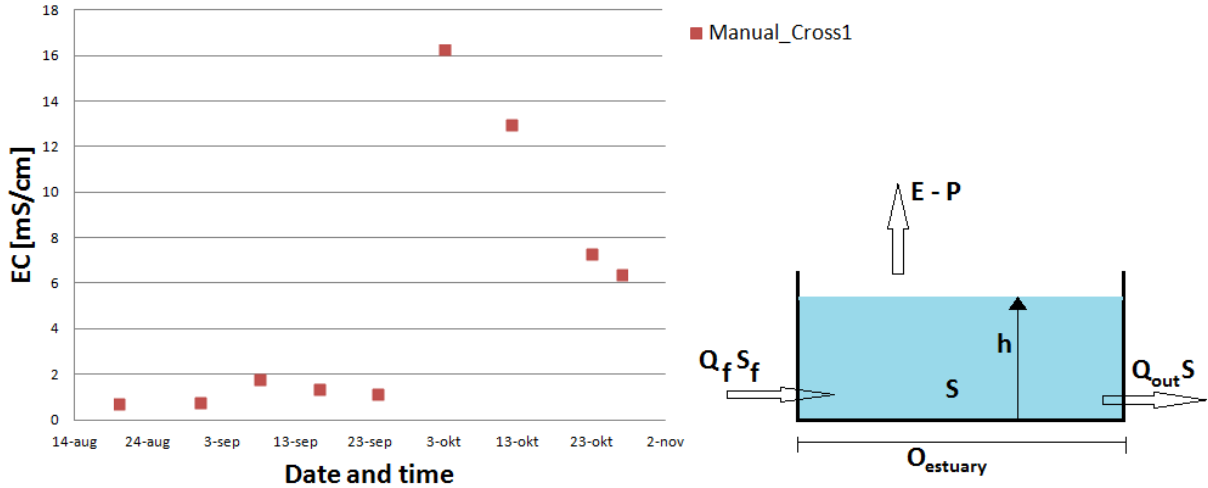


Figure 2.4: On the left graph the manual salinity measurements are depicted at the mouth of the estuary (Cross1). The measurements show the effect of the first over-wash events salt addition and the second salt addition. On the right, a simple representation of the estuary in between over-wash events is shown. In this schematic view, S is the average salinity in the estuary at the time t , and the total volume V of water in the estuary is estimated as $V = O_{estuary}h$.

Parameters				Resulting fresh water inflow Q_f [m ³ /s]		
S_f [kg/m ³]	0.35					
h [m]	0.86					
$O_{estuary}$ [m ²]	9576					
Scenario	1	2				
S [kg/m ³]	1.015	7.91	1	h	Rivas	Ostional
dS/dt [kg/m ³ \d]	0.02625	0.28875	2	h	-0.0043	-0.0044
Used data	Rivas	Ostional	1	$h - 0.1$	-0.0040	-0.0041
$E - P$ [m/d]	0.00305	0.004	2	$h - 0.1$	-0.0038	-0.0040
			1	$h + 0.1$	-0.0036	-0.0037
			2	$h + 0.1$	-0.0047	-0.0049
					-0.0044	-0.0045
Relative influence of terms	Rivas 1	Rivas 2	Ostional 1	Ostional 2		
dS/dt	0.03	0.29	0.03	0.29		
$(Q_f/(O h))*(S-S_f)$	0.03	0.32	0.03	0.33		
$(E - P)/h * S$	0.004	0.017	0.005	0.037		
Scaled on salinity	Rivas 1	Rivas 2	Ostional 1	Ostional 2		
$1/S * dS/dt$	0.03	0.04	0.03	0.04		
$1/S * (Q_f/(O h))*(S-S_f)$	0.03	0.04	0.03	0.04		
$(E - P)/h$	0.004	0.002	0.005	0.005		

Figure 2.5: The calculated fresh water inflow Q_f with the used data and scenarios. The bottom two tables show the relative importance of the separate terms for each scenario, with and without scaling the terms on salinity. The assumption that the water level is constant is checked, by also calculating the fresh water inflow Q_f with water levels $h - 0.1 = 0.76$ and $h + 0.1 = 0.96$.

That resulted in four fresh water flow values, which are all on average $Q_f = 0.004m^3/s$. This is most interesting, since the resulting Q_f is in the same order of magnitude as the used $Q_{f(1/8)}$ derived from the seepage measurements. Even more, it is alike to a calculated amount of seepage when one assumes that over half of the estuary bottom seepage occurs; $Q_{f(1/2)}$. And even though scenario 1 and 2 live through two very different salinity amounts, it results in the same amount

of fresh water discharge. When the separate terms of equation 2.12 are compared, see figure 2.5, the influence of the salinity difference between the two scenarios is apparent. When the terms are then scaled by dividing them by the salinity S , the relative importance of the terms can be seen. It is then apparent that the evaporation term is one tenth smaller compared to the fresh water flow term and the salinity change. For these calculations, it was assumed that the water level in the estuary does not change over time. Figure 2.9 in Part II shows however that even without over-wash events there is a small change in water level. To find whether or not the assumption was valid, figure 2.5 also shows the resulting fresh water inflow Q_f with an exaggerated smaller or higher water level. Apparently a different water level for the complete period, does not influence the results too much. The influence of evaporation on the salt intrusion is perhaps quantitatively less important than first believed.

2.2 Salt intrusion in the subsurface

Measurements in the piezometers in the floodplain aquifer and wells in the alluvial aquifer, show similar diurnal changes in the water table depths as the estuary water levels. These tidal changes are caused by pressure changes in the subsurface, which was already shown in Part II, figure 2.10. The pressure induced by sea level on the subsurface also has an influence on the salt content in the aquifers. Both aquifer systems will be looked into in the following subsections, where after a connection will be sought.

2.2.1 Fresh-salt water interface in the alluvial aquifer

A simple and useful method for estimating the depth to the fresh-salt water interface is known as the Ghyben-Herzberg relation [32], see equation 2.13. When using this relation one assumes that the interface between fresh and salt water is sharp, and thus without mixing, that hydrostatic principles apply, and that the fresh water head is equal to the sea level elevation at the shoreline. The factor 40 is acquired by using the water densities $\rho_{sea} = 1.025g/cm^3$ and $\rho_{fresh} = 1.000g/cm^3$.

$$z_s = 40h \tag{2.13}$$

With equation 2.13, where z_s is the depth of the interface below sea level and h is the fresh water head, the location of the interface can be estimated. Known fresh water heads in the alluvial aquifer can be used for this. The available fresh water heads come from well measurements in W_3 , piezometer $P2W$, and some manual water level measurements in wells W_4 , W_7 , W_8 , and W_9 which were conducted in a previous study by Calderon in 2010 [10]. The resulting estimated depths of the interface are listed in figure 2.6.

Salinity measurements performed in the wells at September 24, also listed in figure 2.6, were plotted against the perpendicular distance between the wells and the shore; low and high tide. This plot is shown in figure 2.7, together with the estimated interface depths z_s . A clear relation between salinity and distance to the sea is found. The area between the high and low tide plots could indicate the location of the mixing zone, induced by pressure changes between low and high tide. The relation between z_s and the distance to the coast is a little bit less pronounced, but does show an overall pattern of a shallow located mixing interface near the coast and a deeper located mixing interface away from the coast. To understand the influence of drought on the interface location however, a long period of monitoring is necessary. The head measurements used to create this estimation are few and sparse, resulting in a vague and uncertain interface.

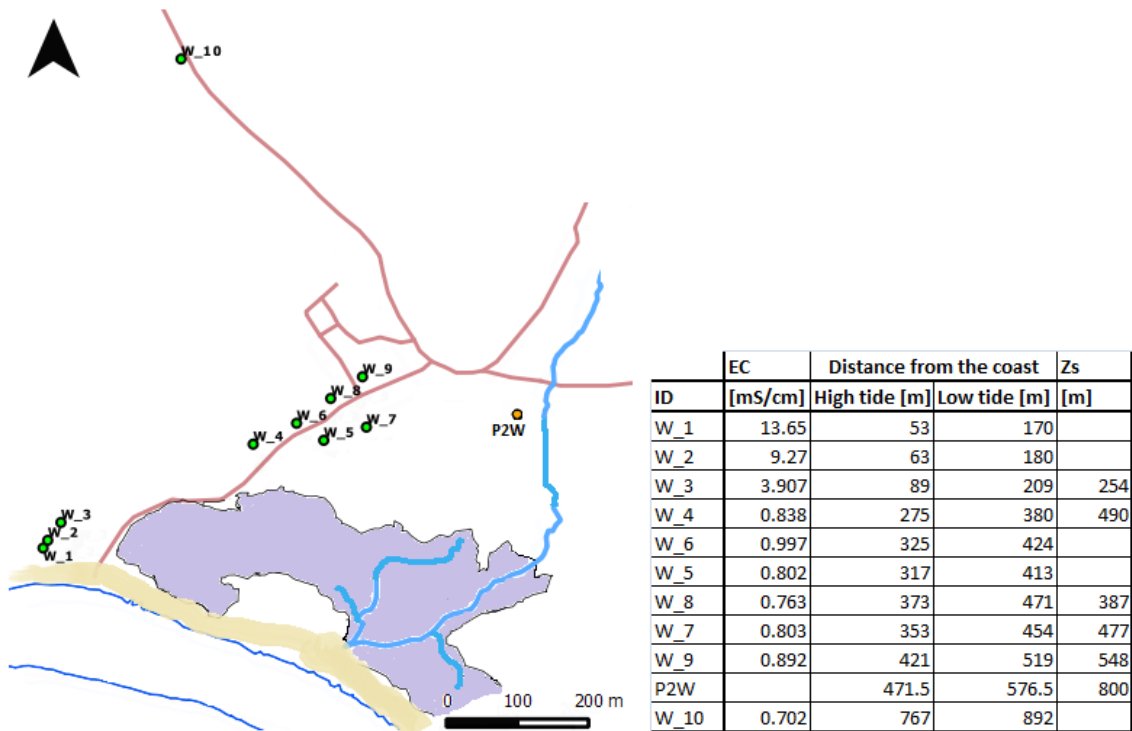


Figure 2.6: On the left, an overview of the separate wells and their relative distance to the shore, high and low sea tide, is shown. These distances are then listed in the table next to it, also showing the measured salinities in those wells and the estimated depth to the interface below mean sea level.

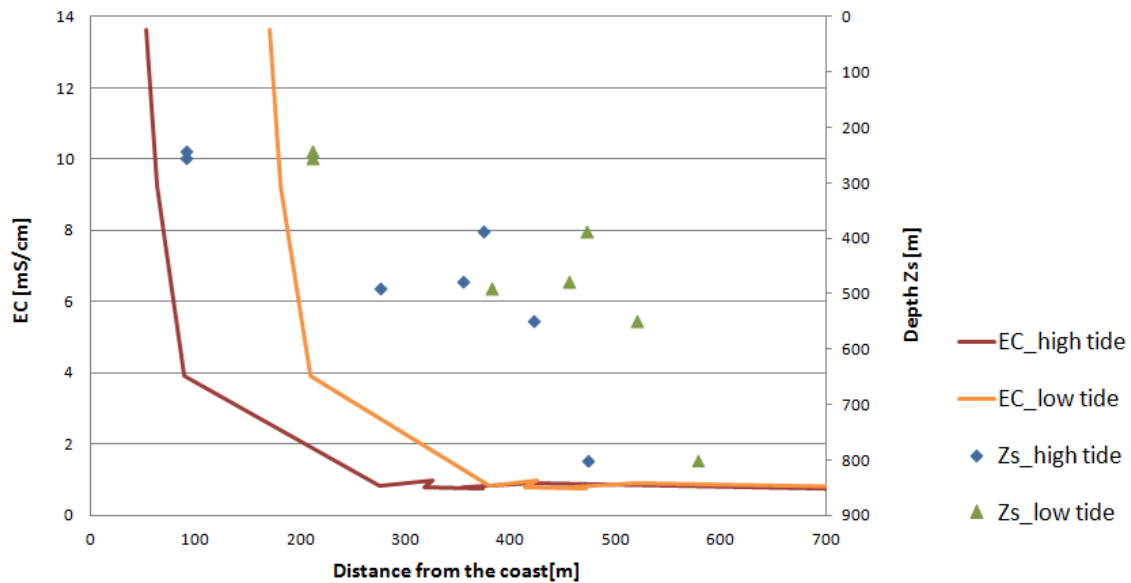


Figure 2.7: Relation between well salinity and the distance of these wells from the coast, as well as the relation between z_s and the distance of these fresh water heads from the coast. Keep in mind that these wells have an approximate depth of 4 to 8 m, thus the comparison between z_s and EC can be sophisticated.

2.2.2 Pore water salinity in the floodplain

Pore water salinity in the floodplain ranged from approximately 10 to 30 mS/cm , as can be seen in figure 2.8. Immediately catching the eye are the differences between previously mentioned levels in

the estuary waters, and pore water salinity levels measured in the floodplain. For example, salinity in piezometer F_5 was 13.85 mS/cm at September 17, while 3 meters next to it the estuary surface water measured only 1.22 mS/cm . That pore water salinities in mangrove swamps can be much higher than those of surface water salinities, has been mentioned also by Taal [13], Jimenez [8], and Myers [83]. According to Myers [83], substrate further from shore is less frequently flushed by tidal action and is thus more susceptible to accumulation of higher salinities.

The Ostional floodplain is less influenced by tidal action, and more by inundation. Four different stages of inundation to be precise, from fresh water inundation to salt water inundation, to no inundation at all. When river discharge is no more, and the sandbar holds most tidal influence, evaporation and infiltration remove all residual inundation. Once in a while this pattern is disturbed by an over-wash event, inundating the area again with sea water. And, as salt water inundation evaporates, salinity of the soil increases.

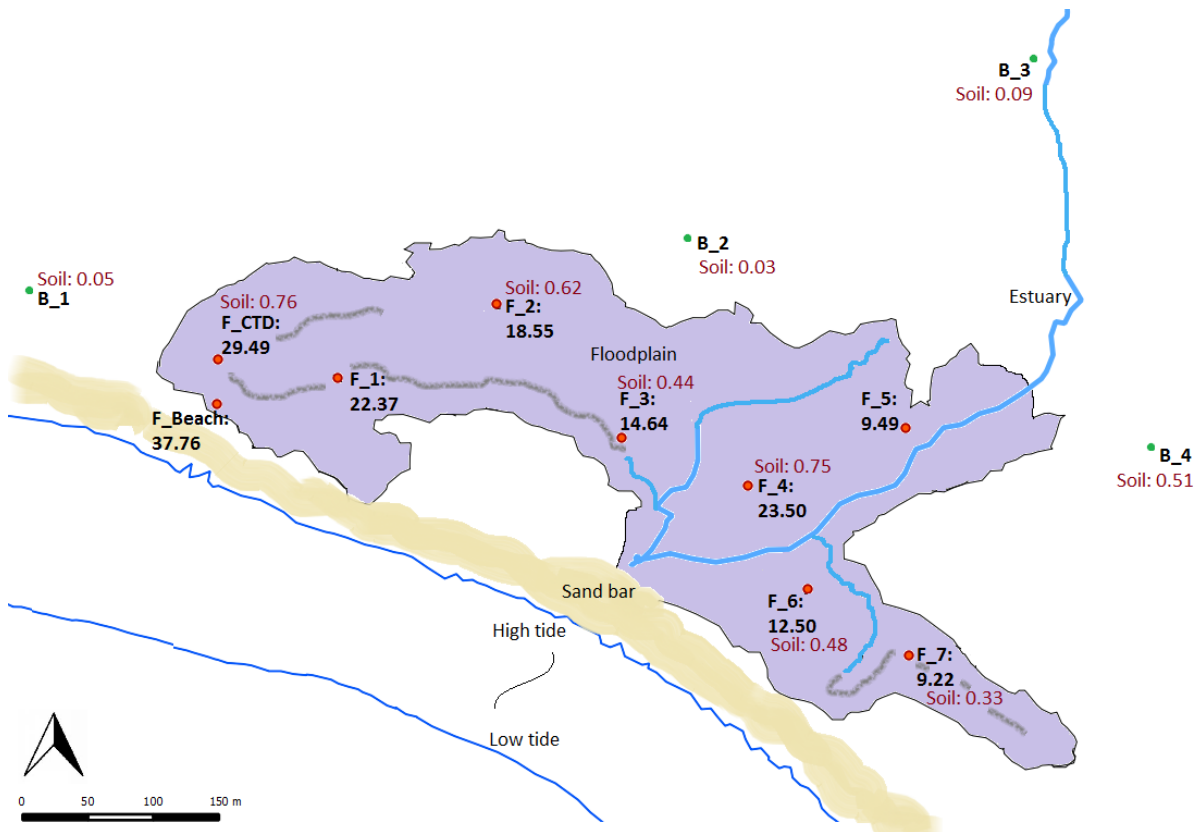


Figure 2.8: Locations of the floodplain piezometers ($F_1 - F_7$, F_{CTD} , and F_{Beach}), showing the average pore water and diluted soil salinity levels [mS/cm], measured throughout the study period. The points B_1 to B_4 show locations of soil salinity measurements outside the floodplain area. Pore water salinities are shown in black and bold, while soil salinities are shown in brown and represent salinities after dissolving the soil in purified water.

Clay soil salinities

This would mean that soil salinities beyond the floodplain are distinguishably lower, since no inundation takes place and therefore also no accumulation of salt. To check if this was indeed the case, soil salinities were measured. This was done next to most piezometers in the floodplain, and at four different locations outside of the floodplain area; points B_1 to B_4 . Every 20 cm a soil sample was taken, resulting in a graph that shows diluted salinity depth profiles at each location, depicted in figure 2.9.

An average of these salinities can be found in figure 2.8, where diluted soil salinities can be compared

with pore water salinities at the same location. And indeed, these values show clearly that all locations outside of the floodplain area contain much lower salt amounts, except for B_4 . When one compares the soil and pore water salinities of F_{CTD} and F_4 , both turn out to be higher compared to the other locations. Likewise, F_2 , F_3 , F_6 , and F_7 show similar relations between soil and pore water salt levels, resulting in a correlation of $R^2 = 0.95$. That B_4 turns out to contain such high soil salinity levels, thus means that it occasionally has been flooded. This was confirmed by residents of El Ostional who described that the area where B_4 is located used to be inundated more frequently. This area is now cleared land, shown in figure 1.1 of Part I. Whether inundation frequency has decreased due to elevation increase (sedimentation) or due to human physical alterations, is unclear.

Looking more carefully at the soil salinity profiles in figure 2.9, two extra observations can be made. First of all, the profile of B_3 shows a sharp increase in salinity at a higher depth. These samples, in contrast to the other soil samples, were taken from the riverbank. B_3 is located in the bay-head delta. When high water levels in the estuary occur, depth 5 and 6 are usually reached, which are depths of 100 to 120 *cm*. That soil salinities at those depths increase, might indicate that indeed the salt intrusion length in the estuary is large enough to increase saline soil conditions in this area. Secondly, the soil salinity profiles of F_4 and F_7 show an interesting curve, being relatively low at first and increasing in depth. Coincidentally or not, these two locations also had the highest amount of crab burrows. Perhaps, flushing of this area is more effective due to the high amount of crab burrows. Increase in salinity with depth thus reflects an increasing dilution by rainwater. Similar findings were done in Brazil [49], where sampling was indeed carried out during the rainy season.

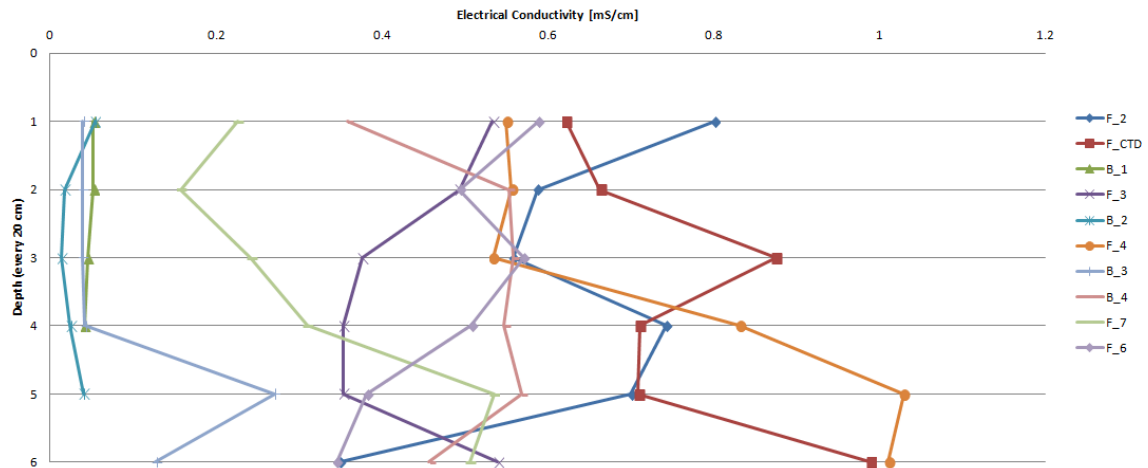


Figure 2.9: Soil salinity profiles for all locations shown in figure 2.8. Every 20 *cm* a sample was taken. The sample was then dissolved in purified water, where after EC of the solution could be measured.

Filling a bowl

Although the presence of high pore water salinities has been explained, the relative salinity variations have not. Like Myers, Jimenez [8] describes the relation between increasing pore water salinities with an increasing distance from the estuary channel. And indeed, F_3 , F_2 , F_1 , and F_{CTD} , show this relation; salinities increase with greater distance from the main estuary channel. However, the other side of the estuary does not show this relationship. Jimenez [8] relation is based on the fact that inundation frequency decreases with increasing distance from the estuary. With less inundation, less flushing of the soil occurs, and more evaporation takes place leaving salt behind.

Thus, looking into the Ostional floodplain, the locations with high pore water salinities should be less often inundated. In figure 1.1 of Part I, a gray mark was already drawn to indicate lower

elevation. These lower elevations run through the branches, into the estuary. The first step after water levels increase in the estuary and over-top the estuary banks, is that these gray bands quasi become part of the branches. The second step is that the floodplain is filled like a bowl of rice. Although elevations were not measured in such detail, these lower bands were quite clearly visible, and are thus also shown in figure 2.8. It immediately accounts for the lower salinities in location F_3 , and F_7 , and indirectly for location F_5 which lies 3 m from the estuary banks. To explain the much higher salinities of F_1 , F_{CTD} , and F_{Beach} , the over-wash events need to be taken into account. During these events, these were the first inundated locations, with pure sea water, what leaves higher salinities after infiltration and evaporation.

2.2.3 Connection between the alluvial and floodplain aquifer

All in all, the subsurface of the Ostional area could be conceptualized as sketched in figure 2.10. This sketch shows both the alluvial aquifer and its connection with sea, as well as the floodplain aquifer located into the alluvial aquifer.

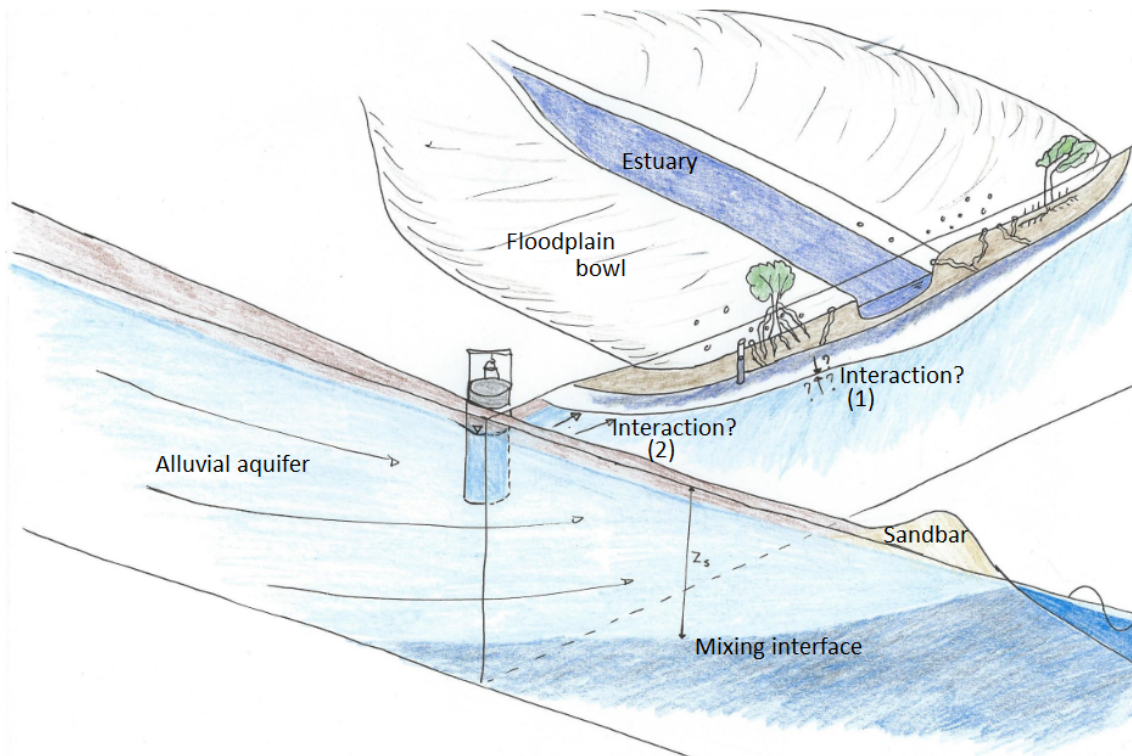


Figure 2.10: Sketch of the subsurface beneath Ostional.

While both separate aquifers now have been analyzed and their occurring salt concentrations have been clarified, this reveals nothing about the interaction between the two aquifers. Material available during the field study did not permit any view into the subsurface deeper than 1.25 m, which is a rather limiting view. The only other available information on the subsurface mostly focuses on the alluvial aquifer, but does reveal that the clay layer is not much thicker than around 3 m [10]. Are thus the remaining 1.75 m that could not be examined part of the floodplain aquifer, that is to say a mixture of clay, silt and organic matter? Or is the bottom again sealed by a confining layer of almost pure clay? Is there a flow of water between the two aquifers?

A couple of factors do suggest that there must be an interaction. For instance (1), since there occurs subsurface flow from the alluvial aquifer into the estuary, and the largest part of the estuary lies in the clayey soil of the floodplain, this might also suggest a subsurface flow from the alluvial aquifer into the floodplain aquifer. According to Jimenez [8], the occurrence of Buttonwood trees

on the edge of the floodplain is an indication that there is a fresh water infiltration into the saline zone. It was however also evident that there was no average water table increase in the floodplain without precipitation or over-wash events. If water infiltrates from the alluvial aquifer into the floodplain aquifer, it should also ex-filtrate somewhere again. Another inkling (2) is provided by the observed water table fluctuations in the floodplain aquifer that imitate the sea tide fluctuations. These fluctuations can only be induced by pressure differences in the subsurface from the sea tide through the alluvial aquifer into the floodplain aquifer.

Would we know whether there is an interaction or not, then it might reveal what happens to the salt that is flushed through the crab burrows. In normal years, the floodplain will be inundated and the aquifer will be flushed with water. When drought occurs, the flushed salt ends up in the floodplain aquifer. It is important to understand whether an accumulation of this salt would take place, or if it will interact with the alluvial aquifer thereafter. If the salt would accumulate, this would have a negative influence on the mangrove trees. Would it infiltrate into the alluvial aquifer, this might have a negative influence on the salinity of the wells used by the village. Either way, an important unanswered question it is.

2.3 Salt intrusion with an opened sandbar

During drought, the singular times salt intrusion genuinely materializes, is when the sandbar is over-topped during an over-wash event. One of these over-wash events was around October 28, and the sea tide from which this over-wash followed is shown in figure 2.11. The same figure shows the water levels in the floodplain and estuary in that period. The result of the over-wash can be seen in the increase of water level in both the floodplain aquifer as in the estuary. All water levels have been assumed a certain level according to the chosen datum b.s.s., and a possible height of the sandbar can be estimated accordingly. It indicates a sandbar that is elevated 40 cm above the floodplain soil surface, which is then over-topped at the highlighted moments in figure 2.11.

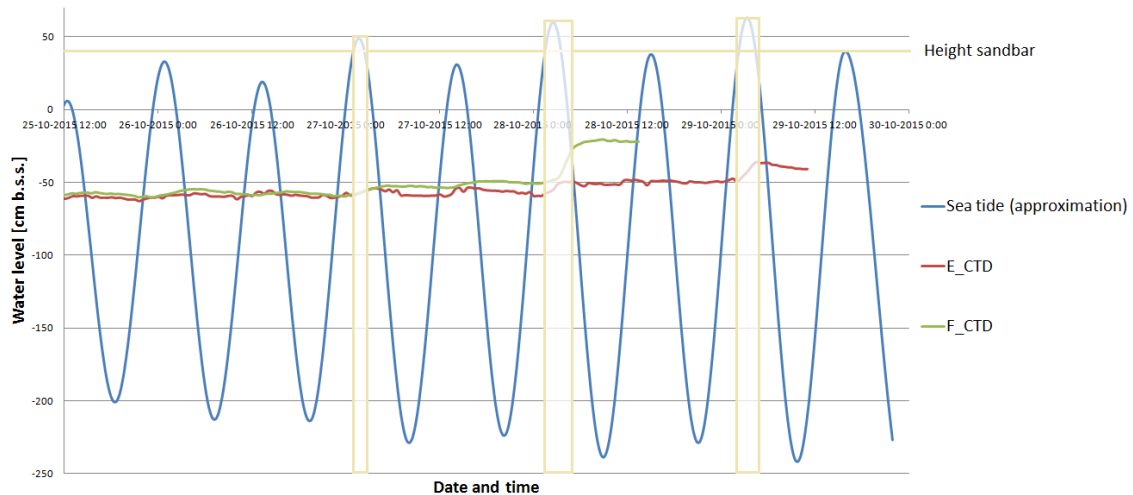


Figure 2.11: Plot of the sea tide (approximated according to datum b.s.s.), the floodplain aquifer water table in F_{CTD} , and the estuary water level at E_{CTD} , during the last spring tide during the field work period. This last spring tide caused the over-wash event around October 28.

The community attempted to manually rupture the sandbar by digging a channel. The attempt failed because according to them, the water level in the estuary was insufficiently high, which meant that the channel should have been dug deeper. A manual rupture is hard labor, and thus the rupture was not considered worth while any more. Considering the case that the communities attempt had succeeded and the sandbar would be opened during the occurring drought, the rupture would have reached at least estuary water level to ensure a good connection. This would consequently lead to:

1. The inflow of sea water during high tide into the estuary and floodplain.
2. The increase in water levels in the estuary and floodplain. Subsequently leading to on and off inundation of the floodplain.
3. Through this, the estuary salt intrusion would be immense. The groundwater inflow is certainly not able to withstand this amount of salt input, and the estuary water would soon reach sea salinity levels.
4. The inundation water in the floodplain will hence contain sea water salinity.
5. The floodplain will be inundated only at high tide, leaving salt behind every time the water level drops.
6. At a certain moment, nature will take over and the sandbar will close again.
7. The closed sandbar leaves an estuary with salt conditions similar to the sea, and a floodplain were again salt water evaporates what leaves behind salt, increasing soil salinity.
8. It might take a long time, but the estuary will reach a steady state again, with unknown salinity levels.

The increase in water level will actually have a positive effect on at least the White mangrove's well-being. After all, it was concluded previously that the lack of water had a negative effect on the White mangrove trees. The increase in salinity however cannot have a positive impact whatsoever. First of all, this increase in salinity will negatively brunt the Tea mangrove trees. These trees will have to cope with a salinity level equal to their tolerance. This might be difficult, but possible. However, the effect it will have on the soil salinities after evaporation has done its work, indirectly will increase salinity levels in the floodplain. How low it will take to increase saline conditions above the Tea mangrove tolerance is unclear, but eventually harmful saline condition might be reached. But it does not stop there. The established Red and White mangrove trees have been able to grow so tall due to low saline conditions. The moment these conditions change however, their height might be a problem again.

Chapter 3

Conclusions

An answer was sought for the question: *Can the salt intrusion of the blind estuary and its surrounding groundwater system be described and predicted during a drought?* Salt intrusion in the estuary was caused by over-wash events and forced by a fresh water inflow together with a muted tide. This could be described with a steady state model. The surrounding groundwater system was divided into two separate systems which were subject to two different causes for salt intrusion. Salt intrusion into the alluvial aquifer was mainly induced via groundwater pressure, and could be described by the Ghyben-Herzberg relation. Salt intrusion into the floodplain was principally caused by evaporation of saline water, and could be related to inundation frequency. Prediction of salt intrusion into the blind estuary proved yet to be impossible. Salt intrusion in the surrounding groundwater system is less dynamic, and prediction is thus less useful. It is important however to keep track of salinities in the groundwater systems in order to know whether salt levels increase, both for the sake of humans and of mangrove trees.

Salt intrusion resulted in a well-mixed estuary. The mechanism that drive this mixing were hard to detect, since separate dimensionless numbers like N , N_R , and K indicated a different balance. Mixing due to wind has not been taken into account, but is suspected to be highly influencing the circulation process. That detecting of the mixing mechanisms is difficult is due to the small tidal and fresh water fluxes, where the latter proved hard to estimate. Several measurements could not be modeled, since these measurements were taken when the estuary was in an unsteady state due to just occurred over-wash events. Evaporation was not taken into account during the model exercises. When applied onto the salt balance, the influence of evaporation on the appearing saline conditions proved to be less important than the fresh water inflow. When the salt balance is used to calculate the fresh water inflow amount, it reveals a similar discharge as measured with the seepage meter.

The mixing interface in the alluvial aquifer was estimated to be at $z_s = 254m$ beneath W_3 at a distance of $89 m$ from the shore, while beneath $P2W$ ($472 m$ from the shore) the interface lay at $z_s = 800m$ depth. These calculations could be compared with manual measurements that showed a mixing zone between approximately 50 to $200 m$ from the coast for wells of around $8 m$ deep.

Pore water salinities in the floodplain are higher due to high soil salinities. Thanks to salt water evaporation or infiltration the floodplain soil is almost saturated with salt. The deeper situated in the floodplain, the fresher the soil, hence the fresher the pore water. Higher elevations are less frequently inundated and in such a way less often flushed. Some anomalies in the salinity pattern occur due to over-wash events that inundate specific areas more near to the shore.

Would the sand bar be ruptured during drought, the effects are an increase in water level and salinity. Saline conditions would increase thus, that they would resemble sea salinity. Although higher water levels might have a positive impact on the water stress of the White mangrove, the higher salinity levels could turn out to be disastrous for the Tea mangrove trees.

Part IV

Concluding remarks and recommendations

Chapter 1

Synthesis

The separate research questions have been answered, and certain knowledge has been gathered to reach the objective. This chapter will thus address the final research objective, and whether or not it has been achieved. The research revealed other insights, which will be proposed as new hypotheses.

1.1 Retrospect on the objective

The research objective was **to understand the influence of a sandbar in front of a blind estuary, on the well being of a mangrove forest during a drought**. The objective is threefold. When understanding is sought on the influence of a sandbar, one has to consider (1) that this landform has a direct influence on the mere existence of the mangrove population by closing the blind estuary from time to time, (2) that the effects the landform imposes on hydrological circumstances in the blind estuary again effect the well being of the mangrove forest, and (3) that these effects can be enlarged or disturbed by drought.

The direct consequence of having a sandbar (mostly temporarily) in front of a blind estuary, is that it provides mangrove trees with a protected environment, shielding them against the harsh sea milieu. It does more than that, it delivers an environment predominantly suited for mangrove trees. In the Ostional area it results thus in an interior mangrove forest, which are known to be one of the most productive types of mangrove forests.

That the environment is predominantly suited for mangrove trees is due to the hydrological circumstances in a blind estuary. A sandbar when closed functions as a natural levee, dike or weir. It thus holds water, mostly fresh, before releasing it to the sea. It stores water, inundating a floodplain and delivering mangroves a modus to reproduce, master other trees, and grow. Due to the sandbar, inundation in the floodplain is infrequent. In contrast with other areas, inundation occurs only for certain periods throughout the year. More sparse, but protracted periods. The Mouthless crab living in the floodplain of Ostional only lives here because of this reason. These type of land crabs do not like inundation too often, so a generally dry floodplain suits them best. Burrows are therefore present anywhere in the floodplain, where they help maintain the forest ecosystem by increasing permeability of the soil. The sandbar in a similar way stems, retards and mostly stops tidal sea water to enter the estuary and floodplain when river discharge is not sufficient. Acting thus, the water in the estuary remains relatively fresh. Mangrove trees are able to withstand saline conditions, but flourish in fresher regimes. Specifically in the Ostional area, the fresh state of the estuary results in the possibility for the Tea mangrove to grow there since their salt tolerance is low.

During drought, the seasonal river remains dry and thus the sandbar remains closed for a longer period of time than usual. This is positive for the mangrove trees for it holds back the sea water that would increase saline conditions dramatically. It also however holds back sea water that

could inundate the mangrove trees, providing them with the necessary water to reproduce, master and grow. It also blocks one of the main functions an estuary and mangrove forest provide; a nursery habitat for many fish and invertebrate species. When opened, sea life can enter through the connection with sea in order to reproduce. This also provides the fishing cooperation with more income, for they have easy prey entering the estuary, and indirectly in the future since reproduction is necessary to sustain a fair fish population. The manual rupture of the sandbar during drought thus has a twofold consequence. The rare Tea mangrove might not like the amount of added salt, but on the other hand water shortage will not be a problem and sea life can enter. Since no river discharge will maintain the rupture, the sandbar is not likely to remain open and damage will perhaps be limited.

1.2 New hypotheses

1.2.1 Survival of the Tea mangrove

The Ostional estuary surface waters are relatively fresh compared to other estuaries during drought. This is caused by the combined efforts of a sandbar closing the estuary, and the persistent inflow of fresh groundwater. The groundwater inflow occurs at the bay-head delta and comes from an alluvial aquifer. Through the sandbar, also flow occurs, with a average flow direction from estuary to sea. In combination with pressure changes in the subsurface, a muted tide is induced in the estuary instead of normal sea tide. The fresh water in the estuary has a positive influence on mangrove production and permits growth of the Tea mangrove.

1.2.2 Not salt but inundation induces zonation

While salt plays a big role for mangrove trees to prefer a certain area, they are not the only trees able to withstand these areas. So are for example Jicaro, Manchineel or Neem trees. Mastery over other trees is only given due to their possibility to grow in inundated areas, because of their root adaptation. Mangrove trees need water not only for their general growth cycle, but also to inundate the area. Inundation both ensures germination of propagules and thus reproduction, as well as the mastery of mangrove trees over other species, like Neem.

1.2.3 Crab burrows

Crabs turn out to play an important ecological role with their burrowing activities in the sediment. It was known that crabs in that way increase permeability of the soil. In this research it is shown that the increased permeability induces an increased soil moisture and a decreased soil salinity. Both effects influence mangrove growth and survival in a positive way.

1.2.4 Mixing in blind estuaries

Closed blind estuaries are not always considered to resemble true estuaries since most of the main driving forces affecting the character of estuaries are undetectable. In-depth research in the Ostional estuary shows that tide, fresh water discharge and density differences do play a role in the mixing and characterization of the estuary. With the help of the steady state model developed by Savenije, it was shown that indeed circulation is induced by fresh water inflow on one hand and tidal flow on the other. Fresh water inflow is represented as groundwater ex-filtration and tidal flow by a muted tide that is induced by pressure changes and seepage through the sandbar. Blind estuaries do differ from other estuaries; over-wash events supply the salt input instead of a tidal flood volume, and the influence of wind is more dominant compared to other estuaries.

Chapter 2

Discussion

All in all, the objective does seem to be reached. In this chapter some dubiety on certain factors of the research are set out in order to estimate how credible and genuine the conclusions are.

2.1 Measurements

2.1.1 Short study period

A great deal of the drawn conclusions are based on measurements conducted in the field, over a period of three months. For constructive conclusions to be drawn, it can be discussed that three months is by far not enough. Long periods of monitoring provide more trustworthy data series, in which unreliable data can be filtered out. A longer period of monitoring also provides the researcher with the possibility to compare the period of interest with other periods. In this way the one is able to see differences between dry and wet circumstances for example. This was not possible during this research, and such patterns needed to be estimated on the basis of village knowledge and the small amount of previous research conducted in the area. On the other hand, the three months of constant research were intense and highly productive. Many measurement were taken and various methods were used.

2.1.2 Error propagation

Collection of data comes with many errors. The errors are due to the measurements device, the person conducting the measurement, or perhaps due to wrongly copied values, etc. Measurement errors then propagate in further analyses, which can result in higher error. The research was conducted under poor funding circumstances, and thus equipment was either old, hand-made, or very simple. Several of the devices, like for example the self-made evaporation pan or seepage meters, resulted in either inaccurate or heterogeneous data. Other measurements, like for example the inverse auger hole infiltration tests, were conducted a little different than required for the method to analyze them. Moreover, some measurements like the salinity measurements in the wells, were only performed once, what reveals a whole lot of other uncertainties.

All these errors give rise to mistrust the data and the conclusions based on them. To contra this uncertainty, the research has focused not on finding precise values for a specific detail, but on conceptualizing the system with averages found in these measurements. Furthermore, various measurements and methods were combined to be able to back the separate findings. This was done primarily by doing continuous and manual measurements of the same parameters. The moment the two measurements revealed a substantial discrepancy, the errors could be distinguished. Another way was by combining observations with several types of experiments and methods. The most elaborate

combinations have been made to determine the fresh groundwater flow. First, observations on salinity levels and Tea mangrove presence gave insight to the plausible existence of such a flow. To back this, seepage measurements were conducted. And to check this, water tables in the alluvial aquifer were measured. Then, the fresh water flow was again estimated by using a water balance. Another example are the evaporation measurements, which have been used together with measurements conducted in Rivas.

2.1.3 Unknown elevation heights

Although DGPS points have been taken, the data could unfortunately not be accessed. For that reason, an assumption was made on behalf of all the water level measurements in the estuary. This assumption was mainly based on observations. The relative difference in height between heads measured separately, can be completely wrong however. This is very important to keep in mind when handling the data and the results. Fortunately, the ultimate conclusions are less dependent on this uncertainty, since the overall scale of the research is less detailed.

2.2 Steady state salt intrusion model

While a blind estuary can certainly be described as an alluvial estuary, the step to use a model developed for open estuaries on a closed blind estuary is big. And although it did seem applicable, some footnotes need to be made. First of all, the model was applied to only five separate measurements. This is probably not enough to say whether or not the model really fits, or that calibration made it fit. Next to that, each of these five measurements were performed over a couple of hours. They were not measured at a fixed tidal average or perhaps high water slack, on which the model is based. And finally, the model calculates salt intrusion due to gravitational and tidal mixing. These fluxes are small in the blind estuary, while wind seems to be a large influence as well. The more mixing is caused by wind, the less appropriate this model becomes. That the model cannot be used to predict the salt intrusion only confirms that suspicion. The use of the model however does confirm the type of salt intrusion and the existence of a fresh water source during drought.

2.3 Blind estuaries in general

The research aims at understanding the influence of a sandbar in a blind estuary on mangrove forests. The conclusions are thus also generalized on all blind estuaries and mangrove forests. However, only one study site, namely the Ostional area, has been thoroughly investigated. Plausible as it seems that other blind estuaries show the same characteristics, this needs further analyses. Two nearby blind estuaries were visited (see Appendix C, Section 4.3), which already revealed differences with the Ostional estuary and mangroves. The La Flor blind estuary for example, contained water with sea salinity. Giving incentive to believe that no fresh water source was available here. The San Juan del Sur blind estuary was also more saline, but did show a similar gradient to the gradient visible in the Ostional estuary. Although it thus seemed to have a fresh groundwater source as well, the Tea mangrove did not grow here. The differences between these three blind estuaries close to each other, makes the potential to generalize less plausible.

Chapter 3

Recommendations

The objective was stated in order to recommend management plans that can combine a healthy ecosystem with an upcoming community life. In the following chapter an attempt is made to set forth recommendations that can provide just that.

3.1 Protection of the ecosystem

The overall results of this research confirm again the fact that separate species in an ecosystem are interdependent of each other. This means that when certain species are removed, this will have a direct or indirect influence on other species in the ecosystem. The ecosystem has found an equilibrium where every biotic and abiotic factor is important. The ecosystem might be able to adapt to slow changes in these separate factors, finding a new equilibrium on its own. In this research the role of the crabs on the well being of the mangrove trees is a clear example of such interdependencies. Another example is the upcoming but non-native Neem tree, that does not participate in the ecosystem but tends to grow rapidly and thus forms a threat. In order to protect and maintain the mangrove population currently existing in Ostional, it is thus very important to keep this in mind. Protection of the mangrove trees goes together with the protection of the complete ecosystem, and the control of this invading species. It is almost impossible to protect only a certain tree like the Tea mangrove, without protecting the complete system maintaining it. Mankind often forms a problem, since changes they induce come sudden, and the impact can thus be large. This does not mean that the influence of humans is ever negative. For example, the cow manure is beneficial for the small crabs in the floodplain. Still, focus on diminishing certain practices as the dumping of litter and trash in the floodplain and surrounding forest, as well as the land clearance of the surrounding area, is certainly important to protect the ecosystem.

3.2 Maintenance of groundwater flow

The occurrence of a fresh groundwater flow into the estuary seems highly important to sustain life in the Ostional area. First of all it creates a relative fresh water estuary, beneficial for the mangrove trees, and indispensable for the Tea mangrove. Furthermore, it makes sure that salt intrusion in the subsurface is minimal. This sustains life for the villagers, them being dependent on groundwater for their water supply. This groundwater flow thus is important to maintain, and is dependent on infiltration more upstream in the catchment. Hence, maintenance of the upstream catchment forests is essential, which will indirectly help to maintain the soil infiltration capacity.

3.3 Manual rupture of the sandbar

One of the main human impacts identified in this research is the manual rupture of the sandbar. It depends on the value of several factors whether this needs to be averted or not:

1. When river discharge is low, but rupture of the sandbar is induced, this could on the long term be destructive for the Tea mangrove, a rare species.
2. Possibly though, when drought is persistent, the opening could provide the (White) mangrove trees with water to survive.
3. And moreover, the estuary needs to connect with sea once in a couple of years at least to be able to function as a nursery for fish and other invertebrates.

3.4 Recommended research topics

As in all researches, it ends with almost more questions than answers. Further research is necessary on the formulated hypotheses, conclusions, and not touched-upon subjects.

3.4.1 In the Ostional area

- Perform research in the estuary when the sandbar is opened, with and without river discharge available. How is salt intrusion propagating in those stages?
- Sedimentation is often influenced by the availability of mangrove trees. The sandbar also highly influences the type and amount of sedimentation in the area. This needs to be researched when the river transports the sediment.
- Monitor the area for longer periods. That will provide longer data series that can be used to update management plans. This includes the estuary, but also the salinity of the wells in order to keep track of the mixing interface location in the subsurface.
- Map the area on elevation, type and amount of species. This information can then be used to manage and sustain the ecosystem.

3.4.2 Blind estuaries and mangroves in general

- Perform similar researches in other blind estuaries to confirm the hypotheses.
- Apply the steady state model in other blind estuaries.
- Research the influence of fresh groundwater inflow on the estuary by performing a research in for example La Flor.
- Investigate the function of nectaries on the White mangrove tree.

Bibliography

- [1] J.H. Day. What is an estuary. *South African Journal*, 1980.
- [2] Hubert H. G. Savenije. *Salinity and Tides in Alluvial Estuaries*. Number First edition. Elsevier, 2005.
- [3] Gerardo ME Perillo. *Geomorphology and sedimentology of estuaries*, volume 53. Elsevier, 1995.
- [4] Edward J Anthony, Lucien M Oyédé, and Jacques Lang. Sedimentation in a fluvially infilling, barrier-bound estuary on a wave-dominated, microtidal coast: the ouémé river estuary, benin, west africa. *Sedimentology*, 49(5):1095–1112, 2002.
- [5] J.A.G. Cooper. Geomorphological variability among microtidal estuaries from the wave-dominated south african coast. *Geomorphology*, pages 99–122, 2001.
- [6] P.S. Roy. New south wales estuaries: their origin and evolution. *Coastal Geomorphology in Australia*, pages 99–121, 1984.
- [7] Stephen J.M. Blaber. *Tropical Estuarine Fishes; Ecology, Exploitation and Conservation*. Blackwell Science Ltd, 2000.
- [8] Jorge A Jiménez-Ramón. *Los manglares del Pacífico Centroamericano*. 1994.
- [9] Yaez-Arancibia A. Jimenez, J. and A. Lara-Domnguez. Ambiente, distribucin y caractersticas estructurales en los manglares del pacifico de centro amrica: contrastes climticos. *Ecosistemas de manglar en Amrica Tropical*, 1999.
- [10] HL Calderon Palma. *Surface and Subsurface Runoff Generation Processes in a Poorly Gauged Tropical Coastal Catchment: A Study from Nicaragua*. CRC Press/Balkema, 2014.
- [11] R.T. Weeda. Hydrogeobiochemistry in a small tropical delta. Technical report, Department of Hydrology, VU Amsterdam, 2011.
- [12] Kai C. Rains and Mark C. Rains. Mangrove and mangrove-fringe wetlands in ostional, nicaragua. Technical report, School of Geosciences, University of South Florida, 2015.
- [13] MD Taal. Flow and salt transport in mangrove swamps. Technical report, TU Delft, 1994.
- [14] Joanna C Ellison. Mangrove retreat with rising sea-level, bermuda. *Estuarine, Coastal and Shelf Science*, 37(1):75–87, 1993.
- [15] Lara Krinsky. Florida’s mangroves: An overview. *University of Florida*, 2010.
- [16] Chris Dolce. El niño: The facts behind the impacts, 2015. Retrieved at 14-12-2015.
- [17] Bob Petz. El niños are growing stronger, 2010. Retrieved at 14-12-2015.
- [18] Judy Z Drexler and Katherine C Ewel. Effect of the 1997–1998 enso-related drought on hydrology and salinity in a micronesian wetland complex. *Estuaries*, 24(3):347–356, 2001.
- [19] Jos Adn Silva. El niño triggers drought, food crisis in nicaragua, 2014. Retrieved at 14-12-2015.

- [20] INETER. Ineter pendiente el niños, 2014. Retrieved at 14-12-2015.
- [21] Carlos M Duarte, Jennifer Culbertson, and BBVA Fundación. *Global loss of coastal habitats: Rates, causes and consequences*. Fundación BBVA Madrid, Spain, 2009.
- [22] Paso Pacifico. Conservation is about making connections, 2006. Retrieved at 14-12-2015.
- [23] Takeuchi-K. Franks S. W. Gupta V. K. Karambiri H. Lakshmi V. Liang X. McDonnell J. J. Mendiondo E. M. O'Connell P. E. Oki T. Pomeroy J. W. Schertzer D. Uhlenbrook S. Sivapalan, M. and E. Zehe. Iahs decade on predictions in ungauged basins (pub), 2003-2012: Shaping an exciting future for the hydrological sciences. *Hydrological Sciences Journal*, 2003.
- [24] L.R. Holdridge. Life zone ecology. *Costa Rica: Tropical Science Center*, 1967. Revised ed.
- [25] Paso Pacifico. Welcome to the ostional mangrove. Retrieved at 13-08-2015 at an information board.
- [26] FAO SDRN Agrometeorology Group. Köppen climate classification, 1997. Accessed on 25-2-2016.
- [27] CIRA. Disponibilidad actual y futura de los recursos hídricos en la franja costera del municipio de san juan del sur. Technical report, Managua: Centro para la Investigación en Recursos Acuáticos de Nicaragua, 2008.
- [28] Google Earth. 11 °06'46.51" n 85 °45'43.84" w. Date of material: 10-12-2011. Accessed on 21-12-2015.
- [29] Maryland School. School improvement in maryland. Online, Accessed at 06-09-2005.
- [30] J Kessler and RJ Oosterbaan. Determining hydraulic conductivity of soils. *Drainage principles and applications*, 24, 1974.
- [31] Hubert H. G. Savenije. *Salinity and Tides in Alluvial Estuaries*. Number First edition. Elsevier, 2005.
- [32] Charles R. Fitts. *Groundwater Science*. Elsevier Inc. Second edition., 2013. doi:10.1016/B978-0-12-384705-8.00001-7.
- [33] SINAPRED. Plan de gestión de riesgos. departamento de rivas. municipio de san juan del sur.(risk management plan), 2005. Online.
- [34] M.E. Donselaar. The holocene holland tidal basin: From outcrop to reservoir model. Presentation course AES1830, number 8, Case Study 1, Delft Technical University.
- [35] Colin D. Woodroffe. *Coasts: Form, process and evolution*. Cambridge University Press, 2002.
- [36] J. Krasny and G. Hecht. Estudios hidrogeológicos e hidroquímicos de la región del pacífico de nicaragua. 1998.
- [37] Hubert H. G. Savenije. *Salinity and Tides in Alluvial Estuaries*. Number First edition. Elsevier, 2005.
- [38] Robert W Dalrymple, Brian A Zaitlin, and Ron Boyd. Estuarine facies models: conceptual basis and stratigraphic implications: perspective. *Journal of Sedimentary Research*, 62(6), 1992.
- [39] Florida Museum of Natural History. South florida aquatic environments: Mangrove species profiles. Accessed at 22-12-2015.
- [40] Mangrove shop. Pelliciera rhizophorae, tea mangrove. Accessed at 22-12-2015.
- [41] Testudines. Hippomane mancinella, manchineel, manzanilla de la muerte. Accessed at 22-12-2015.

- [42] Stephen H. Brown. *Crescentia alata*: Mexican calabash, jicaro, morrito, winged calabash. From the Institute of Food and Agricultural Sciences (IFAS), Florida.
- [43] Waterwereld. Neem tree. Accessed at 22-12-2015.
- [44] Eric Olson. Coastal field guide crabs and fishes, el ostional. Unfinished photo gallery, 2015.
- [45] Foundation for Research and Social Development (FIDES). Recovery of mouthless crab (*cardisoma crassum*) populations in mangrove forests of the Chone river estuary (Ecuador). Accessed at 24-12-2015.
- [46] I Nagelkerken, SJM Blaber, Steven Bouillon, P Green, M Haywood, LG Kirton, J-O Meynecke, J Pawlik, HM Penrose, A Sasekumar, et al. The habitat function of mangroves for terrestrial and marine fauna: a review. *Aquatic Botany*, 89(2):155–185, 2008.
- [47] Peter M Sherman. Influence of land crabs *Gecarcinus quadratus* (Gecarcinidae) on distributions of organic carbon and roots in a Costa Rican rain forest. *Revista de biología tropical*, 54(1):149–161, 2014.
- [48] Erik Kristensen. Mangrove crabs as ecosystem engineers; with emphasis on sediment processes. *Journal of Sea Research*, 59(1):30–43, 2008.
- [49] JMC Araújo Jr, XL Otero, AGB Marques, GN Nóbrega, JRF Silva, and TO Ferreira. Selective geochemistry of iron in mangrove soils in a semiarid tropical climate: effects of the burrowing activity of the crabs *Ucides cordatus* and *Uca maracoani*. *Geo-Marine Letters*, 32(4):289–300, 2012.
- [50] Islam SS Mchenga, Prosper L Mfilinge, and Makoto Tsuchiya. Bioturbation activity by the grapsid crab *Helice formosensis* and its effects on mangrove sedimentary organic matter. *Estuarine, Coastal and Shelf Science*, 73(1):316–324, 2007.
- [51] Edward Castañeda-Moya, Victor H Rivera-Monroy, and Robert R Twilley. Mangrove zonation in the dry life zone of the Gulf of Fonseca, Honduras. *Estuaries and Coasts*, 29(5):751–764, 2006.
- [52] Ken W Krauss, Catherine E Lovelock, Karen L McKee, Laura López-Hoffman, Sharon ML Ewe, and Wayne P Sousa. Environmental drivers in mangrove establishment and early development: a review. *Aquatic Botany*, 89(2):105–127, 2008.
- [53] Cyril Marchand, F Baltzer, Elisabeth Lallier-Vergès, and Patrick Albéric. Pore-water chemistry in mangrove sediments: relationship with species composition and developmental stages (French Guiana). *Marine geology*, 208(2):361–381, 2004.
- [54] Jorge Jimenez. Mangroves in el ostional. Received at 15-10-2015.
- [55] Johan C Winterwerp, William G Borst, and Mindert B De Vries. Pilot study on the erosion and rehabilitation of a mangrove mud coast. *Journal of Coastal Research*, pages 223–230, 2005.
- [56] XL Otero, TO Ferreira, P Vidal-Torrado, and F Macías. Spatial variation in pore water geochemistry in a mangrove system (Pai Matos Island, Cananeia-Brazil). *Applied Geochemistry*, 21(12):2171–2186, 2006.
- [57] Google Earth. 11°06'46.51" N 85°45'43.84" W. Date of material: 1-1-1970. Accessed on 29-12-2015.
- [58] Salvador Manuel Sanchez. Sendero natural educativo. Project proposal to apply for funding, 2015.
- [59] Charles L Hogue and Willis W Wirth. A new central American sand fly breeding in crab holes (Diptera, Ceratopogonidae). Una nueva purruja centroamericana que se desarrolla en los agujeros de cangrejos (Diptera, Ceratopogonidae). *Contributions in Science (Los Angeles)*, (152):1–7, 1968.

- [60] Hall Charles A. Kemp W. Michael. Yañez-Arancibia Alejandro. Day, John W. *Estuarine Ecology*. John Wiley & Sons, 1989.
- [61] Jorge A Jiménez. The structure and function of dry weather mangroves on the pacific coast of central america, with emphasis onavicennia bicolor forests. *Estuaries*, 13(2):182–192, 1990.
- [62] Dick Pasfield. Neem - a new threat to norhern rivers. Sixteenth Australian Weeds Conference.
- [63] Sanchez Salvador Manuel Olson, Eric J. Pruebas preliminares para el control de neem dentro y cerca el manglar de ostional. Research project proposal to apply for funding, 2014.
- [64] Eric Olson. Ostional weather, leaf damage, and burrowing crabs. Conversation started at October 2015.
- [65] Luis Fernando Tavares De menezes and Ariane Luna Peixoto. Leaf damage in a mangrove swamp at sepetiba bay. *Revista Brasil. Bot*, 32(4):715–724, 2009.
- [66] Edward Riley. Questions about flea beetle damage. Received at 18-11-2015.
- [67] Joe Gray. The myth of the salt gland.
- [68] PM Tilney and AE Van Wyk. Extrafloral nectaries in combretaceae: morphology, anatomy and taxonomic significance. *Bothalia*, 34(2):115–126, 2004.
- [69] Jos. van der Zee Sjoerd. Metleaar, Klaas. van Dam. *Ecohydrology. SLM-32806. Soil Physics and Land Management Group*. Wageningen University, 2015.
- [70] J Bouma. Soil morphology and preferential flow along macropores. *Agricultural Water Management*, 3(4):235–250, 1981.
- [71] D Bright. The land crabs of costa rica. los cangrejos terrestres de costa rica. *Revista de Biología Tropical.*, 14(2):183–203, 1966.
- [72] S.I. Smith. Notes on american crustacea. *Trans. Connecticut Academic Arts Science*, 2(1):113–176, 1870.
- [73] Thomas J Smith, Kevin G Boto, Stewart D Frusher, and Raymond L Giddins. Keystone species and mangrove forest dynamics: the influence of burrowing by crabs on soil nutrient status and forest productivity. *Estuarine, coastal and shelf science*, 33(5):419–432, 1991.
- [74] Peter V Ridd. Flow through animal burrows in mangrove creeks. *Estuarine, Coastal and Shelf Science*, 43(5):617–625, 1996.
- [75] S.F. Heron and Peter V Ridd. The use of computational fluid dynamics in predicting the tidal flushing of animal burrows. *Estuarine, Coastal and Shelf Science*, 52:411–421, 2001.
- [76] S.F. Heron and Peter V Ridd. The tidal flushing of multiple-loop animal burrows. *Estuarine, Coastal and Shelf Science*, 78:135–144, 2007.
- [77] Nancy F Smith, Christie Wilcox, and Jeannine M Lessmann. Fiddler crab burrowing affects growth and production of the white mangrove (*laguncularia racemosa*) in a restored florida coastal marsh. *Marine Biology*, 156(11):2255–2266, 2009.
- [78] Christopher J. Martinez. *Seepage Meters for Measuring Groundwater-surface Water Exchange*. University of Florida, 2013. IFAS Extension, AE465.
- [79] Ariel E Lugo and Samuel C Snedaker. The ecology of mangroves. *Annual review of ecology and systematics*, pages 39–64, 1974.
- [80] Björn Kjerfve. *Caribbean coral reef, seagrass and mangrove sites*. UNESCO, 1998.
- [81] Judy Z Drexler and W Eric. Source water partitioning as a means of characterizing hydrologic function in mangroves. *Wetlands Ecology and Management*, 10(2):103–113, 2002.

- [82] Hubert H. G. Savenije. *Salinity and Tides in Alluvial Estuaries*. Number First edition. Elsevier, 2005.
- [83] Ronald L Myers and John J Ewel. *Ecosystems of Florida*. University of Central Florida Press Orlando, 1990.
- [84] Tide-forecast. Tide times for san juan del sur.
- [85] DM Smith and SJ Allen. Measurement of sap flow in plant stems. *Journal of Experimental Botany*, 47(305):1833–1844, 1996.
- [86] P.J. Stuyfzand. Hydrogeochemical (hgc 2.1), for storage, management, control, correction and interpretation of water quality data in excel spread sheet. *KWR-report BTO.2012.244(s)*, 2014. update of 2012 report.
- [87] N.R.G. Walton. Electrical conductivity and total dissolved solids - what is their precise relationship? *Desalination*, 72:275–292, 1989.
- [88] TA Bogaard and Th WJ Van Asch. The role of the soil moisture balance in the unsaturated zone on movement and stability of the beline landslide, france. *Earth Surface Processes and Landforms*, 27(11):1177–1188, 2002.

List of Figures

1.1	The location of the village and estuary, in the Ostional catchment, Nicaragua. Figure was edited from an official map of catchment areas [10], combined with a Google Earth image of the area in 2011 [28].	16
2.1	Locations of the different measurements in the study area.	20
1.1	Schematic overview of the Ostional estuary, showing the key items: (1) the sandbar, (2) the floodplain, (3) a former estuary branch, (4 - 7) examples of locations for Red, White, Tea, and Buttonwood mangrove trees, (8) El Ostional, (9) the fishing cooperation, (10) trails, (11) watering areas for livestock, and (12) cleared land. . .	24
2.1	The sediments found, in the front and top of the sandbar (top figure), in the upstream river catchment (lower three left figures), and the tree trapped in sediment which 25 years ago hung above an estuary branch (lower right figure).	27
2.2	Distribution of energy (top sketch), morphological components in a plan view (middle sketch), and distribution of sedimentary facies in a longitudinal section (bottom sketch), within the Ostional estuary. Based on observations and an idealized wave-dominated estuary of Dalrymple [38].	28
2.3	The different mangrove trees and their seeds, in the Ostional floodplain: The Tea mangrove (left top figure), the Red Mangrove (middle top figure), the Buttonwood (right top figure), and the White mangrove (bottom figure).	29
2.4	Fauna in the Ostional estuary. The Roseate spoonbill (left figure), the Howler monkey (middle figure), and the crab inhabitants, one of them the Mouthless crab (top right figure).	30
2.5	Main components in the root systems of the mangroves. All roots of the species <i>Rhizophora</i> , <i>Avicennia</i> , and <i>Pelliciera</i> consists of the components absorption, ventilation and stability. The figure has been adapted from Jimenez [8].	32
2.6	Noticeable human influences into the estuary of El Ostional. The top left figure shows the excavated trench, whereas the bottom left figure depicts a tree stump. The two right figures show the livestock and its manure, used by the crab as energy supply.	35
2.1	Water table depths below the soil surface (b.s.s.). These measurements were done manually at on average weekly intervals. The displayed trend is a linear interpolation between these moments of measurement. Precipitation in <i>mm/day</i> and the approximate moment of over-wash events are also displayed in the graph.	44
2.2	Seedlings growing in the floodplain; White mangrove (left figures), Red mangrove propagules (middle figure), and the Neem seedlings (right figure).	45

2.3	Effects of damage caused by beetles on leaves of the White mangrove and Buttonwood trees. The beetle is displayed, as are the nectaries. The blue circled nectaries are shown on a relatively undamaged leaf, while the red circled nectaries - blackened - can be seen next to a decaying, largely damaged leaf. The right figure displays the lonely tree away from the floodplain, covered with the sweet tasting substance. . .	46
2.4	Crab burrows in the floodplain, including an example of fresh burrowed clayey material brought up to the surface in the left figure, and a burrow opening partly submerged after water level increase in the right figure.	48
2.5	Continuous water table depths in the floodplain and well below soil surface (b.s.s.) in the upper graph. Continuous electrical conductivity (EC) levels measured in the floodplain in the bottom graph.	49
2.6	Continuous water table depths in the estuary basin E_{CTD} and floodplain at F_4 below soil surface (b.s.s.), for a small period around the over-wash event of 29-09.	49
2.7	Bay-head delta, upstream in the estuary. The picture shows the cross-section where the ten piezometers are installed around. Pools of water can be seen that were mostly not connected to the downstream surface water.	51
2.8	Schematic figure of the average measured head in the ten piezometers approximated with respect to b.s.s. level. These heads can be compared to the surface water level measured at October 5, 2015.	51
2.9	Surface water levels below soil surface (b.s.s.) in the estuary basin, measured continuously.	52
2.10	Water levels below soil surface (b.s.s.) in the estuary basin E_{CTD} , in the floodplain aquifer F_{CTD} , and in the alluvial aquifer W_3 , compared to sea tide from San Juan del Sur which has been leveled approximately to the datum b.s.s.	53
1.1	This sketch represents a longitudinal cross-section of the estuary waters and its subsurface flows. The assumed flows in the shallow aquifer are based on typical flow patterns in coastal aquifers [32]. The boundary between fresh and salt pore water is a diffuse mixing zone, a result of diffusion together with mixing caused by fluctuating tide and fresh water heads.	59
2.1	Schematic longitudinal cross-section of the estuary showing measured EC levels [mS/cm] in green, and recalculated salinity levels [kg/m^3] in blue, at September 8 2015. These measurements were performed at four different cross-sections; cross1 till cross4. Represented in- and outflows are the groundwater seepage Q_f , the tidal period T , the evaporation E , the precipitation P , and the over-wash inflow W . The tide T then causes a certain tidal range H and a tidal excursion E	61
2.2	Shape of the Ostional estuary, depicting a semi-logarithmic plot with the cross-sectional area A in m^2 , the width B in m , and depth h in m . In the table the found convergence lengths a and b are listed, together with the cross-sectional area and width at $x = 0$; A_0 and B_0 . Since a and b are equal, the depth is constant along the estuary; $h = h_0$	62
2.3	The El Ostional salinity curve at 08-09-2015. Measured values are shown, to be compared with the modeled values at tidal average (TA), high water slack (HWS), and low water slack (LWS).	65
2.4	On the left graph the manual salinity measurements are depicted at the mouth of the estuary (Cross1). The measurements show the effect of the first over-wash events salt addition and the second salt addition. On the right, a simple representation of the estuary in between over-wash events is shown. In this schematic view, S is the average salinity in the estuary at the time t , and the total volume V of water in the estuary is estimated as $V = O_{estuary}h$	68

2.5	The calculated fresh water inflow Q_f with the used data and scenarios. The bottom two tables show the relative importance of the separate terms for each scenario, with and without scaling the terms on salinity. The assumption that the water level is constant is checked, by also calculating the fresh water inflow Q_f with water levels $h - 0.1 = 0.76$ and $h + 0.1 = 0.96$	68
2.6	On the left, an overview of the separate wells and their relative distance to the shore, high and low sea tide, is shown. These distances are then listed in the table next to it, also showing the measured salinities in those wells and the estimated depth to the interface below mean sea level.	70
2.7	Relation between well salinity and the distance of these wells from the coast, as well as the relation between z_s and the distance of these fresh water heads from the coast. Keep in mind that these wells have an approximate depth of 4 to 8 m, thus the comparison between z_s and EC can be sophisticated.	70
2.8	Locations of the floodplain piezometers ($F_1 - F_7$, F_{CTD} , and F_{Beach}), showing the average pore water and diluted soil salinity levels [mS/cm], measured throughout the study period. The points B_1 to B_4 show locations of soil salinity measurements outside the floodplain area. Pore water salinities are shown in black and bold, while soil salinities are shown in brown and represent salinities after dissolving the soil in purified water.	71
2.9	Soil salinity profiles for all locations shown in figure 2.8. Every 20 cm a sample was taken. The sample was then dissolved in purified water, where after EC of the solution could be measured.	72
2.10	Sketch of the subsurface beneath Ostional.	73
2.11	Plot of the sea tide (approximated according to datum b.s.s.), the floodplain aquifer water table in F_{CTD} , and the estuary water level at E_{CTD} , during the last spring tide during the field work period. This last spring tide caused the over-wash event around October 28.	74
A.1	Picture of the installed self-made funnel (left figure), and the dimensions of the used evaporation pan (right figure).	103
A.2	Manual measurements in the floodplain piezometers, EC and water level (left top and bottom figures). Manual measurements in the estuary with the kayak (middle top and bottom figures). And well W_3 , together with the already existing piezometers in the alluvial aquifer (right figures).	105
A.3	Self-made seepage meters	105
A.4	Cross-section view showing a typical installation of a seepage meter (a), and for an installation in shallow water (b). Copied from Martinez [78].	106
A.5	Set-up for an inverse-auger hole test.	106
A.6	Retrieving soil samples by digging holes with an auger (left figure), then analyzing them in the lab of CIRA (middle figure), with the sequence of samples for one location depicted in the right figure.	107
A.7	Set-up for elevation measurements using a DGPS device.	107
A.8	Installed Logger into a White mangrove tree (left figure), and the resulting black resin secreted by the tree for protection.	108
B.1	The Ghyben-Herzberg approximation of flow patterns in a coastal aquifer [32]. . .	111

B.2	Definition sketch of an alluvial estuary, with the top figure showing a view from top and the bottom figure depicting a longitudinal cross-section. The figure shows the tidal excursion E , the width B , the tidal range H between High Water (HW) and Low Water (LW), and with a Tidal Average (TA). The fresh water inflow Q_f is shown, as well as the average water depth h . Taken from Savenije [2].	112
B.3	Longitudinal distribution of the salinity for a stratified estuary (a), a partially mixed estuary (b), and a well-mixed estuary (c). Whether the estuary is stratified, partially-, or well-mixed depends on Q_f and can thus change over time. Taken from Savenije [2].	113
B.4	Different shapes of well-mixed salt intrusion curves. Type 1 is the recession shape, type 2 represents the bell shape, type 3 depicts a dome shape, and type 4 is called the humpback shape. Taken from Savenije [2].	113
C.1	Locations of the different measurements in the study area.	117
C.2	Average precipitation and evaporation in the area of El Ostional.	120
C.3	Continuous salinity measurements in the estuary surface water, at the mouth of the estuary.	123
C.4	Set-up of the piezometers at cross-section A-A of figure C.18 of Appendix A. . . .	124
C.5	Table listing the resulting infiltration and ex-filtration rates between groundwater and estuary basin (left). The other table shows the resulting ex-filtration rate measured at the upstream end of the estuary, from which a fresh water velocity v_f has been extracted (right).	131
C.6	Table listing the resulting hydraulic conductivities of the different infiltration tests.	132
C.7	Graph of the measured depths at certain time intervals during the inverse-auger hole tests in the floodplain (left) and in the sand bar (right).	132
C.8	Graph showing the correlation between the calculated hydraulic conductivities and the amount or area of crab burrows counted in a $4 m^2$ area around the hole	133
C.9	Graph showing the measured cross-sections in the estuary basin.	133
C.10	Plotted sap flow values measured in micro-volt in a White mangrove tree in El Ostional.	134
C.11	Overview of the sampled leaves of the White mangrove trees all through the floodplain.	134
C.12	Dimensions x, y, h of the measured locations Cross1 - Cross4 and at the upstream end of the estuary. From these measurements, a cross-section A_{meas} was abstracted, what can be compared to the calculated A_{calc} with equation 2.1.	135
C.13	Graph showing a small period of relative water levels measured by the diver E_{CTD} at the mouth of the estuary. It shows an example for the tidal range H and tidal period T that have been estimated.	135
C.14	Table listing the measured fresh water velocity with seepage measurements that was used to calculate the possible fresh water inflow into the estuary. The section where possibly seepage might occur over the complete estuary bed, here mentioned as $O_{estuary}$, has been estimated with a minimum partition of $p = 1/8$ th of the complete estuary bed (O_{min}) and with max half of the estuary bed (O_{max}). This has then resulted into a minimum and maximum amount of fresh water inflow, Q_{min} and Q_{max}	135
C.15	Table listing the estimated parameters for the estuary necessary for the model calculations.	136
C.16	Model performance correlation coefficient for each measurement.	136

C.17	The relative importance of rainfall and evaporation in relation to discharge and dispersion is indicated here with the non-dimensional coefficients explained in Appendix B, Section 3.3, equations B.12 till B.17.	140
C.18	Location of study area depicting the average piezometric surface of shallow groundwater in the study period as well as cross-sections A-A and B-B. Taken from Calderon [10].	147
C.19	Schematic cross-section of the study area, valid for the area around cross-section B-B in figure C.18. Dashed line indicates river flooding. Figure is not to scale. Taken from Calderon [10].	147
C.20	Stratigraphic correlation in cross-section A-A of figure C.18. Vertical exaggeration times 2. Taken from Calderon [10].	148
C.21	Stratigraphic interpretation at the piezometric cross-section based on macro- and micro-analysis of sediment samples. Piezometer set-up across the river; West (W) and East (E) piezometers, number indicates position with respect to the river banks, 1 is the closest and 3 is the farthest from the river. Secondary numbering indicates same location but different depth (i.e. P1E and P1E-1). Taken from Calderon [10].	148
C.22	Hydraulic conductivity estimates from slug tests, see figure C.18. Taken from Calderon [10].	149
C.23	Tide water level at San Juan del Sur [84].	149
C.24	The estuary of La Flor (left figure), the sandbar closing the estuary (middle figure), and the upstream section of the estuary (right figure).	150
C.25	The mouth of the San Juan del Sur estuary (top figure), the upstream part (left bottom figure), and the Black mangroves with their peg roots (right bottom figure).	151

List of symbols

Symbol	Meaning
K_S	saturated permeability [m/day]
K	van den Burgh coefficient [-]
h	water depth [m]
Q_f	fresh groundwater seepage [m^3/s]
T	tidal period [s]
E	evaporation [mm/day]
P	precipitation [mm/day]
W	over wash [m^3]
H	tidal range [m]
E_0	tidal excursion [m]
x	distance from the mouth [m]
a	cross-sectional convergence length [m]
b	width convergence length [m]
A_0	cross-sectional area at $x = 0$ [m^2]
B_0	width at $x = 0$ [m]
ε	phase lag [-]
δ	rate of longitudinal amplification [$1/m$]
r_s	rate of storage width to stream width [-]
N	Canter-Cremers number [-]
N_R	Estuarine Richardson number [-]
P_t	flood volume or tidal prism [m^3]
F_d	densimetric Froude number [-]
v	tidal velocity amplitude [m/s]
ρ	density of the water [kg/m^3]
D	longitudinal dispersion [m^2/s]
D_0	dispersion at the mouth [m^2/s]
β	dispersion reduction rate [-]
α_0	mixing coefficient [$1/m$]
S_f	fresh water salinity [kg/m^3]
S_0	salinity boundary condition at $x = 0$ [kg/m^3]
R^2	correlation coefficient [-]
L	salt intrusion length [m]
z_s	depth of the mixing interface bsl [m]

Appendices

Appendix A

Establishing the database

This appendix will set forth the survey measurements that have been executed and what material was used for this.

A.1 Survey

A.1.1 Meteorology

Meteorological parameters were measured in El Ostional, located at GPS location Meteo, see Appendix C.

Precipitation was measured with a self-made funnel functioning as a rain gauge. The funnel consisted of an inverted Coke bottle, hung in a steel rack. It is depicted in figure A.1, where all dimensions have been depicted. Every morning the rain gauge was checked upon. After a rain event the amount of water captured was measured in a measuring cup, and thrown away.

Open water evaporation was measured with a pan. However, this was not a standard Class A pan, but a normal cooking pan, sketched in figure ???. Every morning the pan was checked upon, measurements were taken and the pan was filled or emptied to its starting position. Evaporation was measured in two ways. First, a diver was hung in the pan. Unfortunately, the diver seemed unable to capture the fast increase of water added in the morning. The second manner was to check the amount of water added to or removed from the pan. It can be understood that both ways resulted in unreliable values, at most to be used as an estimation.

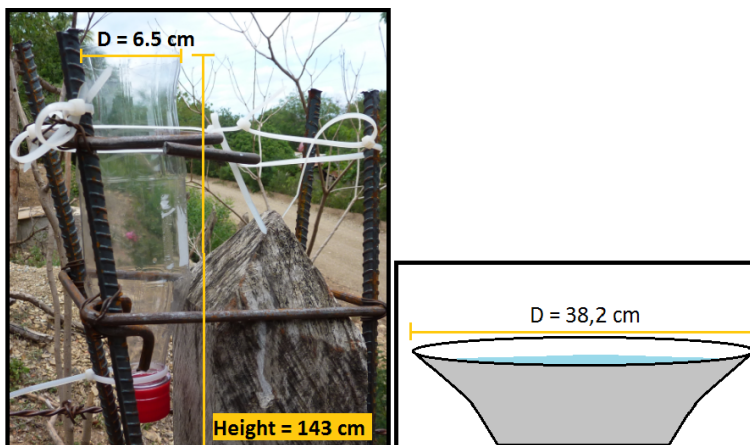


Figure A.1: Picture of the installed self-made funnel (left figure), and the dimensions of the used evaporation pan (right figure).

Air pressure and temperature in El Ostional were measured continuously with a mini Schlumberger diver, used as a baro-diver.

A.1.2 Water level and salinity

The water level and salinity have been measured in the estuary surface water, in the floodplain aquifer, and in the community wells. Salinity was measured in electrical conductivity (EC). These measurements were done continuously and/or manually. The continuous measurements were conducted with mini- and CTD- Schlumberger divers. The manual measurements were performed using either a groundwater sounding device, or a rule for the surface waters, and an EcoSense EC300 portable instrument.

Two piezometers in the floodplain were already available from previous research. Five other piezometers in the alluvial aquifer were also already constructed during earlier research. The two piezometers in the floodplain were not sufficient and thus seven other piezometers were installed in the floodplain, each with an average depth of 1.2 *m* and a screen of around 0.2 *m* deep. All piezometers are depicted in figure 2.1 in the Methodology, and the GPS coordinates can be found in Appendix C. During the research period, piezometers F_2 and F_3 were demolished by unknown villagers. Piezometer F_2 could be reinstalled again.

Continuous measurements

Two divers have been installed in the estuary. One mini-diver at Cross4, upstream in the estuary. And one CTD-diver at Cross 1, at the mouth of the estuary. Locations are shown in figure 2.1 in the Methodology, and the GPS coordinates can be found in Appendix C. The pressure measurements were corrected with baro-pressure measurements performed, see subsection Meteorology. The divers were installed at August 20 and removed at October 29, 2015. By attaching the divers that were installed in the estuary, onto a PVC-pipe with holes, the diver could be installed into the bottom of the estuary, safe for theft or flushing.

One CTD-diver was installed in the floodplain, located in piezometer F_{CTD} . This diver was installed at August 20 and removed at October 28, 2015. Another mini-diver was installed at two different locations in the floodplain subsequently. Its first location was F_7 , installed there at September 7, where it was removed at September 26 because this location was believed not to be safe from theft anymore. The second location was F_4 , where it was installed the same day. This diver was removed at October 26, 2015. The last mini-diver was installed in well W_3 near the shore at September 27, and removed at October 26, 2015.

Manual measurements

Manual measurements in the estuary were done from a kayak on a weekly basis, see figure A.2. Manual measurements in the piezometers was conducted at least every week, and more often whenever possible. The manual measurements in the wells of the community were conducted only once, at September 24. Only the salinity in well W_3 was measured a couple times more often.



Figure A.2: Manual measurements in the floodplain piezometers, EC and water level (left top and bottom figures). Manual measurements in the estuary with the kayak (middle top and bottom figures). And well W_3 , together with the already existing piezometers in the alluvial aquifer (right figures).

A.1.3 Seepage measurements

Seepage in the estuary was measured with two self-made seepage meters, shown in figure A.3. Seepage meters measure the flow of water between groundwater and a surface water body [78]. A number of measurements have been done with these seepage meters all over the estuary. Measurements were taken at locations where the water could be entered. This was not possible at all locations, since mud could sometimes reach until the waist. Figure A.4 shows how the seepage meter was installed. The collection bag was attached with a small amount of water. After a certain time, the bag was removed and the volume of water inside the bag was measured.



Figure A.3: Self-made seepage meters

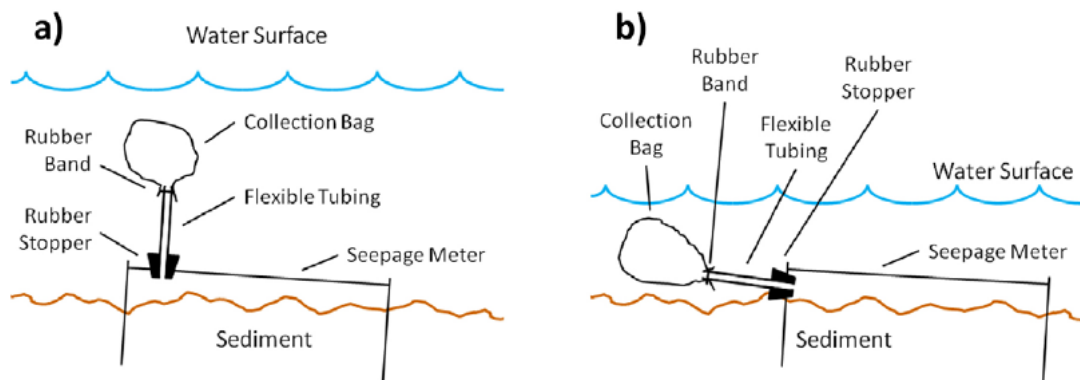


Figure A.4: Cross-section view showing a typical installation of a seepage meter (a), and for an installation in shallow water (b). Copied from Martinez [78].

A.1.4 Inverse-auger hole tests

The inverse-auger hole test is an infiltration test, which is executed in the unsaturated zone. A hole with a diameter of 10 cm is made with an auger to a certain depth, here approximately 1 to 1.2 m. The hole is filled with water and the rate of water level fall is measured. In the study area, 14 tests were executed in the floodplain, and 2 tests were executed in the sand bar. The result of an inverse-auger hole test is the saturated permeability. During this research, the inverse-auger hole tests in the floodplain were performed partly in the saturated zone. It was assumed that the area touching the saturated zone was small enough to be able to disregard the connection. Figure A.5 shows the material used to fill the auger hole and measure the rate of water level fall.



Figure A.5: Set-up for an inverse-auger hole test.

A.1.5 Soil samples

Soil samples were taken in next to several piezometers in the floodplain, next to well W_3 , next to piezometer P_1W , and just outside of the floodplain in the cleared lands and next to the village. Locations can be found in figure 2.1 in the Methodology, and the GPS co ordinates can be found in Appendix C. Samples were taken every 20 cm, over a maximum depth of 120 cm, dug with an auger, see figure A.6.

The samples were then analyzed in the lab, see figure A.6. Soil sample was weighed at 5 g and dissolved in 80 ml of purified water. Subsequently the electrical conductivity was measured, resulting in relative salinity levels for the soil.



Figure A.6: Retrieving soil samples by digging holes with an auger (left figure), then analyzing them in the lab of CIRA (middle figure), with the sequence of samples for one location depicted in the right figure.

A.1.6 Cross-sectional areas

Four cross-sections in the estuary basin were measured in order to create cross-section areas of the basin. This was measured with a rule, while sitting in the kayak.



Figure A.7: Set-up for elevation measurements using a DGPS device.

A.1.7 Sap flow

Sap flow measurements were conducted on a White mangrove tree at the border of the floodplain, see for the location figure 2.1 in the Methodology. For this, the ProsaLog Logger from UP GmbH was used. Sap flow was measured using the thermal dissipation method developed by Granier [85]. Rates of sap flow around two 2 mm diameter probes are measured by determining the difference in

temperature between the two probes. Two cylindrical probes are inserted radially into the stem, with one probe placed approximately 100 mm above the other. The upper probe contains a heater element and a thermocouple junction that is referenced to another junction in the lower probe [85].

Figure A.8 shows the installed Logger, which contained three different sets of probes. One set of probes was installed in the main trunk, while the other two sets were each installed into the two main branches of the mangrove tree. During the research, an attempt was made to change the location of these probes. However, the tree turned out to have activated a defensive mechanism. Around a couple of the probes, resin was secreted by the tree, which turned into a hard black substance. Making it impossible to remove the probes.



Figure A.8: Installed Logger into a White mangrove tree (left figure), and the resulting black resin secreted by the tree for protection.

A.1.8 Leaf damage sampling

Leaves of the White mangrove tree were sampled in order to find a correlation between location and damage amount. All through the floodplain, 8 trees were sampled.

A.2 Further retrieved data

A.2.1 Side sources

Ineter is the Nicaraguan institute for geophysical studies. The institute also has a meteorological department, which measures also in Rivas. Meteorological data from August and September 2015 were obtained. A previous study performed in the El Ostional catchment by Calderon [10], delivered data on subsurface layering and hydraulic conductivities, which was again used during this research. And finally, tidal data was retrieved for the San Juan del Sur bay, that could be used as reference material during this research.

A.2.2 Nearby locations

Two other locations have been visited; the La Flor estuary and the Sand Juan del Sur estuary. In these locations observations and some salinity measurements were conducted.

Appendix B

Used theories

This appendix will set forth the methods used to retrieve applicable data from the conducted survey. Further relations and models to analyze the data are demonstrated.

B.1 Recalculation methods

B.1.1 Converting salinity

Salinity was measured in Electrical Conductivity (EC), which is the conductance per length, and equals the inverse of the electrical resistivity. It is closely related to total dissolved solids (TDS), the mass of all solids in a certain volume of water. EC is a function of the concentrations of all ionic solutes, and commonly reported and used. The units used in this report for electrical conductance are milisiemens per cm, mS/cm . Total dissolved solids are usually displayed in mg/L , and in this report will be reported as kg/m^3 . EC values in the Ostional area ranged from 0.50 - 0.1055 mS/cm for potable water, up to 55 mS/cm for the sea. A linear empirical correlation of EC to TDS is described with equation B.1 [86,87], where A is a constant that is in the range of 0.55 to 0.75 $(mS/cm)/(kg/m^3)$ for a wide range of natural waters [32]. During this research, the value $A = 0.7(mS/cm)/(kg/m^3)$ is used.

$$EC \approx \frac{(TDS)}{A} \quad (B.1)$$

B.1.2 Inverse-auger hole method

The inverse-auger hole tests resulted in depths of the water level in the hole after certain time steps. In the inverse-auger hole method of Kessler and Oosterbaan, this information is then used to calculate the saturated permeability K_S [88]. Equation B.2 is based on Darcy's law, assuming that the hydraulic gradient is 1, and where the amount of infiltrated water can be described with $Q = -\pi r^2(dh/dt)$.

$$K_S = 1.15r \frac{\log(h(t_1) + \frac{r}{2}) - \log(h(t_n) + \frac{r}{2})}{t_n - t_1} \quad (B.2)$$

B.1.3 Seepage measurements

The flow and direction of flow between groundwater and the overlying surface water is measured by the change in volume of water in the collection bag over a known period of time. Subsequently,

this gives the final water volume V_{Final} , which can be used with the starting water volume V_{Start} , and the elapsed time t to determine the rate of seepage with equation B.3. When Q is positive, ex-filtration occurs. When Q is negative, water infiltrates into the groundwater system.

$$Q = \frac{dV}{dt} = \frac{V_{Final} - V_{Start}}{t_{Final} - t_{Start}} \quad (\text{B.3})$$

Subsequently, from this in- or ex-filtration a flow velocity v_f could be extracted using the following calculation:

$$v_f = \frac{Q}{\pi r^2} \quad (\text{B.4})$$

In equation B.4, r is the radius of the seepage meter device.

B.1.4 Sap flow measurements

Constant power is applied to the heater and the difference in temperature between the two probes, ΔT is then dependent on the rate of sap flow around the probes; as sap flow rates increase, heat is dissipated more rapidly and so ΔT decreases [85]. The volumetric sap flux density u can be empirically determined with [?]:

$$u = 0.714 \left(\frac{dT_{night}}{dT_{actual}} - 1 \right)^1 .231 [mL/(cm^2 min^1)] \quad (\text{B.5})$$

In equation B.5, dT_{night} is the temperature-difference at night, to be estimated from the data set, and dT_{actual} is the temperature-difference measured. The mass flow rate of sap F is then calculated using $F = uA$. The area of the tree A without bark, at the point of the heated sensor, thus also needs to be estimated. In this research, only relative differences in sap flow were needed, thus the area was not estimated.

Data was obtained in voltage. In order to convert the data to degrees Celcius, it should be multiplied with a factor that depends on ambient temperature in the tree. For the Ostional area, a factor $40.7 \mu V/^\circ C$ was used that belonged to an ambient temperature in the tree between 20 and $30^\circ C$.

B.2 Ghyben-Herzberg approximation

At a point on the interface at a depth z_s below sea level, the calculated pressure in the salt water is $P_s = \rho_s g z_s$. For this static salt water is assumed. The pressure in the fresh water at the same point should then be $P_f = \rho_f g (z_s + h)$. Hydrostatic fresh water needs to be assumed. The head h in the fresh water should be measured from the sea level datum. Since there is only one pressure at any points in a fluid, the pressure on the interface equals $P_s = P_f$. This yields the Ghyben-Herzberg relation [32]:

$$z_s = \frac{\rho_f}{\rho_s - \rho_f} h = \frac{1.000}{1.025 - 1.000} h = 40h \quad (\text{B.6})$$

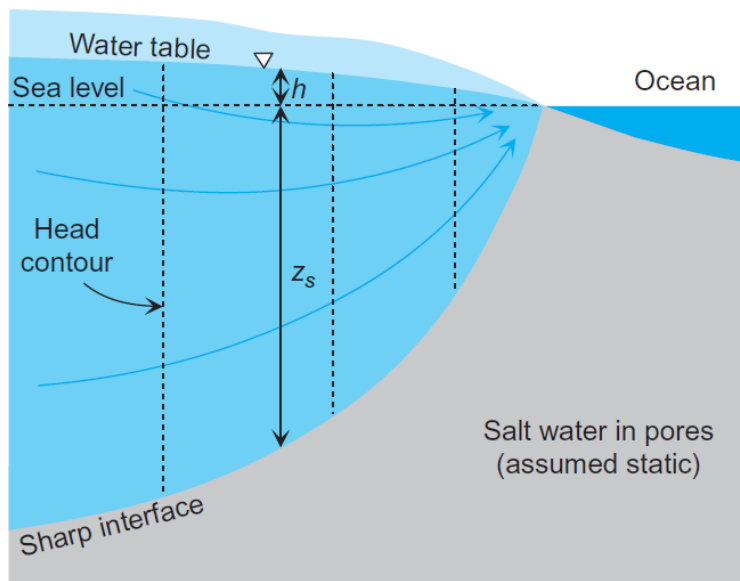


Figure B.1: The Ghyben-Herzberg approximation of flow patterns in a coastal aquifer [32].

B.3 Steady state model

In this section the background assumptions and definitions for the steady state model developed by Savenije [2, 31, 37] are explained. For more information, please use the book *Salinity and tides in alluvial estuaries* by Savenije.

B.3.1 Definition sketches of an alluvial estuary

Figure B.2, B.3, B.4 show the different aspects of an alluvial estuary that are driven by the oceanic and riverine forces. These forces, represented by the fresh-water inflow Q_f and the tide generally create three different salt intrusion mechanisms; stratified, partially mixed, or well-mixed. For the well-mixed estuary, different salt intrusion curves can be distinguished over the longitudinal cross-section of an estuary. Type 1 is the recession shape, which occurs in narrow estuaries with a near-prismatic shape and a high river discharge. Type 2, the bell shape, occurs in estuaries that have a trumpet shape, hence a long convergence length in the upstream part, but a short convergence length near the mouth. Type 3 shows the dome shape, which occurs in strong funnel-shaped estuaries that have a short convergence length. And finally type 4, the humpback shape, which is a negative or hypersaline estuary. The driver for hypersalinity is evaporation. If evaporation exceeds rainfall and fresh water inflow, and if the estuary is shallow, it can become hypersaline. Estuaries with dome-shaped salt intrusion are most susceptible to hypersalinity.

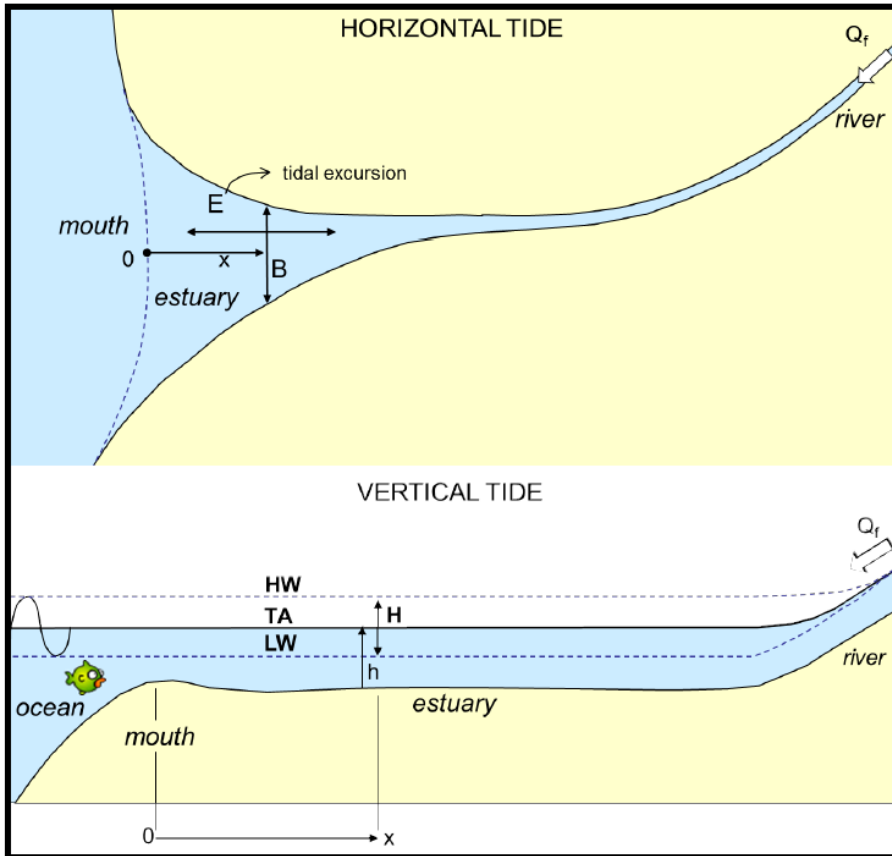


Figure B.2: Definition sketch of an alluvial estuary, with the top figure showing a view from top and the bottom figure depicting a longitudinal cross-section. The figure shows the tidal excursion E , the width B , the tidal range H between High Water (HW) and Low Water (LW), and with a Tidal Average (TA). The fresh water inflow Q_f is shown, as well as the average water depth h . Taken from Savenije [2].

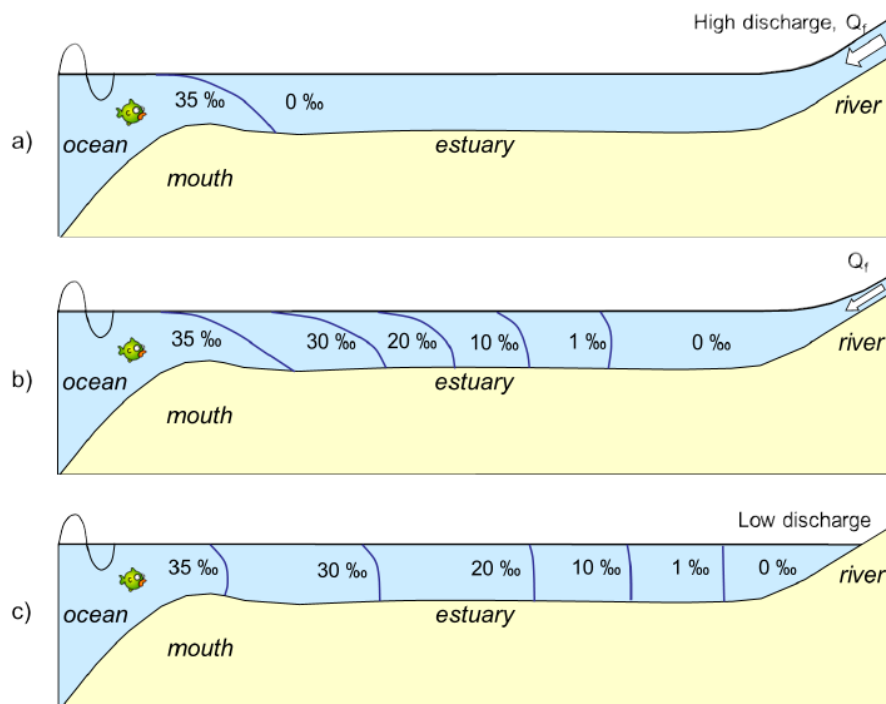


Figure B.3: Longitudinal distribution of the salinity for a stratified estuary (a), a partially mixed estuary (b), and a well-mixed estuary (c). Whether the estuary is stratified, partially-, or well-mixed depends on Q_f and can thus change over time. Taken from Savenije [2].

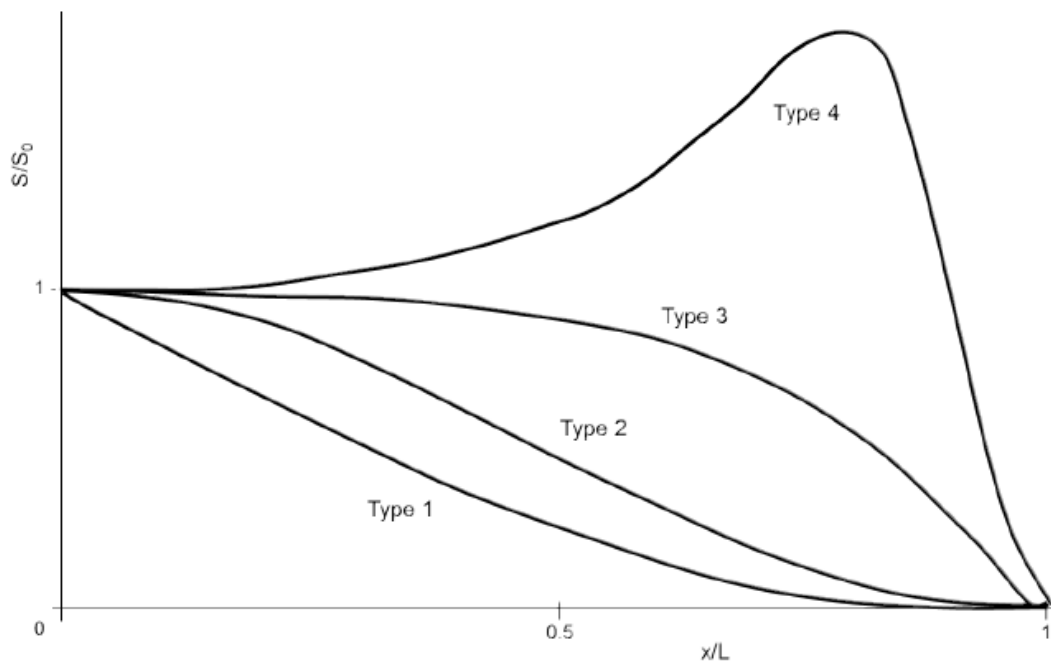


Figure B.4: Different shapes of well-mixed salt intrusion curves. Type 1 is the recession shape, type 2 represents the bell shape, type 3 depicts a dome shape, and type 4 is called the humpback shape. Taken from Savenije [2].

B.3.2 Base of the model

The steady state model is based on salt balance equations and on the dispersion in an estuary. The salt balance for the special case when equilibrium occurs between the advection and dispersion and steady state occurs, is shown in equation B.7.

$$Q_f(S_{TA} - S_f) - A_{TA}D_{TA}\frac{\delta S_{TA}}{\delta x} = 0 \quad (\text{B.7})$$

Where S_{TA} represents the mean tidal steady state salinity, S_f is the fresh water salinity, A_{TA} and D_{TA} are respectively the cross-sectional area and the dispersion, both at the tidal average (TA) situation. The boundary condition used is that $S_{TA} = S_f$ and $(\delta S_{TA})/(\delta x) = 0$ when x goes to infinity.

The dispersion equation used is the following, with the dispersion D , the salinity S , and the boundary conditions at the mouth D_0 and S_0 .

$$\frac{D}{D_0} = \frac{S}{S_0}^K \quad (\text{B.8})$$

When this equation is integrated with Van den Burgh's equation, B.9, taking into account that the exponential variation of the cross-sectional area, it yields equation 2.7 in Part III.

$$\frac{\delta D}{\delta x} = KU_f \quad (\text{B.9})$$

Integration of equation B.7 and B.8 results in equation 2.6 in Part III of the report, which is used for the calculations.

B.3.3 Fresh water inflow

The fresh water inflow Q_f is one of the most difficult parameters to determine. During this research, seepage measurements have been conducted in order to be able to estimate this parameter. Seepage measurements resulted in a certain fresh water flow velocity v_f . This could then be used to calculate a probable amount of fresh water inflow. An estimation of the area of ex-filtration in the estuary bed ($O_{estuary}$) needs to be defined, assuming the following:

1. A minimum amount; $p = 1/8$ of the total estuary bed is expected to let seepage pass into the estuary.
2. A maximum amount; $p = 1/2$ of the total estuary bed can let seepage pass into the estuary at a max.

With p being the partition of the estuary bed that is expected to let seepage pass. Then, a minimum and maximum amount of possible fresh water inflow can be estimated with equation B.10.

$$Q_f = v_f \cdot O_{estuary} \cdot p \quad (\text{B.10})$$

B.3.4 Influence of rainfall and evaporation

When the influence of rainfall and evaporation is taken into account in the salt balance, equation B.7 modifies into equation B.11.

$$r_S A \frac{\delta s}{\delta t} + (Q_r - Brb) \frac{\delta s}{\delta x} - \frac{\delta}{\delta x} \left(AD \frac{\delta s}{\delta x} \right) = -sBr \quad (\text{B.11})$$

Depending on the relative size of each term in equation B.11, the effect of rainfall and evaporation is important or small. To analyze the relative size of the terms in equation B.11, these terms have been scaled. The scaling results in five non-dimensional coefficients, $N_1 - N_5$, that can determine the relative importance of the terms with respect to the rate of change of the salinity.

$$N_1 = \frac{r_0 T}{h_0} \quad (\text{B.12})$$

$$N_2 = \frac{-r_0 T b}{h_0 L} \quad (\text{B.13})$$

$$N_3 = \frac{Q_0 T}{A_0 L} \exp -x' L/a \quad (\text{B.14})$$

$$N_4 = \frac{D_0 T}{a L} \quad (\text{B.15})$$

$$N_5 = \frac{-D_0 T}{L^2} \quad (\text{B.16})$$

In equations B.12 - B.16, r_0 is the net rainfall rate during the dry season (negative in case of net evaporation), T is the tidal period, b and a are the width and cross-sectional convergence lengths, L is the tidal average salt intrusion length that corresponds to Q_0 , the dry season fresh water discharge. The cross-sectional area and dispersion at the mouth are respectively represented by A_0 and D_0 . The coefficients N_1 and N_2 weigh the impact of the net rainfall r on the rate of change of salinity; N_1 through dilution, N_2 through advection. Thus, combining these two coefficients, it results in equation B.17, where N_r weighs the overall importance of rainfall.

$$N_r = \frac{N_1}{2} - N_2 \quad (\text{B.17})$$

N_3 weighs the impact of the fresh water inflow on the rate of change of salinity, while N_4 and N_5 weigh the importance of the dispersion at the downstream boundary to the rate of change of salinity. Combination of N_4 and N_5 gives $N_D = -0.5N_4 + N_5$.

Appendix C

Complete results

The acquired data and results of the analysis are exhibited here.

C.1 Applicable data

C.1.1 Measurement locations

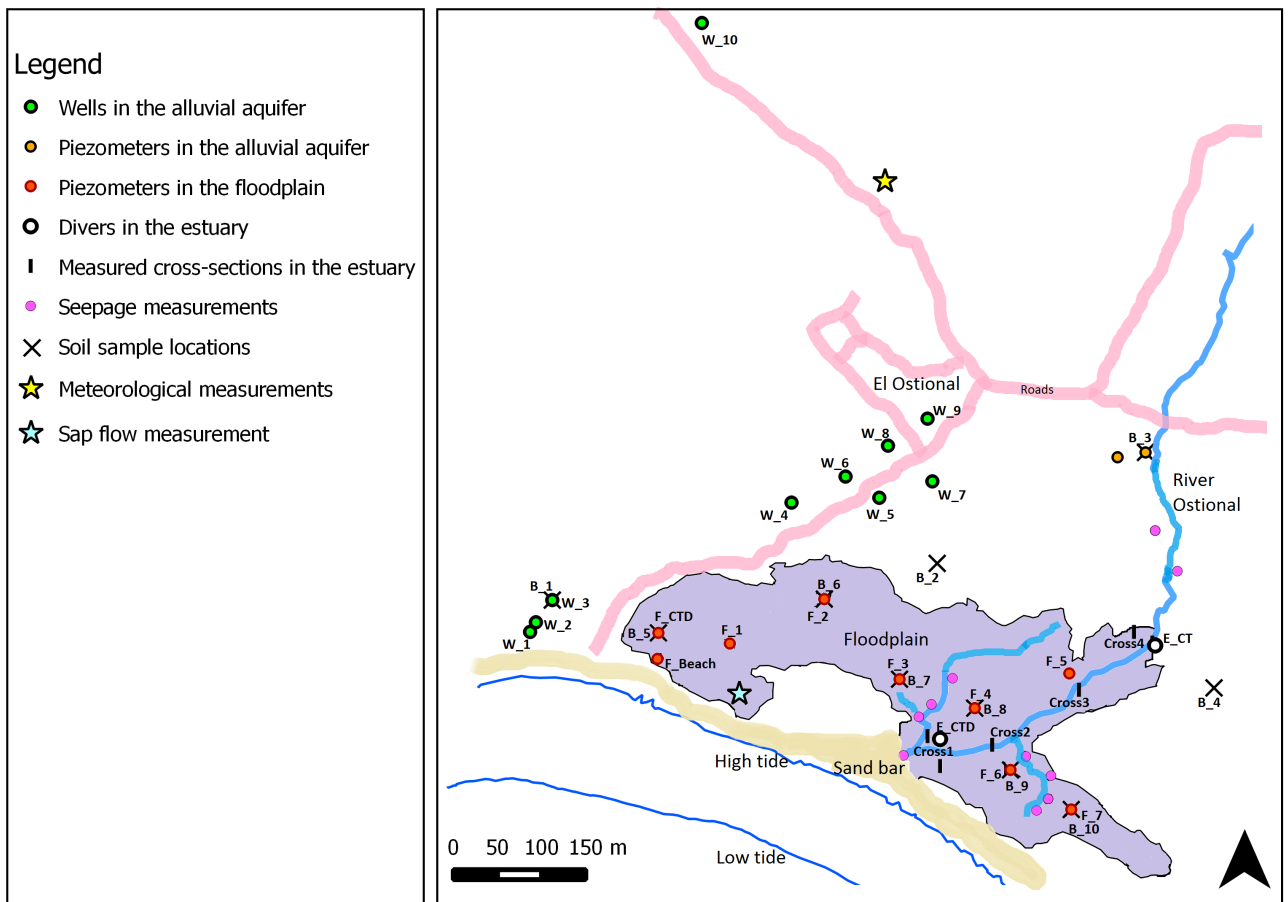


Figure C.1: Locations of the different measurements in the study area.

Type	ID	Latitude	Longitude
General	Meteo	11.11453	-85.76211
	Sap flow tree	11.10922	-85.76362
Estuary basin	E_CTD	11.10875	-85.76154
	E_CT	11.10972	-85.75931
	Cross1A	11.10847	-85.76154
	Cross1E	11.10878	-85.76167
	Cross2	11.10869	-85.76095
	Cross3	11.10926	-85.76010
	Cross4A	11.10975	-85.75934
	Cross4B	11.10986	-85.75953
Floodplain piezometers	F_CTD	11.10985	-85.76446
	F_Beach	11.10958	-85.76447
	F_1	11.10974	-85.87372
	F_2	11.11020	-85.76274
	F_3	11.10937	-85.76196
	F_4	11.10907	-85.76118
	F_5	11.10943	-85.76020
	F_6	11.10843	-85.76081
	F_7	11.10802	-85.76018
Alluvial piezometers	P1W	11.11172	-85.75941
	P2W	11.11167	-85.75970
Community wells	W_1	11.10986	-85.76579
	W_2	11.10996	-85.76573
	W_3	11.11019	-85.76556
	W_4	11.11120	-85.76308
	W_5	11.11125	-85.76217
	W_6	11.11147	-85.76252
	W_7	11.11142	-85.76162
	W_8	11.11179	-85.76208
	W_9	11.11207	-85.76167
	W_10	11.11617	-85.76401
Seepage measurements	Seepage1	11.10858	-85.76192
	Seepage2	11.10898	-85.76176
	Seepage3	11.10938	-85.76141
	Seepage4	11.10911	-85.76163
	Seepage5	11.10813	-85.76042
	Seepage6	11.11091	-85.75931
	Seepage7	11.11091	-85.75931
	Seepage8	11.11091	-85.75931
	Seepage9	11.11049	-85.75908
	Seepage10	11.10813	-85.76042
	Seepage11	11.10813	-85.76042
	Seepage12	11.10837	-85.76039

	Seepage13	11.10801	-85.76054
	Seepage14	11.10857	-85.76065
Soil samples			
	B_1	11.11019	-85.76556
	B_2	11.11057	-85.76157
	B_3	11.11172	-85.75941
	B_4	11.10928	-85.75870
	B_5	11.10985	-85.76446
	B_6	11.11020	-85.76274
	B_7	11.10937	-85.76196
	B_8	11.10907	-85.76118
	B_9	11.10843	-85.76081
	B_10	11.10802	-85.76018
Leaf samples			
	Tree1	11.11063	-85.75918
	Tree2	11.10985	-85.76467
	Tree3	11.10857	-85.76065
	Tree4	11.10941	-85.76181
	Tree5	11.10914	-85.76342
	Tree6	11.10907	-85.76118
	Tree7	11.10943	-85.76020
	Tree8	11.10802	-85.76018

C.1.2 Meteorological data collected in El Ostional

Meteorological data was collected in El Ostional, at location Meteo in figure C.1.

This resulted in the averages depicted in figure C.2, and in the daily precipitation, evaporation, temperature and vapor pressure listed in the following tables.

Diameter [m] raingauge	0.065
Surface area [m ²] raingauge	0.003
Average precipitation [mm/d]	2.5
Diameter [m] pan	0.4
Surface area [m ²] pan	0.1
Average evaporation [mm/d]	6.5

Figure C.2: Average precipitation and evaporation in the area of El Ostional.

Date	Precipitation	Evaporation	Temperature		Vapour pressure	
	[mm/d]	[mm/d]	Actual	Wet	Saturation	Actual
15-8-2015	0		26.9	24.0	3.0	2.8
16-8-2015	NV	NV	NV	NV	NV	NV
17-8-2015	3		27.0	25.0	3.2	3.0
18-8-2015	0		27.3	25.5	3.3	3.2
19-8-2015	0		28.5	25.3	3.2	3.0
20-8-2015	0		27.8	25.5	3.3	3.1
21-8-2015	0		26.8	24.8	3.1	3.0
22-8-2015	0		27.8	25.5	3.3	3.1
23-8-2015	7		28.0	25.5	3.3	3.1
24-8-2015	0		27.5	25.3	3.2	3.1
25-8-2015	0		27.0	24.5	3.1	2.9
26-8-2015	0		25.3	24.0	3.0	2.9
27-8-2015	0		28.0	25.3	3.2	3.0
28-8-2015	0		27.0	24.5	3.1	2.9
29-8-2015	0		30.0	25.5	3.3	3.0
30-8-2015	1		31.5	26.8	3.5	3.2
31-8-2015	0		27.8	25.8	3.3	3.2
1-9-2015	0		28.3	25.5	3.3	3.1
2-9-2015	0		27.8	22.8	2.8	2.4
3-9-2015	0		27.3	24.0	3.0	2.8
4-9-2015	NV	NV	NV	NV	NV	NV
5-9-2015	0		26.8	23.8	2.9	2.8
6-9-2015	14		28.5	25.8	3.3	3.1
7-9-2015	0		28.3	25.5	3.3	3.1
8-9-2015	0	8	27.5	24.8	3.1	3.0
9-9-2015	0	6	27.5	25.3	3.2	3.1
10-9-2015	2	2	24.8	23.5	2.9	2.8
11-9-2015	0	4	25.8	23.5	2.9	2.8
12-9-2015	0	8	29.5	25.8	3.3	3.1
13-9-2015	26		28.3	25.5	3.3	3.1
14-9-2015	NV	NV	NV	NV	NV	NV
15-9-2015	0	16	29.3	25.8	3.3	3.1
16-9-2015	0	8	28.0	25.3	3.2	3.0
17-9-2015	0	12	27.5	25.0	3.2	3.0
18-9-2015	0	8	27.0	25.0	3.2	3.0
19-9-2015	0	12	26.3	24.3	3.0	2.9
20-9-2015	0	8	28.3	25.3	3.2	3.0
21-9-2015	NV	13	NV	NV	NV	NV
22-9-2015	2	13	26.0	25.3	3.2	3.2
23-9-2015	1	5	26.5	24.8	3.1	3.0
24-9-2015	5	NV	26.3	24.5	3.1	3.0
25-9-2015	0	10	25.5	23.8	2.9	2.8
26-9-2015	0	3	26.5	24.8	3.1	3.0
27-9-2015	3	3	27.0	25.5	3.3	3.2
28-9-2015	18	NV	26.0	25.3	3.2	3.2
29-9-2015	0	8	NV	NV	NV	NV
30-9-2015	0	8	NV	NV	NV	NV
1-10-2015	0	8	NV	NV	NV	NV

2-10-2015	0	8	NV	NV	NV	NV
3-10-2015	0	8	27.5	25.0	3.2	3.0
4-10-2015	1	8	29.5	26.3	3.4	3.2
5-10-2015	0	12	28.3	25.0	3.2	3.0
6-10-2015	0	12	28.0	25.0	3.2	3.0
7-10-2015	0	19	28.5	25.0	3.2	2.9
8-10-2015	1	7	26.5	24.0	3.0	2.8
9-10-2015	3	3	28.8	26.5	3.5	3.3
10-10-2015	0	4	27.5	25.5	3.3	3.1
11-10-2015	NV	NV	NV	NV	NV	NV
12-10-2015	1	8	26.3	25.3	3.2	3.2
13-10-2015	9	NV	26.3	24.5	3.1	3.0
14-10-2015	3	3	26.0	25.0	3.2	3.1
15-10-2015	11	NV	NV	NV	NV	NV
16-10-2015	2	NV	NV	NV	NV	NV
17-10-2015	39	NV	NV	NV	NV	NV
18-10-2015	0	NV	NV	NV	NV	NV
19-10-2015	0	NV	NV	NV	NV	NV
20-10-2015	10	NV	NV	NV	NV	NV
21-10-2015	14	NV	NV	NV	NV	NV
22-10-2015	0	NV	27.0	23.5	2.9	2.7
23-10-2015	0	4.8	26.3	25.0	3.2	3.1
24-10-2015	0	5.1	26.8	25.3	3.2	3.1
25-10-2015	0	8.0	28.0	25.3	3.2	3.0
26-10-2015	0	2.4	26.5	24.3	3.0	2.9
27-10-2015	0	6.4	26.5	24.8	3.1	3.0
28-10-2015	0	NV	24.8	23.5	2.9	2.8
29-10-2015	2	NV	24.5	23.5	2.9	2.8
30-10-2015	0	NV	25.5	24.5	3.1	3.0

C.1.3 Water level and salinity

Continuous data

The continuous water levels and salinities have been demonstrated in report part II, figures 2.5, 2.6, and 2.9.

In these figures, a couple of error measurements have been removed. For instance, measurements in well W_3 became untrustworthy after October 21, when the owner of the well began extracting water for personal use. Measurements in the estuary at E_{CT} failed after October 5. Perhaps the installed diver floated upwards, although it might also be possible that the diver did not function well any more.

The continuous salinity measurements at E_{CTD} are depicted in figure C.3. Unfortunately, these measurements also show some peculiar patterns. The continuous measurements deviate from the manual measurements taken in the estuary surface water, starting from September 26 and further. Also, after October 22 the measurements somehow seem to stagnate around 2.5 mS/cm , as if the diver could not measure higher levels. Probably, the deviation between the continuous and manual measurements is due to the fact that the diver was installed into a mud layer. Diffusion differences between water and soil, and probably the change in salinity in the pores of the mud did not change as rapidly as the salinity in the surface water.

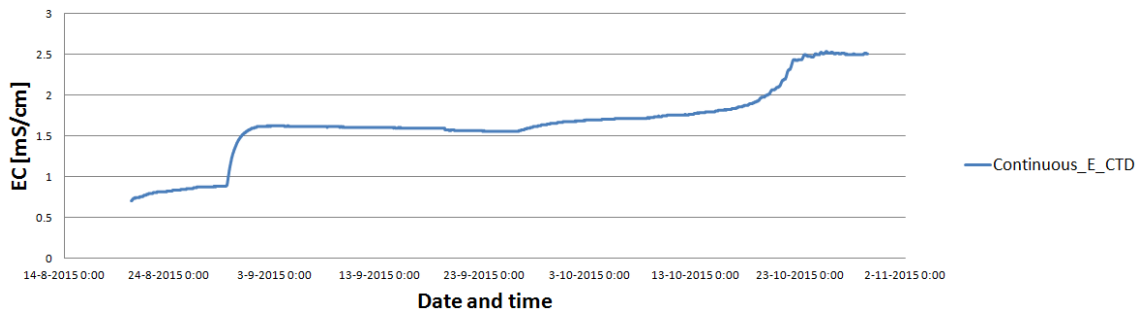


Figure C.3: Continuous salinity measurements in the estuary surface water, at the mouth of the estuary.

Manual data

The water levels and salinities measured manually in the wells, the floodplain piezometers, and in the alluvial piezometers installed by Calderon [10], are listed in the tables below. The depths of the wells range from 4 to 10 m , the floodplain piezometers are 1.25 m deep, and the alluvial piezometers are shown below in figure C.4. The locations of the wells and piezometers are shown in figure C.1, where also the GPS coordinates are listed.

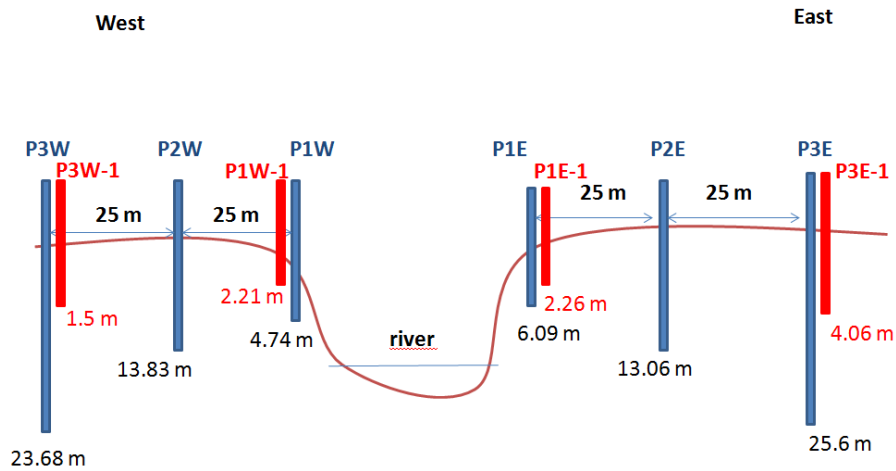


Figure C.4: Set-up of the piezometers at cross-section A-A of figure C.18 of Appendix A.

Then, following these tables, graphs of the manual salinity measurements in the estuary basin are shown for every moment of measurement. Measurements were taken over the complete depth, and thus also measurements at 1 meter below the water level are shown.

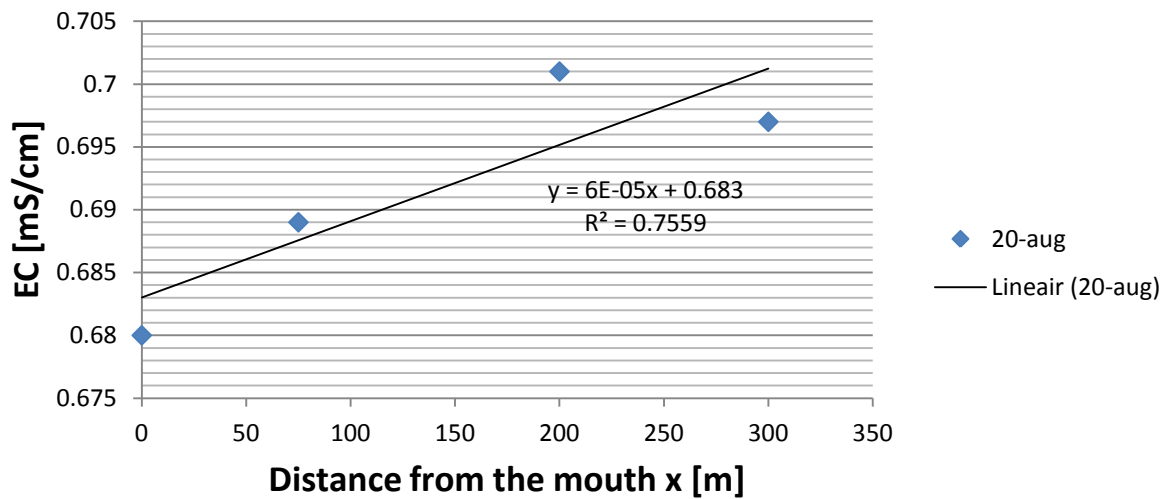
Well measurements		
ID	Date	EC [mS/cm]
W_1	24-sep	13.650
W_2	24-sep	9.270
W_3	24-sep	3.907
	5-okt	4.084
	8-okt	4.021
	13-okt	4.268
	22-okt	3.600
	26-okt	4.940
W_4	24-sep	0.838
W_5	24-sep	0.802
W_6	24-sep	0.997
W_7	26-okt	0.803
W_8	24-sep	0.763
W_9	24-sep	0.892
W_10	24-sep	0.702

Floodplain piezometers measurements			
ID	Date	WL [cm b.s.s.]	EC [mS/cm]
F_1	26-sep	-40	21.23
	26-sep	-39	23.40
	3-okt	0	18.00
	4-okt	0	23.57
	8-okt	-30	23.66
	13-okt	-30	23.74
	22-okt	-13	22.00
	26-okt	-33	23.35
Average			22.37
F_2	26-sep	-91	14.17
	26-sep	-93	14.88
	3-okt	-69	16.67
	4-okt	-66	12.43
	8-okt	-75	24.31
	13-okt	-84	23.00
	22-okt	-38	20.42
	26-okt	-64	20.50
	28-okt	-67	20.61
Average			18.55
F_3	7-sep	-75	15.63
	17-sep	-74	14.42
	22-sep	-85	15.64
	23-sep	-86	14.85
	26-sep	-80	15.32
	26-sep	-80	15.48
	3-okt	-38	15.58
	4-okt	-36	15.55
	8-okt	-58	9.28
Average			14.64

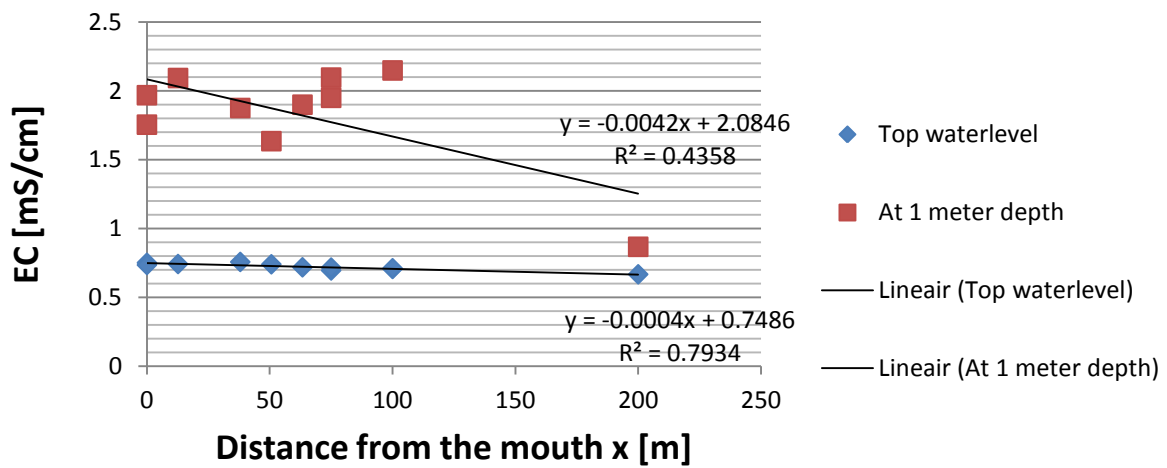
F_4	26-sep	-99	28.16
	26-sep	-100	28.43
	4-okt	-44	20.55
	8-okt	-64	21.29
	13-okt	-73	21.86
	22-okt	-49	21.88
	26-okt	-61	22.37
	29-okt	-32	23.47
Average			23.50
F_5	11-sep	-76	4.45
	17-sep	-65	13.85
	26-sep	-82	10.71
	26-sep	-82	10.48
	4-okt	-51	9.67
	8-okt	-62	9.70
	13-okt	-70	9.33
	22-okt	-52	7.28
	26-okt	-62	9.44
	29-okt	-57	10.02
Average			9.49
F_6	7-sep	-90	13.46
	17-sep	-93	11.63
	23-sep	-105	11.80
	26-sep	-102	12.45
	26-sep	-102	12.69
	4-okt	-66	12.26
	8-okt	-77	13.07
	14-okt	-87	12.90
	22-okt	-56	12.05
	26-okt	-73	11.74
	30-okt	-62	13.50
Average			12.50
F_7	7-sep	-70	10.63
	17-sep	-80	8.00
	23-sep	-85	9.55
	26-sep	-80	9.20
	26-sep	-80	9.49
	4-okt	-23	10.91
	8-okt	-28	10.89
	14-okt	-43	10.59
	22-okt	-15	7.33
	26-okt	-30	7.32
	30-okt	-6	7.47
Average			9.22
F_Beach	3-okt	-220	38.40
	8-okt	-245	38.05
	13-okt	-247	38.84
	22-okt	-240	35.75
Average			37.76

Alluvial piezometers measurements			
ID	Date	WL [cm b.s.s.]	EC [mS/cm]
P1W1	17-sep	-55	0.601
	5-okt	-50	0.591
	13-okt	-62	0.548
	24-okt	-54	0.567
Average		-55	0.577
P1W	17-sep	-59	0.527
	5-okt	-60	0.496
	13-okt	-72	0.554
	24-okt	-65	0.535
Average		-64	0.528
P2W	17-sep	2	0.546
	5-okt	12	0.557
	26-okt	-1	0.531
Average		4	0.545
P1E1	17-sep	-45	0.560
	26-okt	-41	0.552
Average		-43	0.556
P1E	17-sep	-65	0.573
	26-okt	-66	0.542
Average		-66	0.558
P2E	17-sep	-85	0.543
	26-okt	-90	0.542
Average		-88	0.543
P3E	17-sep	-185	1.443
	26-okt	-165	1.464
Average		-175	1.454

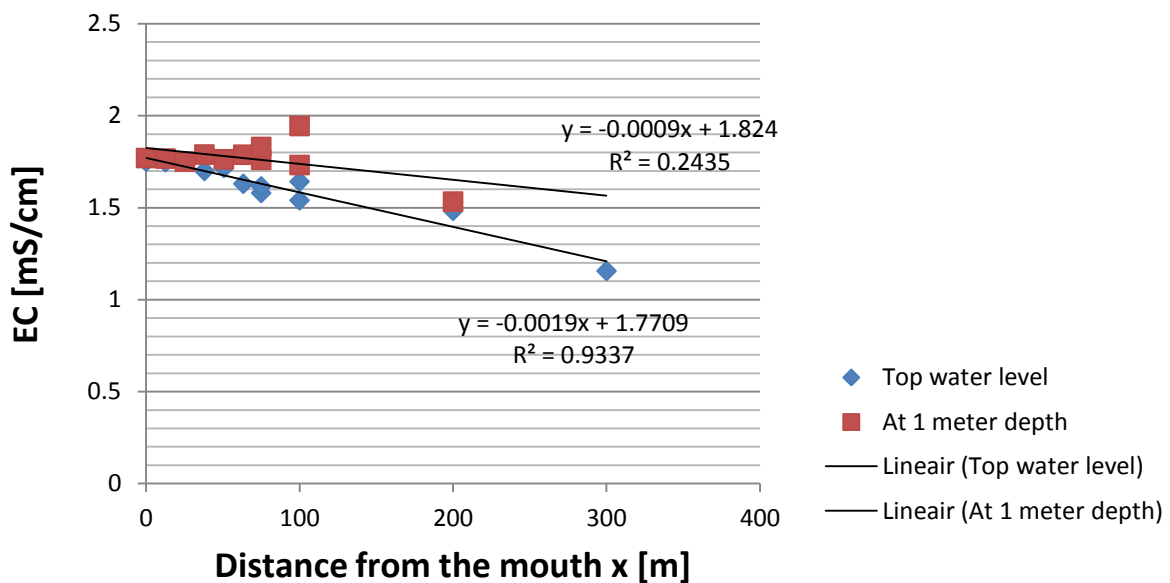
20-aug



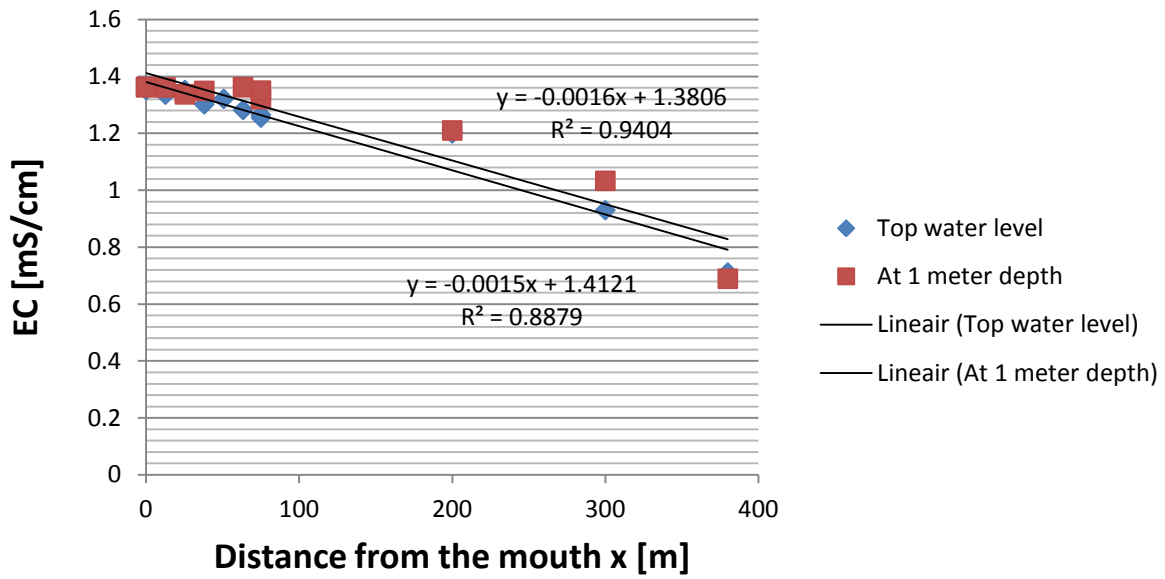
31-08



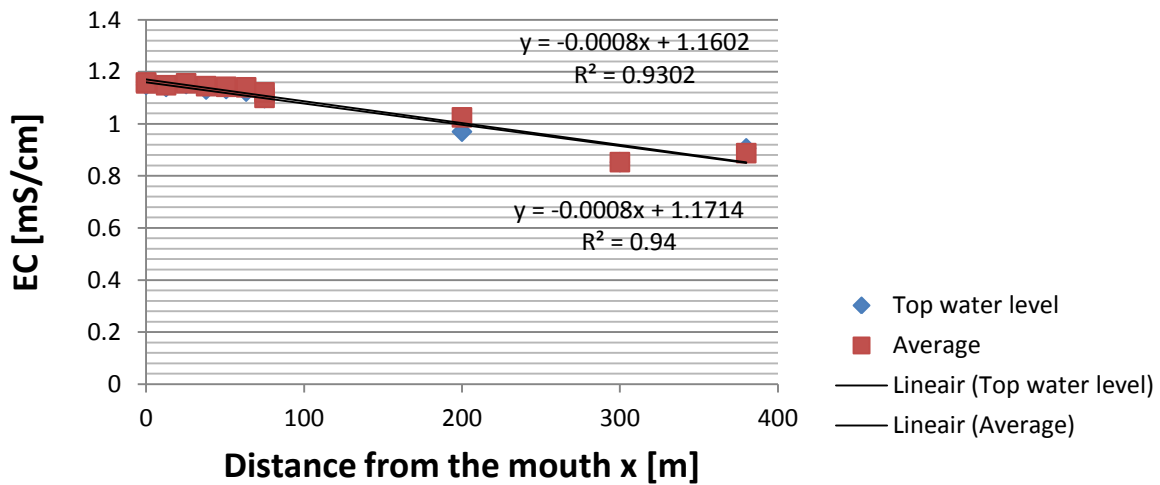
08-09



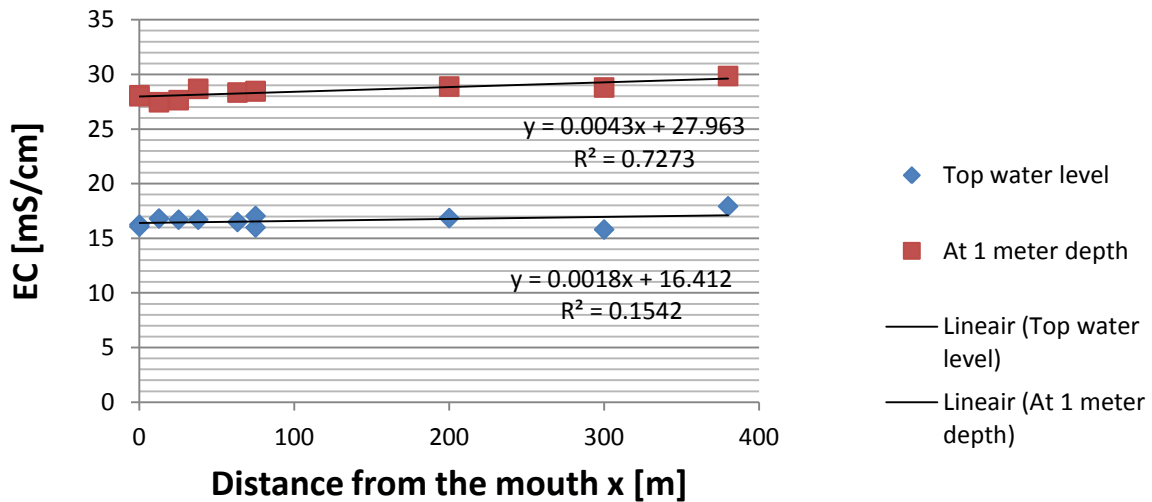
16-09



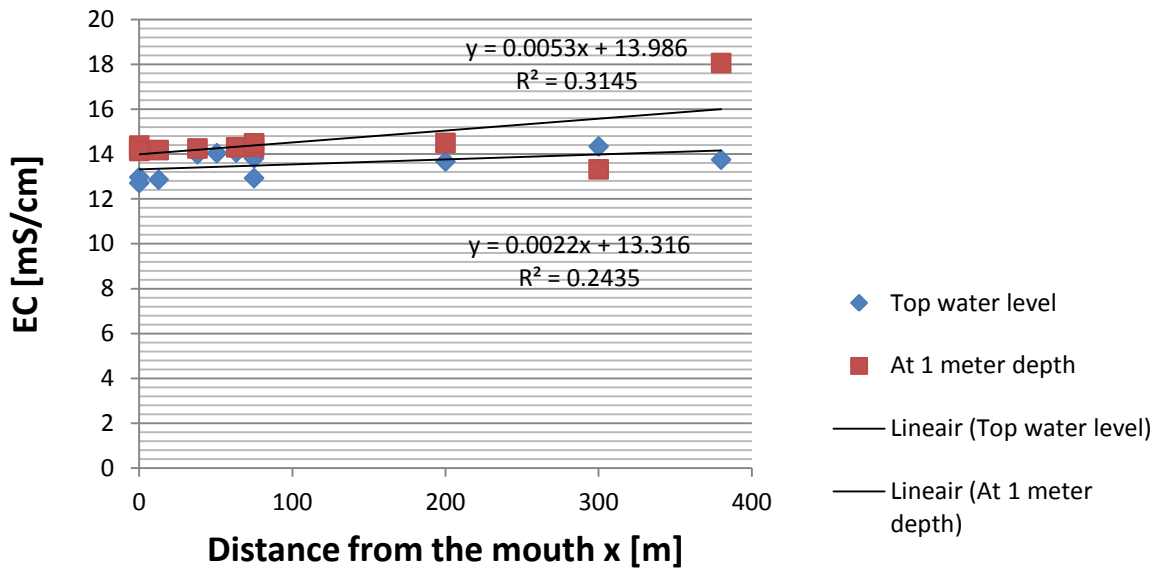
24-09



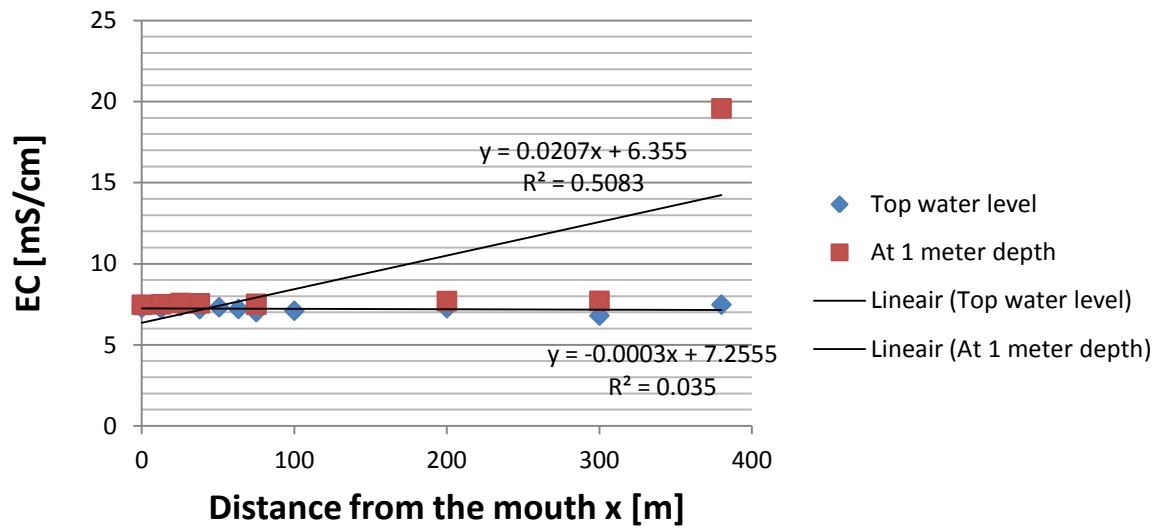
03-10



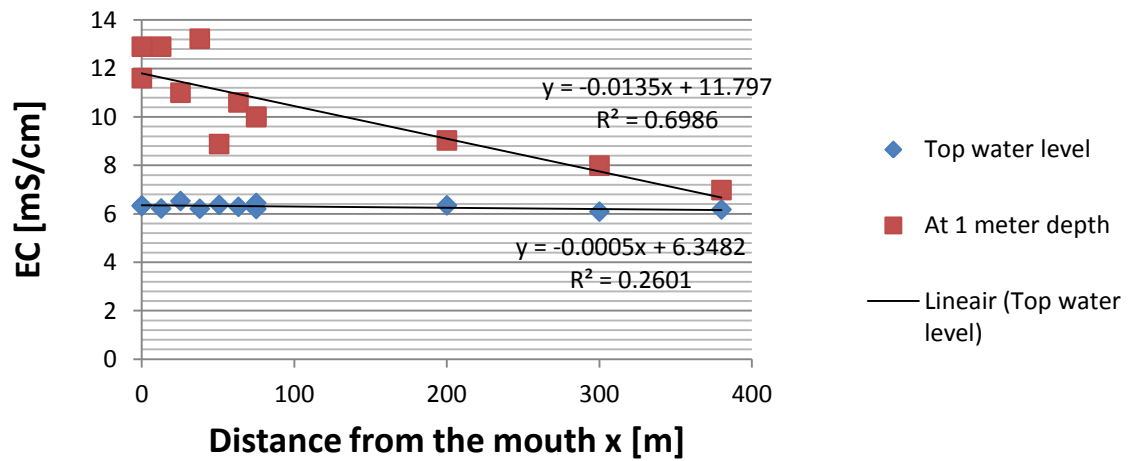
12-10



23-10



27-10



C.1.4 Infiltration and ex-filtration rates

Seepage measurements gave infiltration and ex-filtration rates, listed in figure C.5.

Measurement	Seepage rate [cm ³ /min]
Seepage1	0.07
Seepage2	-0.09
Seepage3	-0.12
Seepage4	-0.03
Seepage5	-0.06
Seepage6	0.27
	0.63
Seepage7	0.35
Seepage8	0.27
	1.39
Seepage9	1.20
	13.33
Seepage10	-0.01
Seepage11	0.22
Seepage12	0.11
	0.04
Seepage14	0.01
Seepage15	-0.17
Seepage16	0.81
	3.33
Seepage17	-0.18
Seepage18	9.17
Seepage19	5.00
Seepage20	1.25
Seepage21	1.70

Seepage upstream end estuary		
Ex-filtration	3.51	[cm ³ /min]
	5.85E-08	[m ³ /s]
D_seepage	0.3	[m]
A_seepage	0.07	[m ²]
v_f	8.28E-07	[m/s]

Figure C.5: Table listing the resulting infiltration and ex-filtration rates between groundwater and estuary basin (left). The other table shows the resulting ex-filtration rate measured at the upstream end of the estuary, from which a fresh water velocity v_f has been extracted (right).

C.1.5 Permeability

Hydraulic conductivities have been calculated from the inverse-auger hole tests performed in the floodplain and sand bar. Resulting K -values of these measurements are listed below in figure C.6. The measured depth per time interval have been plotted in figure C.7. And finally, the calculated K -values have been compared to the amount of crab burrows in a 4 m² area around the auger hole, and to the total area of burrows in this 4 m² area around the auger hole. The resulting correlations can be found in figure C.8.

Location	ID	K [m/day]
Sand bar	SB1	15
	SB2	25
	SB3	22
	SB4	22
	SB5	26
	SB6	31
	Average	23
Floodplain	B_1	1.07
	B_2	0.41
	B_4	1.18
	B_6	1.79
	B_9	1.22
	B_10	0.27
	B_11	0.96
	B_12	1.21
	B_13	0.14
	B_14	0.11
	B_15	0.33
	B_16	0.86
	B_17	1.43
	B_18	0.06
Average	0.79	

Figure C.6: Table listing the resulting hydraulic conductivities of the different infiltration tests.

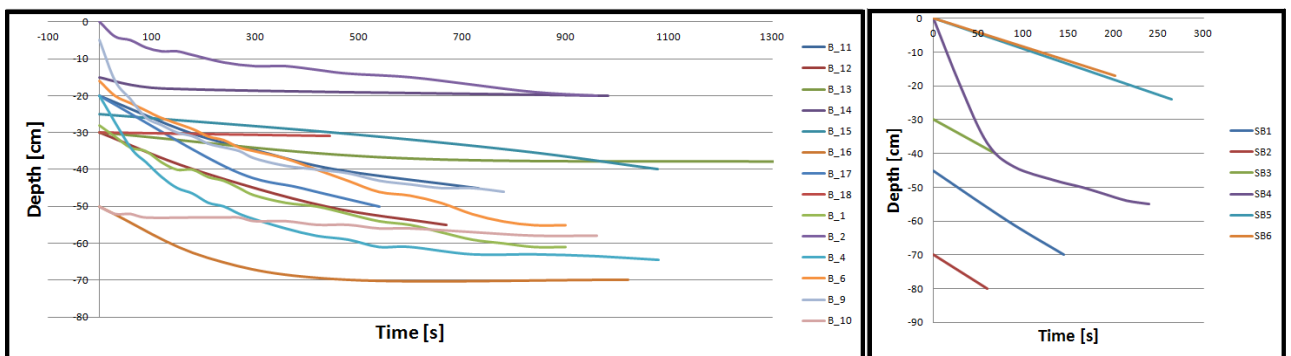


Figure C.7: Graph of the measured depths at certain time intervals during the inverse-auger hole tests in the floodplain (left) and in the sand bar (right).

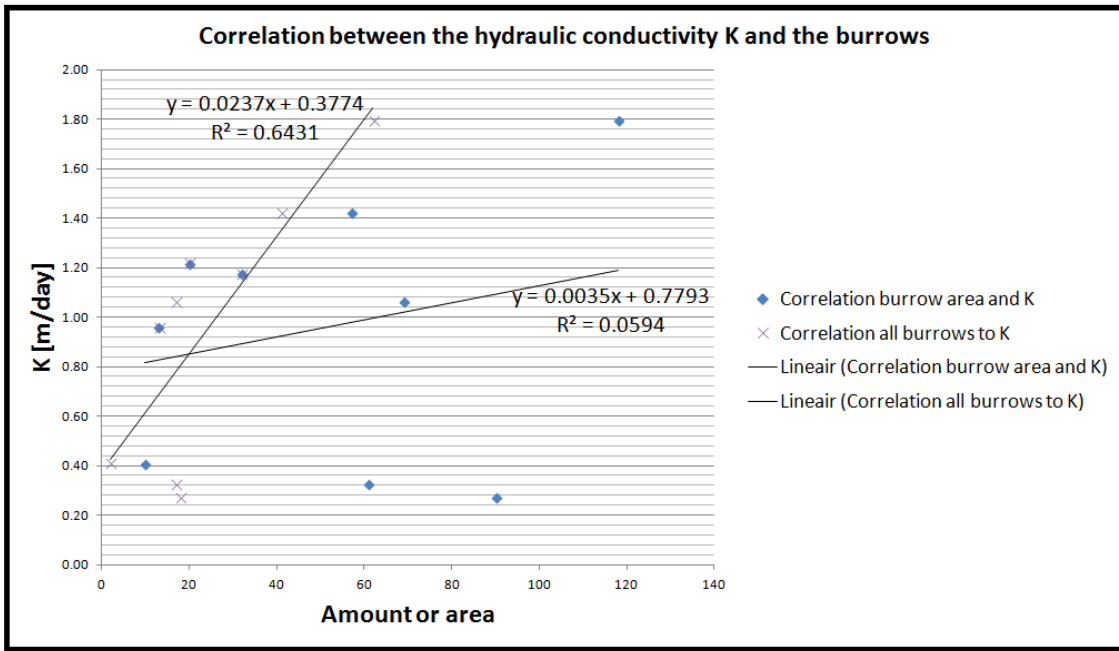


Figure C.8: Graph showing the correlation between the calculated hydraulic conductivities and the amount or area of crab burrows counted in a 4 m^2 area around the hole.

C.1.6 Cross-sectional areas

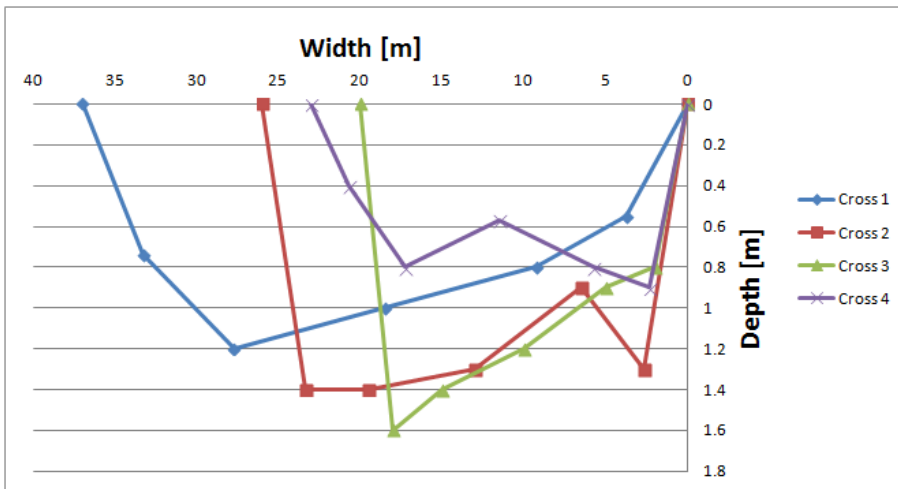


Figure C.9: Graph showing the measured cross-sections in the estuary basin.

C.1.7 Sap flow data

Sap flow measurements could not be converted into sap flow density rates due to the negative values that were measured. A small part of the measurements from 2 sensors is shown in figure C.10. The rest of the measurements shows even further fluctuations and nonsensical values.

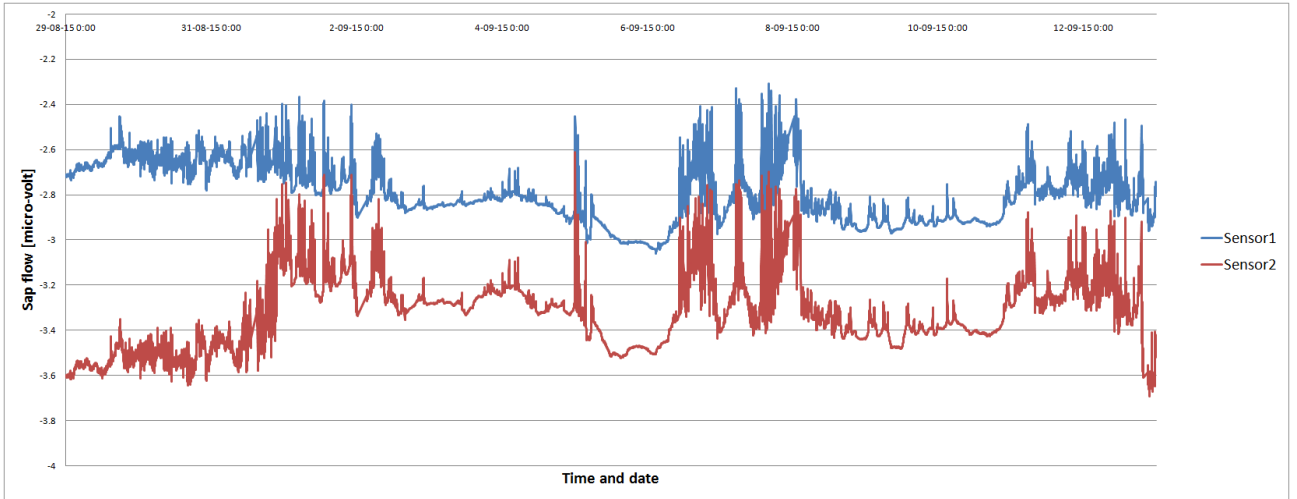


Figure C.10: Plotted sap flow values measured in micro-volt in a White mangrove tree in El Ostional.

C.1.8 Leaf damage sampling

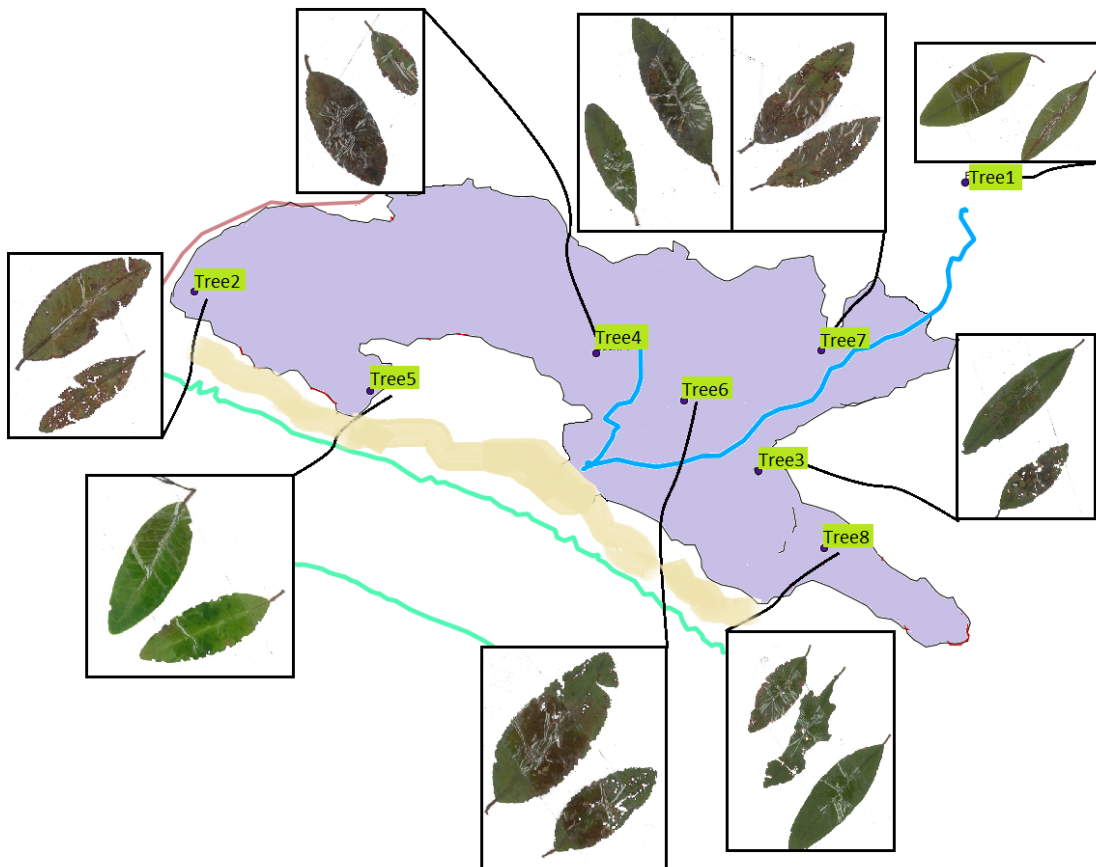


Figure C.11: Overview of the sampled leaves of the White mangrove trees all through the floodplain.

C.2 Fresh-salt water interface

C.3 The 1-D analytical salt intrusion model

C.3.1 Parameter estimation

From the measurements conducted in the estuary, several parameters could be estimated. The estimations are shown in figures C.12 and C.13.

Location	x [m]	B_meas [m]	B_calc [m]	h_meas [m]	h_calc [m]	A_meas [m ²]	A_calc [m ²]	
Cross 1	0	37	37	0.9	0.9	32	32	
Cross 2	75	26	31	1.3	0.9	33	27	
Cross 3	200	20	24	1.2	0.9	24	20	
Cross 4	300	23	19	0.7	0.9	16	16	
Upstream end	380	20	16	0.3	0.9	6	14	
Average:		25	25	0.9	0.9	22	22	
a [m] =		450	b [m] =		450	O_estuary [m ²] =		9576

Figure C.12: Dimensions x, y, h of the measured locations Cross1 - Cross4 and at the upstream end of the estuary. From these measurements, a cross-section A_{meas} was abstracted, what can be compared to the calculated A_{calc} with equation 2.1.

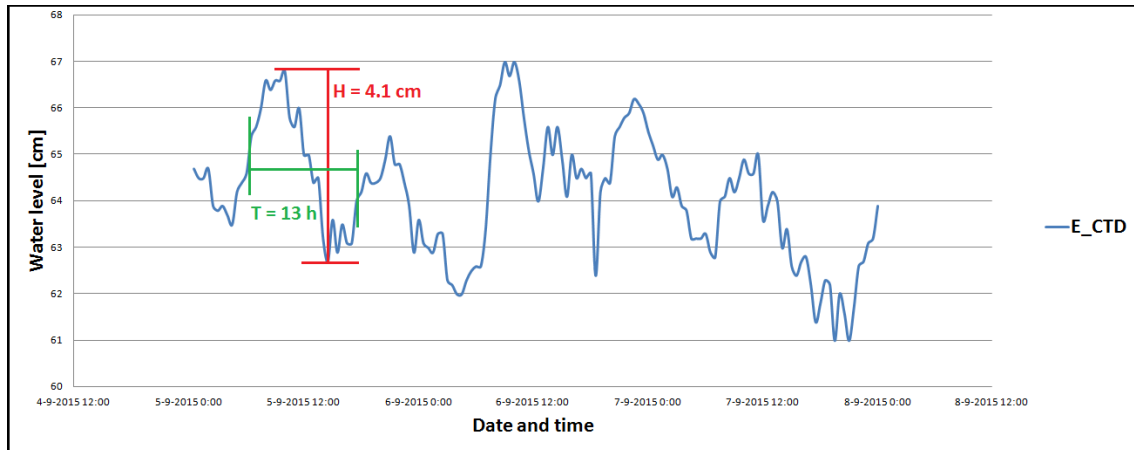


Figure C.13: Graph showing a small period of relative water levels measured by the diver E_{CTD} at the mouth of the estuary. It shows an example for the tidal range H and tidal period T that have been estimated.

Estimation of fresh water inflow		
O_estuary	9576	[m ²]
O_seepage_est_min	1197	[m ²]
O_seepage_est_max	4788	[m ²]
v_f	8.28E-07	[m/s]
Q_f_min	0.001	[m ³ /s]
Q_f_max	0.004	[m ³ /s]

Figure C.14: Table listing the measured fresh water velocity with seepage measurements that was used to calculate the possible fresh water inflow into the estuary. The section were possibly seepage might occur over the complete estuary bed, here mentioned as $O_{estuary}$, has been estimated with a minimum partition of $p = 1/8$ th of the complete estuary bed (O_{min}) and with max half of the estuary bed (O_{max}). This has then resulted into a minimum and maximum amount of fresh water inflow, Q_{min} and Q_{max} .

Estimated parameters						
Tidal excursion	E_0 [m]	21.45				
Velocity amplitude	v [m/s]	1.44E-03				
Flood volume	P [m3]	681				
Canter-Cremers number	N [-]	0.07				
Densimetric Froude number	F_d [-]	9.83E-06				
Estuarine Richardson number	N_R [-]	6988				
van den Burgh coefficient	K [-]	0.1				
Measurement dependend parameters		31-aug	8-sep	16-sep	24-sep	27-okt
Boundary dispersion	D_0 [m2/s]	0.01	0.04	0.03	0.03	0.13
Dispersion reduction rate	β [-]	0.18	0.04	0.06	0.05	0.01
Intrusion length	L [m]	852	1461	1316	1380	2038

Figure C.15: Table listing the estimated parameters for the estuary necessary for the model calculations.

C.3.2 Salinity curves

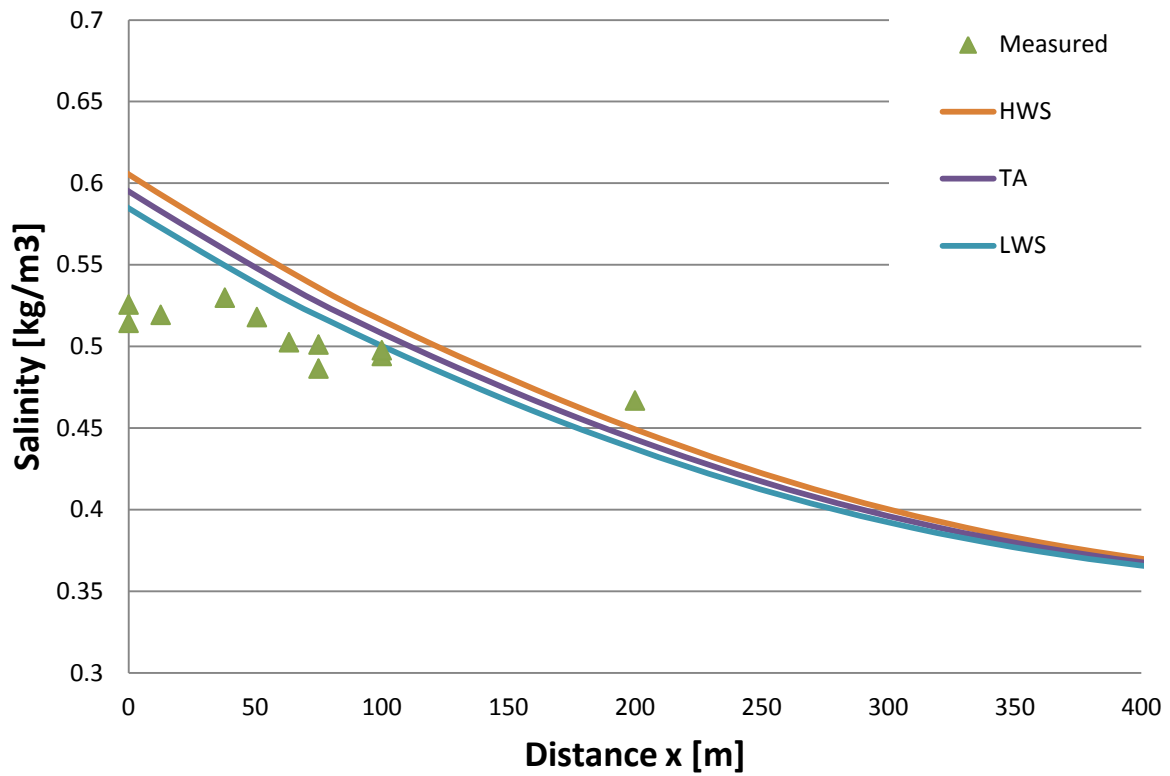
The following graphs show the best fit of the model with the estimated parameters from figure C.15. For each measurement moment, the model performance has been calculated with a correlation coefficient, displayed in the table below.

Q_f = 0.001 m3/s		
Measurement date	D_0 [m2/s]	Correlation coefficient
31-8-2015	0.008	0.883
8-9-2015	0.035	0.973
16-9-2015	0.025	0.973
24-9-2015	0.029	0.960
27-10-2015	0.130	0.509

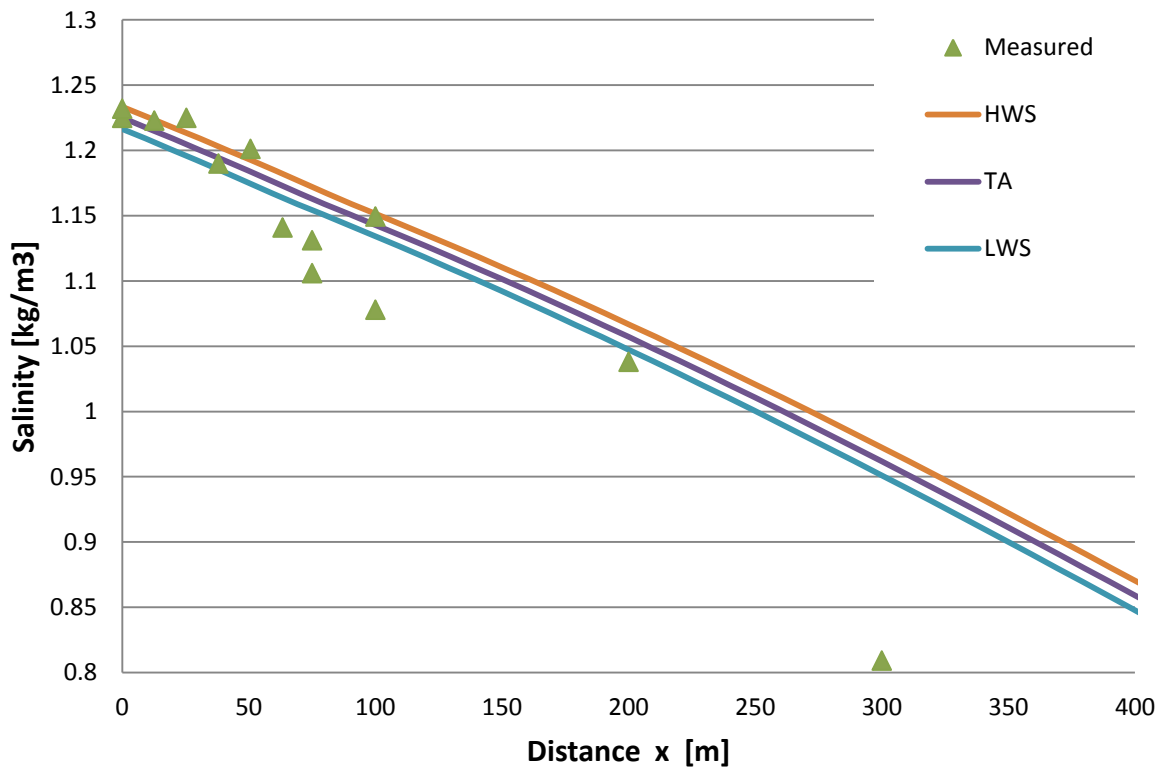
Q_f = 0.004 m3/s		
Measurement date	D_0 [m2/s]	Correlation coefficient
31-8-2015	0.008	0.883
8-9-2015	0.140	0.973
16-9-2015	0.025	0.973
24-9-2015	0.029	0.960
27-10-2015	0.130	0.509

Figure C.16: Model performance correlation coefficient for each measurement.

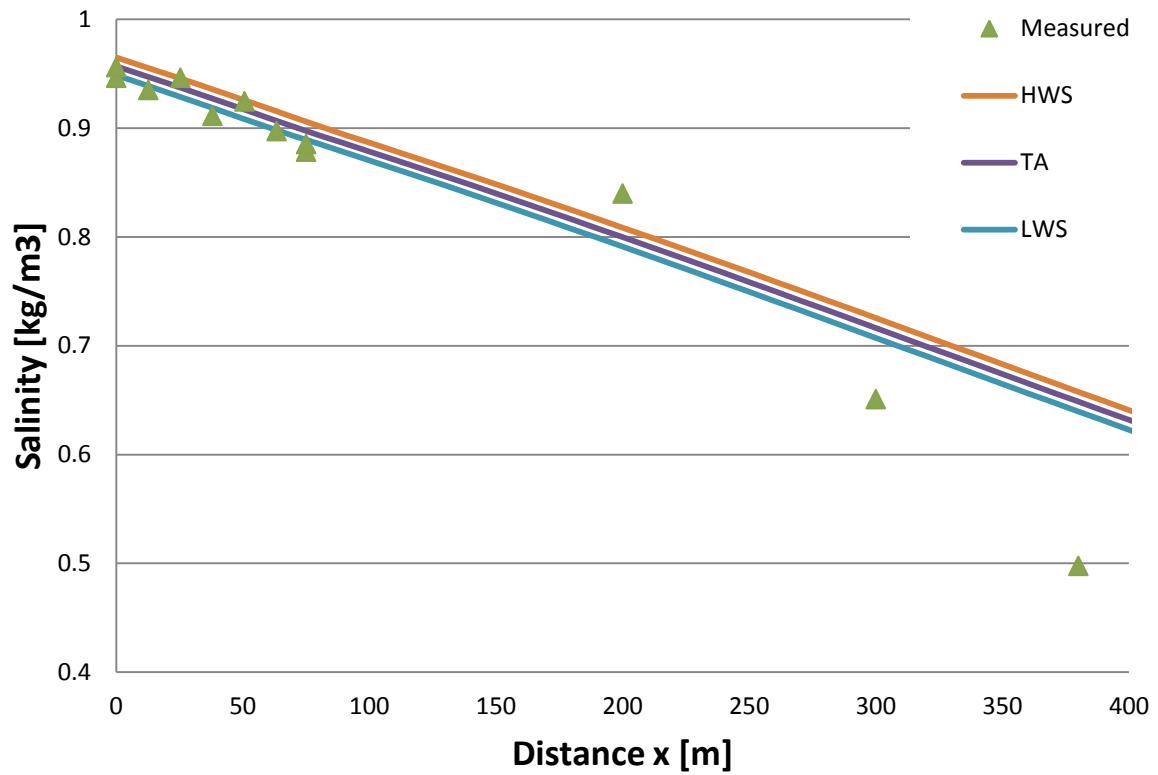
El Ostional 31-8-2015 Salinity Curve



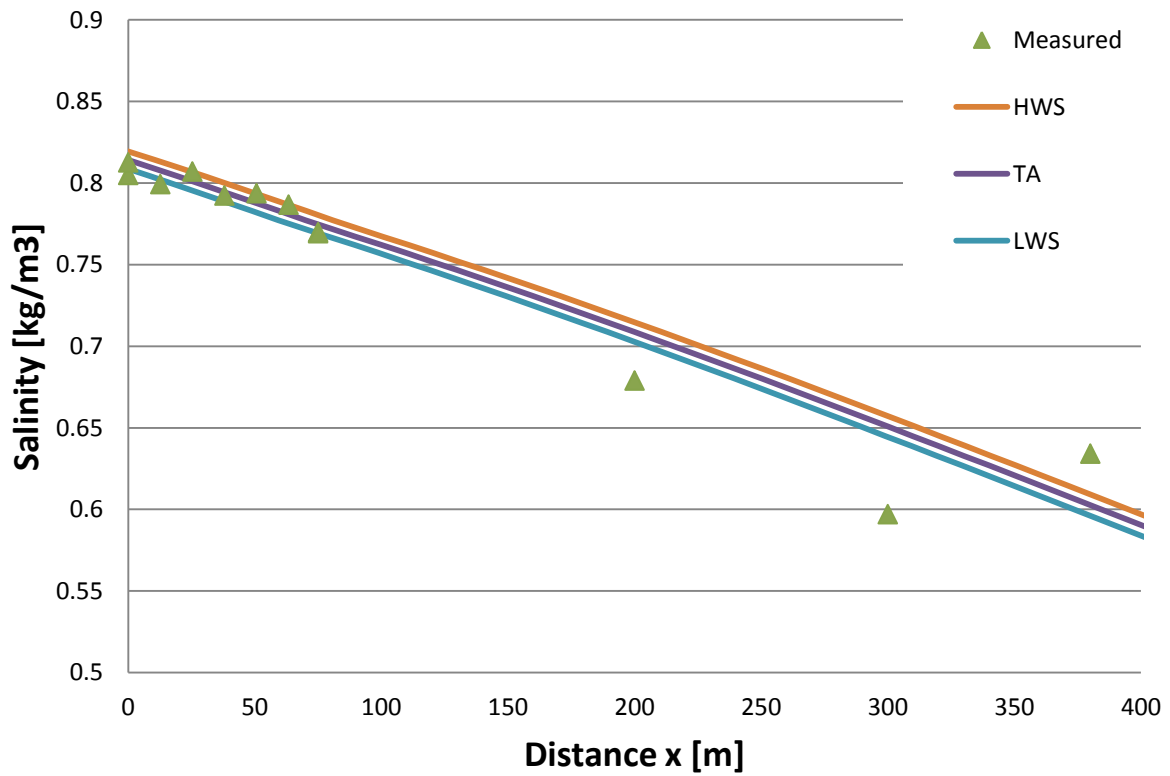
El Ostional 08-09-2015 Salinity Curve



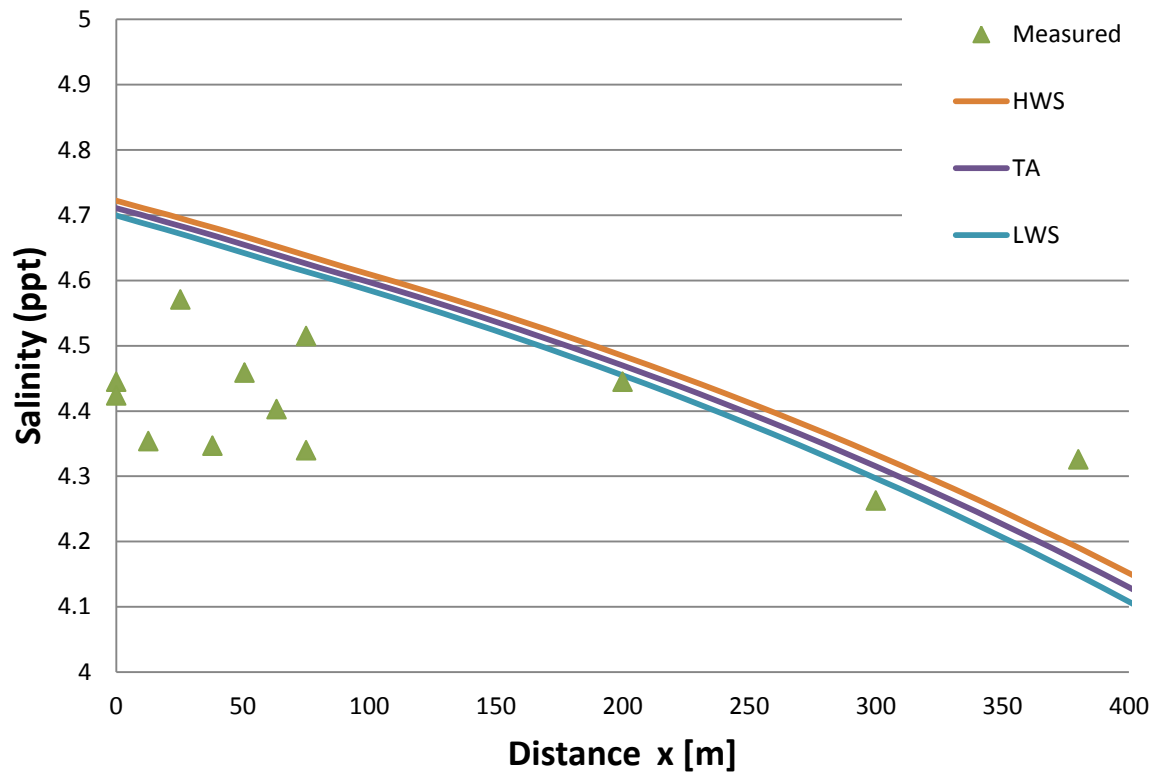
El Ostional 16-9-2015 Salinity Curve



El Ostional 24-9-2015 Salinity Curve



El Ostional 27-10-2015 Salinity Curve



C.3.3 Rainfall influence

Relative importance of rainfall		
r	-6.02E-08	m/s
N1	-3.28E-03	-
N2	1.01E-03	-
N3	5.12E-03	-
N4	2.49E-03	-
N5	-7.68E-04	-
Nr	-2.65E-03	-
Nq	-5.12E-03	-
Nd	-2.01E-03	-
Nr/Nq	5.17E-01	-
Nr/Nd	1.31E+00	-

Figure C.17: The relative importance of rainfall and evaporation in relation to discharge and dispersion is indicated here with the non-dimensional coefficients explained in Appendix B, Section 3.3, equations B.12 till B.17.

C.4 Further retrieved data

C.4.1 Side sources

Ineter

INSTITUTO NICARAGUENSE DE ESTUDIOS TERRITORIALES
I.N.E.T.E.R.
DIRECCIÓN GENERAL DE METEOROLOGÍA
DEPARTAMENTO DE CONTROL DE CALIDAD T/R
TABLAS CLIMATICAS DE RESUMEN MENSUAL.
ESTACION RIVAS MES DE AGOSTO DE 2015

DIA	TEMPERATURA °C					HUMEDAD		Precipitac.	EVAPORACIÓN
	MAX	MIN	MED.	TH	P-ROCIO	H. Relat.	T. Vapor	(mm)	Piché
1	31.3	24.9	27.7	25.3	24.4	83	22.9	1.9	3.9
2	33.7	25.1	28.9	25.7	24.3	79	23.3	0.0	5.5
3	33.3	25.7	29.1	24.8	23.2	72	21.4	0.0	6.3
4	33.7	25.7	29.1	25.1	23.6	74	21.9	0.0	8.4
5	33.5	26.5	29.2	25.8	24.6	77	23.2	0.0	7.2
6	33.9	26.4	29.0	25.5	24.3	77	22.7	0.0	6.1
7	33.1	25.6	28.7	25.3	24.1	77	22.5	0.0	6.2
8	32.8	25.7	28.7	25.7	24.6	79	23.2	0.0	5.5
9	32.5	25.4	28.6	25.5	24.4	79	23.0	0.0	5.0
10	32.1	25.8	28.3	25.3	24.2	79	22.6	0.0	4.7
11	32.0	25.0	27.6	24.4	23.3	78	21.5	0.0	4.3
12	32.6	25.8	27.9	24.7	23.5	77	21.8	0.1	5.4
13	32.9	24.9	29.0	25.3	24.0	76	22.4	0.0	6.5
14	32.5	24.0	27.5	24.7	23.7	80	22.0	5.0	4.7
15	31.9	23.7	27.0	24.9	24.0	84	22.4	7.0	3.1
16	30.7	24.5	26.7	24.8	24.2	86	22.6	1.7	2.7
17	30.9	25.4	27.5	25.5	24.9	86	23.6	0.0	3.0
18	34.0	25.9	29.3	25.2	23.8	73	22.1	0.0	5.4
19	31.8	26.0	28.5	24.9	23.6	75	21.9	0.0	5.2
20	32.7	25.5	28.1	25.2	24.1	79	22.6	1.0	4.5
21	34.2	25.8	29.4	25.5	24.0	74	22.5	3.3	5.8
22	30.5	24.3	26.7	25.2	24.7	89	23.4	3.5	3.9
23	31.7	25.0	27.4	25.6	25.0	87	23.8	4.9	1.8
24	32.4	25.8	28.8	24.7	23.2	73	21.4	0.0	4.8
25	32.5	24.5	28.3	25.2	24.1	79	22.5	0.0	6.0
26	33.3	23.9	28.6	25.4	24.2	78	22.6	0.0	6.7
27	32.8	25.9	28.3	25.4	24.3	80	22.8	0.0	4.8
28	33.3	26.3	29.0	25.3	24.7	77	22.9	0.0	5.2
29	33.7	26.4	29.0	25.8	24.7	78	23.3	0.0	5.8
30	34.0	25.9	29.4	25.9	24.7	77	23.3	0.0	4.7
31	34.0	26.5	29.2	26.1	25.0	79	23.7	0.1	4.5
SUMA	1014.3	787.8	880.5	783.7	749.4	2441.0	701.8	28.5	157.6
MEDIA	32.7	25.4	28.4	25.3	24.2	78.7	22.6	0.9	5.1
MAX	34.2	26.5	29.4	26.1	25.0	89.0	23.8	7.0	8.4
MIN	30.5	23.7	26.7	24.4	23.2	72.0	21.4	0.0	1.8
>=0,5	-	-	-	-	-	-	-	0	-
DIA MAX/MIN	21	15	-	-	-	-	-	15	-
DIA	MAX	MIN	MED.	TH	P-ROCIO	H. Relat.	T. Vapor	21.0	Piché

		INSO	Nh	VIENTO (m/seg.)				Presion A Nivel de la Estación		
Tanque		Horas y	Nubes							
DIA	(ml)	Decim.	bajas	MED.	MAX.	MIN.	DD.PP	Med-mb	Max-mb	Min-mb
1	4.6	4.2	4	2.7	4	2	E	1003.2	1004.3	1001.5
2	6.9	9.9	2	3.9	5	2	N	1001.5	1002.8	999.5
3	9.0	8.6	3	4.9	6	3	E	1001.5	1002.8	999.8
4	8.6	9.6	2	5.1	7	4	E	1002.3	1003.5	1001.1
5	6.9	9.3	2	4.7	6	4	N	1002.3	1003.8	1000.7
6	6.7	6.8	2	4.8	6	4	N	1001.9	1003.2	999.6
7	6.9	6.3	6	4.2	6	3	E	1002.4	1003.8	1000.3
8	6.5	6.3	3	3.3	4	2	E	1003.6	1005.5	1001.8
9	6.2	7.3	3	2.9	4	2	SE	1003.7	1005.0	1001.8
10	5.8	4.5	5	3.1	4	2	N	1002.3	1004.2	999.9
11	6.4	4.0	6	3.8	5	2	E	1003.5	1005.1	1001.8
12	6.7	3.6	4	4.2	5	3	E	1003.6	1005.3	1002.5
13	6.8	9.2	1	4.1	6	2	N	1003.3	1005.0	1001.0
14	6.1	5.9	4	3.7	5	2	E	1004.1	1005.5	1002.4
15	5.1	3.4	6	2.3	4	2	E	1003.9	1005.4	1002.4
16	2.5	0.5	4	2.6	4	2	E	1004.2	1005.8	1003.3
17	1.5	2.8	4	3.5	4	2	SE	1004.0	1005.8	1002.3
18	7.4	9.6	2	4.3	6	3	N	1003.6	1005.4	1001.4
19	7.8	9.3	4	3.9	5	3	E	1002.9	1004.7	1001.1
20	5.0	6.7	6	2.9	5	3	E	1002.9	1004.6	1000.8
21	6.2	5.8	4	3.5	4	3	SW	1002.7	1004.2	1000.8
22	2.7	1.8	6	2.6	4	2	N	1003.3	1004.4	1001.9
23	2.7	1.1	7	1.8	4	2	E	1002.7	1004.0	1001.1
24	6.7	6.4	0	4.6	6	3	NE	1002.5	1005.4	1000.2
25	7.6	9.5	2	2.7	6	2	E	1003.5	1005.1	1001.0
26	6.6	9.0	4	2.4	4	2	E	1004.2	1006.6	1002.0
27	7.8	5.3	5	3.3	5	2	E	1003.5	1006.0	1001.5
28	5.4	7.8	3	3.5	5	2	E	1002.4	1004.3	999.8
29	6.3	10.0	1	4.1	6	2	N	1002.4	1004.8	999.9
30	6.9	9.4	2	2.8	4	2	N	1002.8	1004.5	1000.6
31	8.4	6.7	3	2.8	4	3	E	1003.7	1005.5	1002.0
SUMA	190.7	200.6	110.0	109.0	153.0	77.0	E18	31094.4	31146.3	31035.8
MEDIA	6.2	6.5	3.5	3.5	4.9	2.5	-	1003.0	1004.7	1001.2
MAX	9.0	10.0	7.0	5.1	7.0	4.0	-	1004.2	1006.6	1003.3
MIN	1.5	0.5	0.0	1.8	4.0	2.0	-	1001.5	1002.8	999.5
>=0,5	-	-	-	-	-	-	-	-	-	-
DIA MAX/MIN	-	-	-	-	-	-	-	-	-	-
DIA	Tanque	INSOL	Nh	MED.	MAX.	MIN.	DD.PP	Med-mb	-	-

PRECION			
	Presion A Nivel del Mar		
DIA	Med-mb	Max-mb	Min-mb
1	1010.4	1011.6	1008.8
2	1008.7	1010.0	1006.7
3	1008.7	1010.0	1007.0
4	1009.5	1010.7	1008.3
5	1009.5	1011.0	1007.9
6	1009.1	1010.4	1006.8
7	1009.6	1011.0	1007.5
8	1010.8	1012.8	1009.0
9	1011.0	1012.2	1009.0
10	1009.5	1011.4	1007.1
11	1010.7	1012.5	1009.0
12	1010.9	1012.7	1009.7
13	1010.5	1012.2	1008.2
14	1011.3	1012.8	1009.6
15	1011.2	1012.8	1009.7
16	1011.5	1013.1	1010.6
17	1011.3	1013.2	1009.6
18	1010.8	1012.7	1008.6
19	1010.2	1011.9	1008.3
20	1010.1	1011.8	1008.0
21	1010.0	1011.5	1008.0
22	1010.6	1011.6	1009.2
23	1010.0	1011.2	1008.4
24	1009.7	1012.7	1007.4
25	1010.8	1012.4	1008.2
26	1011.5	1013.9	1009.3
27	1010.7	1013.3	1008.8
28	1009.6	1011.5	1007.0
29	1009.6	1012.0	1007.1
30	1010.0	1011.7	1007.8
31	1010.9	1012.7	1009.2
SUMA	31318.7	31371.3	31259.8
MEDIA	1010.3	1012.0	1008.4
MAX	1011.5	1013.9	1010.6
MIN	1008.7	1010.0	1006.7
>=0,5	-	-	-
DIA MAX/MIN	-	-	-
DIA	Med-mb	-	-

INSTITUTO NICARAGUENSE DE ESTUDIOS TERRITORIALES
I.N.E.T.E.R.
DIRECCIÓN GENERAL DE METEOROLOGÍA
DEPARTAMENTO DE CONTROL DE CALIDAD T/R
TABLAS CLIMATICAS DE RESUMEN MENSUAL.
ESTACION RIVAS MES DE SEPTIEMBRE DE 2015

DIA	TEMPERATURA °C							Precipitac. (mm)	EVAPORACIÓN Piché (mm)
	MAX	MIN	MED.	TH	P-ROCIO	H. Relat.	T. Vapor		
1	32.7	26.0	28.4	25.5	24.5	80	23.1	0.0	4.0
2	32.0	25.1	27.5	25.0	24.1	82	22.5	1.4	3.8
3	31.0	24.6	27.1	24.3	23.2	80	21.3	0.0	4.1
4	32.5	24.8	27.9	24.9	23.8	79	22.2	0.2	4.5
5	31.1	25.2	27.7	24.8	23.7	79	22.1	0.1	4.0
6	30.5	25.9	27.1	25.0	24.3	85	22.8	1.2	2.7
7	32.4	25.6	28.5	25.5	24.5	80	23.1	0.3	4.4
8	34.3	26.1	28.6	25.3	24.1	77	22.5	0.2	5.4
9	33.5	25.8	27.9	25.5	24.6	83	23.3	3.3	3.6
10	30.2	24.2	26.7	24.6	23.8	85	22.1	0.0	2.3
11	32.0	23.8	25.9	24.6	23.7	82	21.9	0.0	3.1
12	33.0	24.3	27.7	25.4	24.5	84	23.1	10.4	2.9
13	32.0	24.0	27.9	25.4	24.5	82	23.1	0.0	2.8
14	32.2	26.0	28.3	25.3	24.3	80	22.8	0.0	4.3
15	32.9	26.4	29.1	26.2	25.2	80	24.0	0.0	5.7
16	33.8	26.7	29.5	25.5	24.1	74	22.5	0.0	6.1
17	32.7	26.0	29.0	24.6	22.8	71	20.9	0.0	6.3
18	32.3	24.6	27.8	25.2	24.2	82	22.7	9.1	3.7
19	32.2	24.0	27.4	25.4	24.7	86	23.4	0.0	2.8
20	33.3	25.9	29.2	25.9	24.7	77	23.3	0.0	4.1
21	34.0	26.2	29.3	25.9	24.7	77	23.3	0.0	5.0
22	31.0	25.8	27.5	25.1	24.2	83	22.7	5.8	3.5
23	30.6	24.9	26.7	25.1	24.6	89	23.2	0.6	2.3
24	29.6	24.3	26.8	24.7	23.9	85	22.3	0.1	2.2
25	31.7	23.5	28.0	24.9	23.8	79	22.1	0.2	2.9
26	33.0	24.3	28.1	25.0	23.8	79	22.2	11.8	3.6
27	32.5	23.8	27.3	25.4	24.8	88	23.5	9.5	2.6
28	32.1	24.2	28.3	26.1	25.4	85	24.4	3.0	2.6
29	33.0	25.5	29.4	26.6	25.6	81	24.7	0.6	3.3
30	33.5	26.0	29.4	26.0	24.7	78	23.5	0.0	4.7
31	-	-	-	-	-	-	-	-	-
SUMA	967.6	753.5	840.0	758.7	728.8	2432.0	684.6	57.8	113.3
MEDIA	32.3	25.1	28.0	25.3	24.3	81.1	22.8	1.9	3.8
MAX	34.3	26.7	29.5	26.6	25.6	89.0	24.7	11.8	6.3
MIN	29.6	23.5	25.9	24.3	22.8	71.0	20.9	0.0	2.2
>=0,5	-	-	-	-	-	-	-	0	-
DIA MAX/MIN	8	25	-	-	-	-	-	26	-
DIA	MAX	MIN	MED.	TH	P-ROCIO	H. Relat.	T. Vapor	13.0	Piché

		INSO	Nh	VIENTO (m/seg.)				Presion A Nivel de la Estación		
Tanque		Horas y	Nubes							
DIA	(ml)	Decim.	bajas	MED.	MAX.	MIN.	DD.PP	Med-mb	Max-mb	Min-mb
1	5.0	5.5	5	3.8	5	3	NE	1004.1	1005.7	1002.6
2	4.9	3.3	5	2.8	4	2	SE	1004.5	1006.0	1003.5
3	4.9	6.1	4	3.3	5	2	SE	1003.7	1005.4	1002.4
4	7.3	7.8	4	3.2	4	3	E	1003.6	1005.6	1001.5
5	6.2	4.2	2	2.7	4	2	E	1003.7	1005.5	1001.1
6	2.3	2.3	5	2.7	4	2	SE	1003.9	1005.9	1001.9
7	6.2	7.1	3	2.8	4	2	SE	1003.2	1004.8	1001.1
8	6.7	7.2	2	3.8	5	2	E	1002.3	1003.9	1000.4
9	3.7	3.3	3	2.7	4	2	NE	1002.2	1004.2	1000.6
10	3.3	0.3	4	1.7	3	2	SE	1003.5	1004.6	1001.1
11	5.4	3.9	3	2.3	3	2	SE	1004.1	1005.8	1002.2
12	3.7	4.8	5	1.2	3	2	N	1002.8	1004.6	999.2
13	5.5	8.3	4	2.1	3	2	N	1002.6	1005.0	1000.2
14	7.5	7.4	3	2.9	4	2	N	1003.2	1004.6	1001.9
15	8.0	9.1	2	4.3	7	2	SE	1003.9	1005.4	1001.9
16	10.8	9.5	2	3.9	6	2	N	1003.7	1005.3	1001.6
17	6.7	8.2	2	2.6	4	2	SE	1002.0	1003.8	1000.0
18	7.9	4.8	5	1.7	3	2	N	1001.2	1003.0	998.6
19	2.3	4.9	3	1.1	3	2	E	1001.9	1004.2	999.4
20	6.3	8.2	3	2.7	4	2	E	1002.1	1004.4	999.6
21	7.7	8.8	3	2.8	5	2	E	1001.3	1003.1	998.2
22	5.1	2.2	5	2.9	4	2	SE	1001.2	1002.8	999.5
23	3.8	1.3	6	0.5	2	1	N	1001.6	1003.2	999.8
24	2.0	0.1	6	0.0	0	0	C	1001.9	1003.9	1000.0
25	4.4	5.9	3	1.7	3	2	SE	1001.8	1003.5	999.6
26	4.1	6.4	4	1.9	3	2	SE	1001.5	1003.1	999.1
27	5.1	6.0	5	0.5	2	1	N	1001.8	1003.6	998.8
28	4.6	7.6	3	1.6	3	2	SE	1001.3	1003.6	998.8
29	4.3	9.2	4	1.9	4	2	SE	1000.8	1002.2	998.4
30	7.7	9.2	2	1.9	4	2	SE	1001.1	1002.8	998.7
31	-	-	-	-	-	-	-	-	-	-
SUMA	163.4	172.9	110.0	70.0	112.0	58.0	SE14	30076.5	30129.5	30011.7
MEDIA	5.4	5.8	3.7	2.3	3.7	1.9	-	1002.6	1004.3	1000.4
MAX	10.8	9.5	6.0	4.3	7.0	3.0	-	1004.5	1006.0	1003.5
MIN	2.0	0.1	2.0	0.0	0.0	0.0	-	1000.8	1002.2	998.2
>=0,5	-	-	-	-	-	-	-	-	-	-
DIA MAX/MIN	-	-	-	-	-	-	-	-	-	-
DIA	Tanque	INSOL	Nh	MED.	MAX.	MIN.	DD.PP	Med-mb	-	-

PRECION			
DIA	Med-mb	Max-mb	Min-mb
1	1011.4	1013.0	1009.9
2	1011.8	1013.3	1010.8
3	1011.0	1012.8	1009.7
4	1010.9	1013.0	1008.7
5	1011.0	1012.9	1008.4
6	1011.2	1013.3	1009.2
7	1010.4	1012.1	1008.3
8	1009.5	1011.1	1007.7
9	1009.4	1011.8	1007.9
10	1010.9	1011.9	1008.4
11	1011.4	1013.2	1009.5
12	1010.1	1011.9	1006.4
13	1009.8	1012.3	1007.5
14	1010.5	1011.8	1009.1
15	1011.1	1012.7	1009.1
16	1011.0	1012.6	1008.8
17	1009.2	1011.0	1007.2
18	1008.5	1010.2	1005.8
19	1009.2	1011.5	1006.6
20	1009.3	1011.7	1006.8
21	1008.5	1010.3	1005.4
22	1008.4	1010.0	1006.8
23	1008.9	1010.5	1007.1
24	1009.2	1011.2	1007.3
25	1009.0	1010.8	1006.9
26	1008.8	1010.4	1006.3
27	1009.1	1010.9	1006.0
28	1008.5	1010.9	1006.0
29	1008.0	1009.4	1005.6
30	1008.3	1010.0	1005.9
31	-	-	-
SUMA	30294.3	30348.5	30229.1
MEDIA	1009.8	1011.6	1007.6
MAX	1011.8	1013.3	1010.8
MIN	1008.0	1009.4	1005.4
>=0,5	-	-	-
DIA MAX/MIN	-	-	-
DIA	Med-mb	-	-

C.4.2 A study of the Catchment

Previous study El Ostional

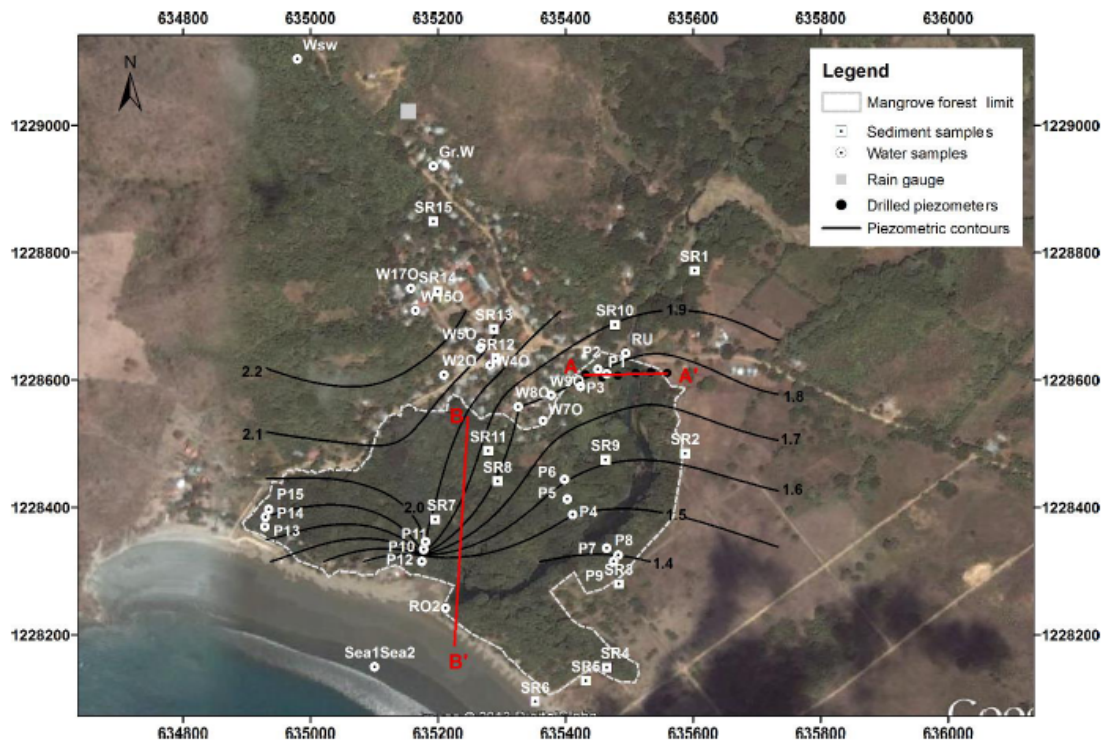


Figure C.18: Location of study area depicting the average piezometric surface of shallow ground-water in the study period as well as cross-sections A-A and B-B. Taken from Calderon [10].

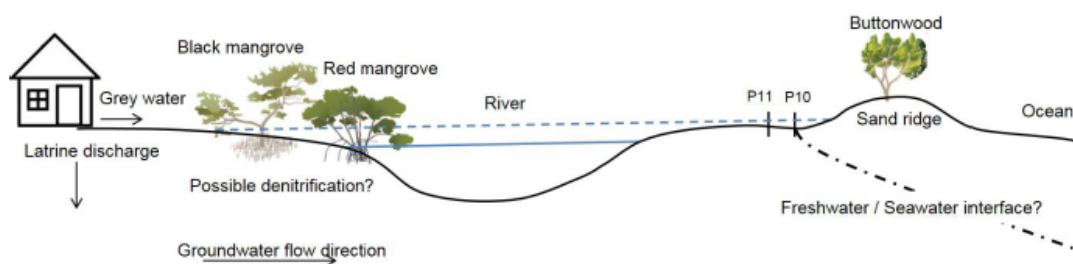


Figure C.19: Schematic cross-section of the study area, valid for the area around cross-section B-B in figure C.18. Dashed line indicates river flooding. Figure is not to scale. Taken from Calderon [10].

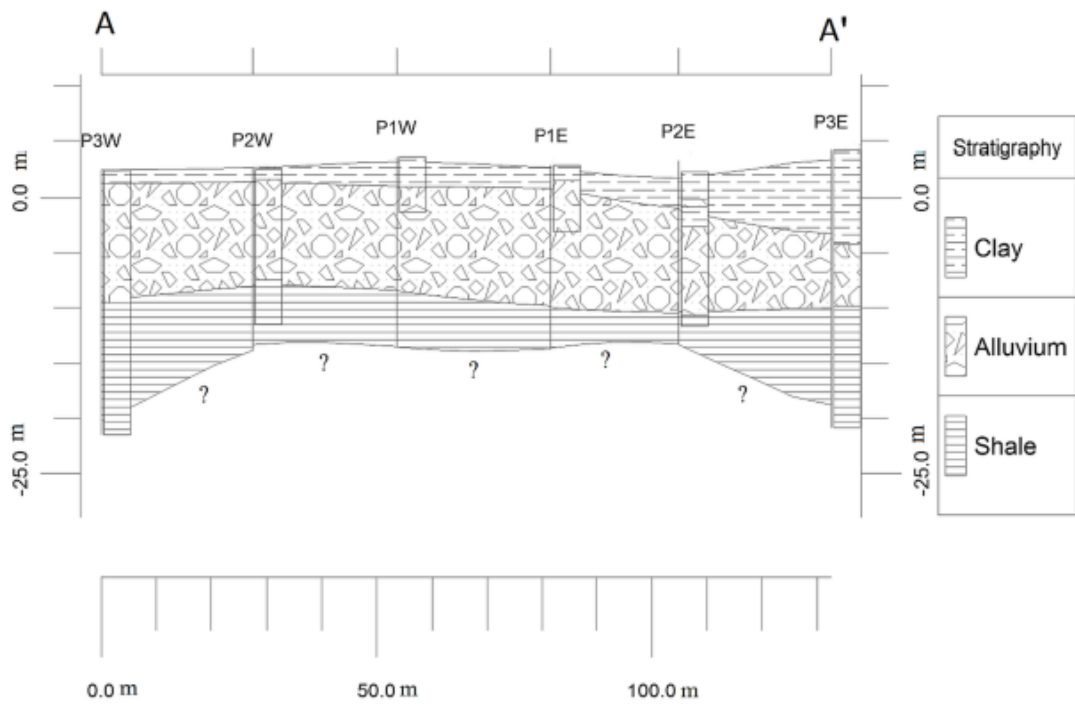


Figure C.20: Stratigraphic correlation in cross-section A-A of figure C.18. Vertical exaggeration times 2. Taken from Calderon [10].

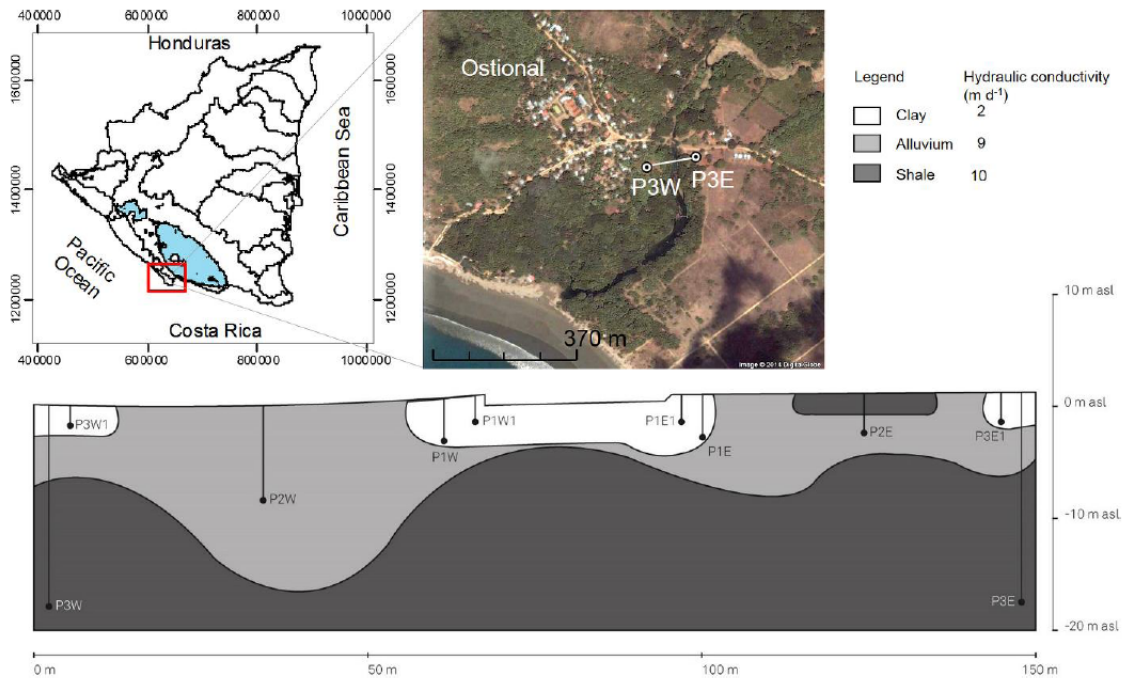


Figure C.21: Stratigraphic interpretation at the piezometric cross-section based on macro- and micro-analysis of sediment samples. Piezometer set-up across the river; West (W) and East (E) piezometers, number indicates position with respect to the river banks, 1 is the closest and 3 is the farthest from the river. Secondary numbering indicates same location but different depth (i.e. P1E and P1E-1). Taken from Calderon [10].

Stratum	Piezometer	K (m d ⁻¹)	Average K (m d ⁻¹)
Clay	P1	0.043	0.33
	P4	1.18	
	P5	0.23	
	P7	0.0006	
	P8	0.001	
	P10	0.88	
	P11	0.05	
	P12	0.29	
Alluvium	P1E	5.60	6.70
	P1W	7.80	
Shale	P3W	12.96	9.07
	P3E	5.18	

Figure C.22: Hydraulic conductivity estimates from slug tests, see figure C.18. Taken from Calderon [10].

Tidal data

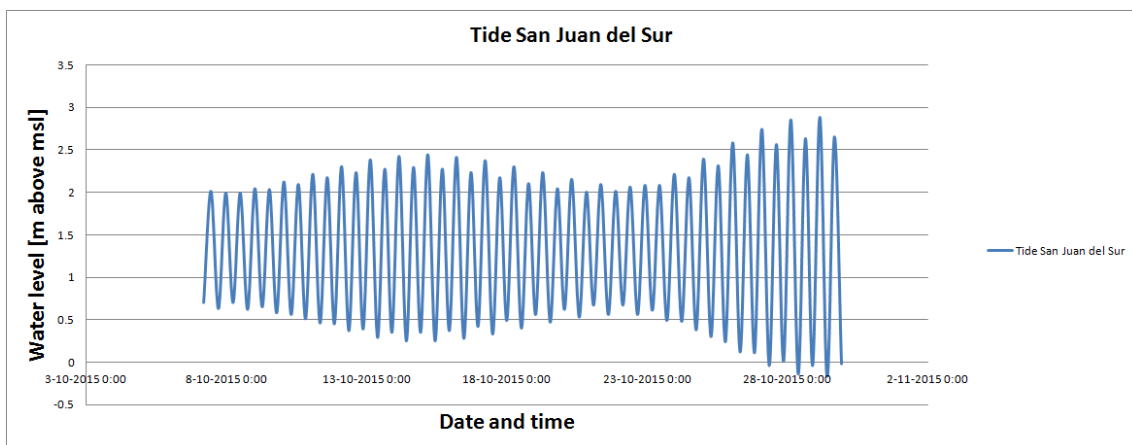


Figure C.23: Tide water level at San Juan del Sur [84].

C.4.3 Nearby locations

At October 6, a visit was paid to two estuaries close to El Ostional. The visit was meant to give an indication of the differences between El Ostional and other small blind estuaries in Nicaragua.

La Flor estuary

The estuary of La Flor is located approximately 5 km up the coast of El Ostional, and lies next to a secluded beach that has the privilege of being one of the few spawning spots where Pasmala and Tora turtles leave their eggs. Months later, one can successfully observe the birth of this reptiles. Because of this, La Flor has been classified as Wildlife Refuge. This beach is bordered by rocky formations. In front of it, there is a small island (which has the same name) in which a great number of seabirds have their nests. There is a large presence of wildlife animals, mainly near the small estuary. There are no hotels or restaurants in the reserve, and the living infrastructure

that does exist belongs to the Ministry of Environment and Natural Resources (MARENA). The institution has established representatives there in order to protect the arrival and birth of the small turtles. They are the ones who manage the lodging options, by giving spaces to camp in the middle of fruit trees and in front of the beach.

The La Flor estuary also is a blind estuary, and due to drought it was closed off from the sea at the moment of visit. Only a part of the estuary could be visited, due to the fact that it is part of a Natural Reserve. Several observations were made:

- The estuary was saline compared to the Ostional estuary. Electrical conductivity levels ranged from 40 - 42 mS/cm . This is almost as salt as sea water.
- The estuary banks seemed higher, especially the left bank. It might be possible that the floodplain behind this sandbar is smaller, and perhaps does not exist at all.
- The river and estuary contained a higher level of meandering near the shore.
- Only the Red and White mangrove trees were found.
- The White mangrove trees were damaged even worse than in the Ostional estuary.

There had just been a major over-wash event in Ostional. Presumably, the same over-wash event occurred in La Flor, what explains the high salinity levels. It does however also indicate that groundwater inflow is low or non-existent, what would explain the absence of the Buttonwood tree as well. Further, a high meander and small floodplain could indicate that the river La Flor generally receives less discharge, also in the rainy season.



Figure C.24: The estuary of La Flor (left figure), the sandbar closing the estuary (middle figure), and the upstream section of the estuary (right figure).

San Juan del Sur estuary

The San Juan del Sur estuary is bordered with the upcoming tourist town San Juan del Sur. This includes a very small slum next to the estuary banks, where the waste water flows directly into the estuary. The estuary is larger, and certainly a blind estuary, being closed from the sea during the visit by a sandbar.

Several observations were made:

- The estuary had a falling gradient in salinity from downstream to upstream. Electrical conductivity levels started around 26 mS/cm at the mouth of the estuary, and for the main part of the estuary this remained the same. Almost completely upstream, this suddenly changed, and levels went down quickly to 16, 12, 6 and finally 0.7 mS/cm .
- In between the mangrove trees, submerged crab burrows were found. The salinity of the water in the burrows was high; 40 - 65 mS/cm .
- The mangrove forest contained Red, Black and White mangrove trees, and was bordered by Buttonwood trees. Due to the occurrence of Blank mangrove trees, a whole forest of peg roots could be seen.

- The White mangrove trees were damaged even worse than in the Ostional estuary. In this estuary the Black mangroves also showed similar damage, but much less.
- The zonation between the different mangrove trees was very clear and similar to literature described zonation patterns. First the Red mangrove next to the water, then the Black mangrove, followed by the White mangrove, and finally the Buttonwood, fringing the forest.

The same over-wash event in San Juan del Sur, resulted in lower salinity levels than in La Flor, but still higher than in Ostional. The salinity gradient does indicate however, that at least a small groundwater inflow is present. And again, the presence of Buttonwood trees are possible and indication of this groundwater inflow as well.



Figure C.25: The mouth of the San Juan del Sur estuary (top figure), the upstream part (left bottom figure), and the Black mangroves with their peg roots (right bottom figure).



El Ostional, Nicaragua



**Blind Estuaries during Drought:
The Influences of a Sandbar
on Mangrove Trees**

S. de Vries
MSc. Thesis
Water Resources Management
Delft University of Technology

